Assessing water connectivity in rural and urban watersheds for improved water management

AI Project #: 2616 (G2020000030)

Public Final Report

Initially submitted on: October 2025

Prepared for

Alberta Innovates, Vicki Lightbown

Prepared by

University of Calgary

Edwin Cey, Professor

403-220-8393, ecey@ucalgary.ca

With partnership financial support from:
The City of Calgary
The Town of Okotoks

Disclaimer

Alberta Innovates (AI) and His Majesty the King in right of Alberta make no warranty, express or implied, nor assume any legal liability or responsibility for the accuracy, completeness, or usefulness of any information contained in this publication, nor that use thereof infringe on privately owned rights. The views and opinions of the author expressed herein do not necessarily reflect those of AI or His Majesty the King right of Alberta. The directors, officers, employees, agents and consultants of AI and the Government of Alberta are exempted, excluded and absolved from all liability for damage or injury, howsoever caused, to any person in connection with or arising out of the use by that person for any purpose of this publication or its contents.

Executive Summary

This Alberta Innovates (AI) supported project investigated surface water-groundwater (SW-GW) connectivity in urbanizing watersheds to support more sustainable water management. To achieve this goal, the project examined both urban and natural hydrologic systems to improve understanding of linkages among surface water, groundwater, and stormwater. Emerging low impact development (LID) practices, such as rain gardens and bioretention systems, were a focal point, assessing their influence on hydrologic processes, water quality, and watershed resilience in Alberta. Three primary field studies were completed: (1) a paired-watershed comparison of streamflow response in developed and undeveloped catchments; (2) monitoring of two community rain gardens; and (3) study of bioretention mesocosm cells at the Okotoks Bioretention Facility (OBF). Together, these studies provided a robust framework for assessing the impact of urban development on water movement, storage, and exchange between surface and subsurface systems.

Key findings highlighted the importance of SW-GW interactions across the landscape, from recharge to discharge zones. Results from the paired-watershed study showed that groundwater was the dominant source of streamflow in both developed and undeveloped catchments, accounting for 86-95% of total discharge. Urban development altered flow pathways and routed water away from the headwater streams, resulting in more static seasonal flows. These insights provide a foundation for improving integrated watershed management through LID-based stormwater optimization and evidence-based guidelines and policies.

Multi-year monitoring of infiltration-based LID systems provided real-world insights into their hydrologic and water quality performance. The OBF mesocosm study revealed that media composition, vegetation, and time since installation were key determinants of performance. All bioretention media types leached nutrients, particularly early on, with non-typical clay-loam (CL) media providing improved water quality compared to sand-based mixes, and equivalent or better hydraulic performance. These findings highlight the potential to adopt more flexible, performance-based media specifications, but also emphasized the need for proper soil amendments to reduce impacts on downgradient water systems. Monitoring demonstrated that the rain gardens effectively infiltrated all captured runoff, with no surface discharge observed during the study period. Subsurface seepage dominated the hydrologic response accounting for 50-70% of inflow, while evapotranspiration contributed significantly at seasonal timescales. The importance of subsurface seepage from unlined rain gardens points to the need to consider subsurface soil and hydrogeologic conditions in LID designs.

The project has produced a large, high-quality hydrologic dataset that remains available for continued use in research, modeling, and municipal planning. Results have already informed new modeling approaches and design considerations for LID systems in cold climates. Through hands-on fieldwork, data analysis, and engagement with project partners, highly qualified personnel gained skills and experience needed to address Alberta's complex water management challenges. The project has also provided important community engagement and educational outreach, using field sites as interactive learning spaces for students, professionals, and youth groups. Collectively, these outcomes strengthen Alberta's capacity for sustainable, evidence-based water management and innovation.

Table of Contents

1.0 INTRODUCTION... 1

2.0 METHODOLOGY 2

2.1 Sage Hill and Glacier Ridge Watersheds..3
2.1.1 Monitoring Equipment...5
2.1.2 Streamflow Analysis and Hydrograph Separation 6
2.2 West Nose Creek and Spy Hill Station...6
2.3 Okotoks Bioretention Facility..6
2.3.1 OBF Mesocosm Cells 8
2.3.2 Inlet Bioswale Monitoring..10
2.4 Highland Park and Cambrians Heights Rain Gardens 11
2.4.1 Monitoring Equipment..12
2.4.2 Simulated Events..12
2.4.3 Water Budget and Subsurface Flow Analysis..14
2.4.4 LID Numerical Simulations 16

3.0 RESULTS 16

3.1 Sage Hill and Glacier Ridge Paired Watersheds 16
3.2 OBF Mesocosm Cells...22
3.2.1 Hydrologic Performance - Growing Season 22
3.2.2 Water Quality Performance - Growing Season..26
3.2.3 Winter Season Performance 28
3.3 OBF Inlet Bioswales...32
3.4 Highland Park and Cambrian Heights Rain Gardens 34
3.4.1 Seasonal Water Budgets..34
3.4.2 Event Water Budgets 37
3.4.3 Infiltration 40
3.4.4 Vertical and Lateral Subsurface Flows 40
3.5 Numerical Simulations 42

4.0 KEY LEARNINGS... 46

4.1 Task 1 Hydrologic Performance of LID Systems...46
4.2 Task 2 Pre- and Post-Development SW-GW Interactions..47
4.3 Task 3 Water Quality Performance Assessment 48
4.4 Task 4 Frozen Ground Hydrology 48
4.5 Task 5 Hydrologic Assessment Tools..49

5.0 OUTCOMES AND IMPACTS 49

5.1 Performance Metric: Highly Qualified Personnel (HQP) Training 49
5.2 Performance Metric: Best Practices Advanced and Guidelines Informed 50

6.0 BENEFITS... 52

6.1 Economic..52
6.2 Environmental 52
6.3 Social 53
6.4 Building Innovation Capacity..53

7.0 RECOMMENDATIONS... 53

8.0 KNOWLEDGE DISSEMINATION 54

9.0 REFERENCE LIST **58**

10.0 PROJECT PUBLICATIONS AND PRESENTATIONS **61**

List of Figures

Figure 1. Map showing field study sites in West Nose Creek, City of Calgary, and Town of Okotoks, including the locations of Sage Hill and Glacier Ridge watersheds and rain garden facilities in Highland Park and Cambrian Heights that were established in 2021. Base map courtesy of Google Earth, 2018. 3

Figure 2. Map with outlines of SHR (blue; developed) and GRR (orange; developing) relative to WNC (green). Main map and inset maps show the locations of monitoring equipment, groundwater springs, and relevant land use. Land use is representative of conditions circa July 2022 and was delineated manually (Johnson, 2024). The top-right inset map shows SHR, GRR, and WNC relative to the regional topography. mASL: meters above sea level. 4

Figure 3. Okotoks Bioretention Facility (a) aerial view image of the full site, and (b) photograph of eight (of 24) mesocosm test cells in the research area. The top diagram (a) shows the location of the mesocosm research cells, and stormwater inlet swales that feed into the main macrocosm bioretention area. Dark and light grey shading represents the parking lot and rooftop sources of runoff, while blue arrows show the direction of stormwater flow through the system. The four monitoring wells shown as white dots were used to record the water table position beneath the adjacent swales (19-1, 19-2) and in background regions across the site (17-1, 17-2). 7

Figure 4. Schematic diagram of a bioretention test cell at the OBF used for artificial stormwater application. Blue arrows show the water budget components that were monitored, including water inflow, drainage outflow, and evapotranspiration (ET), as well as internal changes in soil moisture and soil temperature at two depths in the growing medium. The OBF site contains 24 total test cells consisting of three different growing media types. 8

Figure 5. Schematic diagram (not to scale) of monitoring instrumentation installed at rain garden facilities in (a) Cambrian Heights, and (b) Highland Park. 12

Figure 6. Photographs of rain garden sites showing instrumentation and evolution of vegetative cover. Cambrian Heights rain garden in (a) September 2021 during the construction phase, (b) August 2022 after one full growing season, and (c) June 2023 showing established vegetation. Highland Park rain garden in (d) October 2021 during the construction phase, (e) June 2022 after a large rain event in the first full growing season, and (f) June 2023 after near complete establishment of the native plants. 13

Figure 7. Conceptual approach and model domain for 3D flow simulations of the HP rain garden, showing (a) schematic model geological cross-section, (b) subsurface control volume with relevant water budget components, and (c) isometric view of 3D model domain showing soil moisture conditions during a rainfall event. All images not to scale. 15

Figure 8. Hydrograph and daily precipitation for SHR-SW5, GRR-SW4, and WNC in 2022. Daily precipitation was recorded for each individual catchment at SHR-TB, GRR-TB, and SpH-TB. Spring is defined by the months of April-May, Early-summer is June, Late-summer is July-August, and Fall is September-October. Precipitation data starts on April 7, due to instrument deployment timing. 17

Figure 9. Comparison of runoff ratios from SHR-SW5, GRR-SW4, and WNC for 2022. Each runoff ratio was calculated using the contributing area to the stream gauging station used in this analysis. 18

Figure 10. Comparison of daily average stream discharge (Q_s) to daily average groundwater level fluctuations. a) Daily average baseflow (Q_b) (solid lines) separated from the daily average streamflow (Q_s) (dotted lines) for SHR and GRR in 2022. b) Daily average local groundwater levels from shallow wells (light colors) in the glacial overburden and deep wells (dark colors) completed at the overburden-bedrock interface. Groundwater levels are reported relative to an arbitrary datum to compare relative fluctuations. 20

Figure 11. Differential gauging plot for SHR and GRR in 2022. Each data point is the mean of the daily flows for a 9–11-day period representative of the Spring, Early-summer, Late-summer, and Fall phases of the flow season. The dotted lines are straight line interpretations of the gaining and losing fluxes and represent the net change in streamflow for a given reach. The exact locations of the gaining and losing fluxes require higher resolution streamflow measurements. Error bars are the standard deviation of the daily average flows used to calculate the mean for that given period...21

Figure 12. Infiltration performance showing (a) temporal evolution of infiltration capacity over time (the simulated event number), solid black line indicating the mean infiltration across 24 mesocosms, bars representing 95% confidence intervals (CI); and (b) The relationship between infiltration and simulated event magnitude, whiskers representing the 95% confidence interval (CI), empty circles are for potential outliers outside the 1.5-times inter-quartile range (1.5xIQR), and stars represent extreme outliers outside 3-times the inter-quartile range (3xIQR). 23

Figure 13. Temporal variation (along with the simulated event number) of the infiltration rates across design parameters. The solid lines are the linear regression lines. 24

Figure 14. Relationship between simulated event magnitude and water retention expressed as (a) percentage water retention, and (b) volume of water retention. Circles are outliers at 1.5 interquartile range (IQR), and stars are outliers at 3.0 IQR. 25

Figure 15. Relationship between volume retained per event and antecedent media storage; (a) mean of 24 mesocosms per simulated event, and (b) per simulated event per mesocosm. 26

Figure 16. Mean nutrient concentrations in simulated runoff effluent and corresponding extractable media nutrient content for each media type. Reactive phosphorous (RP) and nitrate-N (NO3) nutrient components are shown. Influent nutrient concentrations are shown as the blue baseline on the effluent graphs...27

Figure 17. Nitrate-N leaching across the simulated events and design factors. Numbers in top-left of the plots indicates the peak nitrate-N concentration recorded if values are off scale...........28

Figure 18. (A) Bioretention cell infiltration rates for simulated frozen and unfrozen events based on media type. (B) Magnification of infiltration rates under frozen conditions. Colored boxes represent the lower and upper quartiles, with the centre line denoting the median, and x denoting the mean. Whiskers represent the extreme values...29

Figure 19. Percent water retention for unfrozen (Average of Summer events) and frozen (Spring 2021 -S21 and Spring 2022 - S22) simulated events based on media type. The box represents the

lower and upper quartiles, with the centre line denoting the median, and x denoting the mean. Whiskers represent the extreme values. 30

Figure 20. Nutrient concentrations from cell outflows from the Spring 2021 and Spring 2022 frozen simulated events based on vegetation type. The red lines indicate inflow concentrations. The box represents the lower and upper quartiles, with the centre line denoting the median, and x denoting the mean. Whiskers represent the extreme values. 31

Figure 21. Groundwater recharge estimates for storm events at (a) bioswale 19-1 and (b) bioswale 19-2 showing mounding estimates (circles) and water budget estimates (triangle). The black line represents a 1:1 recharge relationship based on the runoff coefficient for the catchment. "Hydraulic Load" is the estimated volume of runoff into the swale divided by swale area. The green trend-line displays the linear-regression relationship mounding recharge estimates. Right-hand Y axis applies only to the recharge data estimated through mounding and shows the recharge estimates obtained using the calibrated estimate of saturated hydraulic conductivity. 33

Figure 22. Seasonal water budgets of the Highland Park (HP) and Cambrian Heights (CH) rain gardens, depicted as equivalent water depth (mm) normalized to the garden area. Water budgets ran from May 24–October 16 in 2023, and May 13–October 15 in 2024. 35

Figure 23. Event scale water budgets at the Highland Park rain garden 12, 24, and 48 hours after the start of nine large precipitation events (>25 mm) in 2023 and 2024. GM soil moisture refers to water stored in the growing media and seepage refers to water that drained out of the growing media. The box represents the upper and lower quartiles, the centre line denotes the median, the x denotes the mean, and whiskers represent the extreme values. 37

Figure 24. Event scale water budgets at the Cambrian Heights rain garden 12, 24, and 48 hours after the start of ten large precipitation events (>25 mm) in 2023 and 2024. GM soil moisture refers to water stored in the growing media and seepage refers to water that drained out of the growing media. The box represents the upper and lower quartiles, the centre line denotes the median, the x denotes then mean, and whiskers represent the extreme values. 38

Figure 25. Water budget calculated in hourly intervals for the five simulated events at Highland Park in 2023 and 2024. All events simulated approximately 26 mm of rainfall, except H-sim5 which simulated a 48 mm rainfall. Soil moisture refers to water stored in the growing media and seepage refers to water that has drained out of the growing media. 39

Figure 26. Infiltration rates calculated at each rain garden using two methods: (1) flooding tests where infiltration rate was estimated by observing the rate at which ponded water level declined during large precipitation events, and (2) spot measurements using the MPD (Modified Philip-Dunne) infiltrometer. 41

Figure 27. Groundwater response to event H24-25 and daily precipitation at Highland Park rain garden from September 10-18, 2024. Groundwater level is depicted as depth relative to the ground surface at MW1..42

Figure 28. Simulated influence of varying hydraulic conductivity (K_s) on lateral flow away from the rain garden for different soil layers. Values are expressed relative to the initial calibrated K_s

values for each layer, using percent difference (left axis) and total volumetric flow (right axis). See Figure 7a for soil layer delineation....43

Figure 29. Simulated influence of varying hydraulic conductivity (K_s) for different soil layers on event-based rain garden water budget components for two large (26 mm) events under (a) dry antecedent soil moisture, and (b) wet antecedent soil moisture conditions. Values are expressed as a percentage of total runoff inflow to the garden for each modeled scenario. See Figure 7a for soil layer delineation. 44

Figure 30. Simulated influence of varying hydraulic conductivity (K_s) for different soil layers on total cumulative rain garden water budget components for all events over the full simulation period. Values are expressed as a percentage of total runoff inflow to the garden for each modeled scenario. See Figure 7a for soil layer delineation. 45

1.0 Introduction

A holistic understanding of surface water and groundwater connectivity is needed to ensure proper water management in Alberta, especially in the face of population growth, increasing water demand, and climate change. This project was specifically designed to improve understanding of surface water, stormwater, and groundwater connectivity in water-stressed urbanizing areas of Alberta to support sustainable water management. Urban development introduces numerous impervious surfaces to the landscape, such as rooftops, roads, and parking lots, that limit infiltration and promote runoff of rainfall or snowmelt. Historically, urban centres have relied on traditional stormwater infrastructure (e.g., drainage pipes, storm sewers, stormwater ponds) to deal with the large runoff volumes from impervious surfaces. However, this approach to stormwater management drastically alters natural hydrological processes, and can lead to adverse outcomes such as increased runoff and flooding, altered streamflows, water quality degradation, greater erosion, reduced groundwater recharge, and decreased drought resiliency.

Low impact development (LID) has been proposed as a green or nature-based approach to manage the negative impacts of stormwater runoff and help restore more natural hydrological conditions in urban environments. There are a wide variety of LID technologies available to serve different purposes, including rain gardens, bioretention systems, vegetated or bio-swales, green roofs, soil cells, and permeable pavements. While the design and construction of different LID systems vary, they are generally designed to restore natural hydrologic function by reducing or delaying the amount of runoff during precipitation events and promoting the storage, retention, infiltration, or evapotranspiration of water. The benefits of LID systems are clear and important, however risks and knowledge gaps remain. Most LID systems have been tested in warmer and more humid climates, with little attention paid to performance under freezing or dry/arid conditions. In addition, infiltration-based LID technologies, such as rain gardens and bioretention, rely on infiltration or evapotranspiration to manage stormwater runoff, yet the impacts on groundwater and subsurface infrastructure (e.g., road bases or basements) in urban settings is not clear. Thus, it is important to carefully examine the function and performance of LID systems in Alberta's distinct climatic and geological setting to ensure they are properly designed and implemented.

The City of Calgary and Town of Okotoks, two key partners in this study, are implementing LID systems to improve stormwater management. These and other municipalities are seeking guidance on the design and function of LID systems at a site or local level. They are also in need of relevant information to ensure the proper implementation of LID technologies at regional or watershed scales, and to assess the impacts of urban development on hydrological systems more broadly. This project addresses these concerns directly and is aimed at providing the necessary data and scientific knowledge to support municipalities in their development of sustainable water management plans.

The **overarching goal of this project** was to comprehensively evaluate surface water-groundwater (SW-GW) connectivity in urban and peri-urban settings, thereby supporting more sustainable water management during development. The **specific project goals** were:

- Obtaining high-quality hydrological data in urban and natural settings, with particular emphasis on frozen soil processes, to improve understanding of surface water, stormwater and groundwater linkages.

- Assessing the hydrologic function and water quality treatment performance of LID systems and their associated influence on groundwater.
- Developing and refining hydrologic assessment tools for improved characterization of water flows and quality prior to and after urban development.
- Informing best management practices for LID system design for stormwater management in the unique geologic and climatic (cold and dry) setting of Alberta.

2.0 Methodology

The project was undertaken from 2020 to 2025 and was based on a series of experiments and activities to address the scientific challenges and opportunities listed in the project goals above. Specific project objectives were developed and aligned to a corresponding **project task list** as follows:

1. **Hydrologic Performance of LIDs**: Assess the hydrologic performance of LID systems by characterizing the water balance of multiple stormwater bioretention and rain garden systems, and examining the associated impacts on local groundwater.

2. **Pre- and Post-Development SW-GW Interactions**: Characterize pre- and post-development SW-GW interactions by using relevant investigation techniques to quantify the spatial and temporal variability of hydrologic fluxes in urban and rural settings.

3. **Water Quality Performance Assessment**: Assess water quality treatment performance of engineered bioretention systems at the Okotoks Bioretention Facility. (**Note: Solely part of another joint NSERC CRD project with partial reporting here)

4. **Frozen Ground Hydrology**: Investigate and describe the influence of frozen ground on water movement within natural and engineered systems.

5. **Hydrological Assessment Tools**: Develop, refine and test improved models or assessment tools for describing hydrological behaviour and LID performance in urban settings.

6. **Knowledge Transfer**: Work with partners and end users to ensure successful knowledge transfer and implementation of project results to support water management.

To achieve the project objectives, hydrological field studies were conducted at several research sites within and near the City of Calgary and the Town of Okotoks in southern Alberta (**Figure 1**). Pre-existing hydrological observatories operated by the University of Calgary (UofC) were leveraged in this study, including monitoring instrumentation in the West Nose Creek (WNC) watershed, the Spy Hill hydrometeorological station, and the Okotoks bioretention facility (OBF). Additional field research sites that were developed for this project included the paired Sage Hill and Glacier Ridge watersheds on the northwest perimeter of Calgary, and two community rain gardens, Highland Park (HP) and Cambrian Heights (CH) in Calgary.

The climate in the study area is typical of the Canadian prairies and is characterized by hot, dry summers and cold winters with low precipitation. The 1991–2020 normal monthly mean air temperature at the Calgary International Airport was −7.6 °C in January and 16.9 °C in July

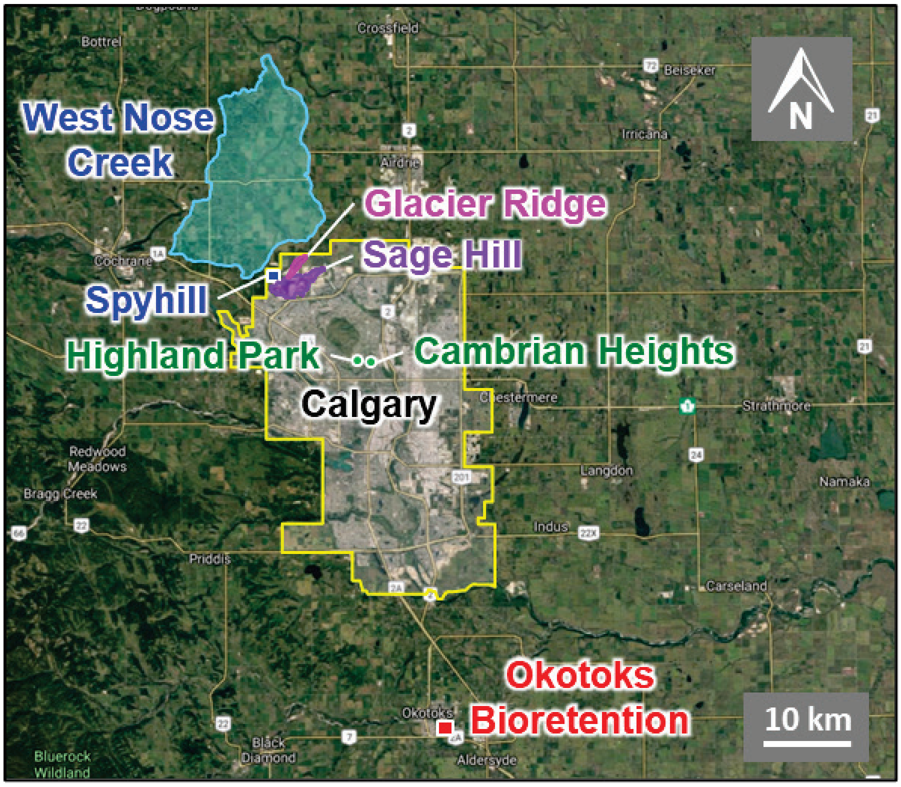

Figure 1. Map showing field study sites in West Nose Creek, City of Calgary, and Town of Okotoks, including the locations of Sage Hill and Glacier Ridge watersheds and rain garden facilities in Highland Park and Cambrian Heights that were established in 2021. Base map courtesy of Google Earth, 2018.

(Environment Canada, 2025). Mean annual precipitation over the same period was 445 mm, of which 124 mm was attributed to winter snowfall. The semi-arid climate of the region is typified by an estimated average annual potential evapotranspiration of 1040 mm (Government of Alberta, 2013; Morton, 1983) that far exceeds annual precipitation. The location east of the Rocky Mountains makes the area prone to Chinook (or föhn) winds that facilitate midwinter melt events throughout the winter, which can create soil freeze-thaw dynamics that alter hydrological processes of infiltration, runoff, and deep percolation.

More details about each of the field study sites, monitoring equipment, and investigation methods is provided in the following subsections.

2.1 Sage Hill and Glacier Ridge Watersheds

Two headwater catchments with perennial streams, but distinct differences in urban development, were selected in northwest Calgary for this project (Figure 2). The Sage Hill ravine (SHR) catchment has a total area of 10.1 km^2 with an estimated impervious cover of 20% (City of Calgary, 2023). Based on air photos, urban development in Sage Hill began around 2003, except for prior landfill

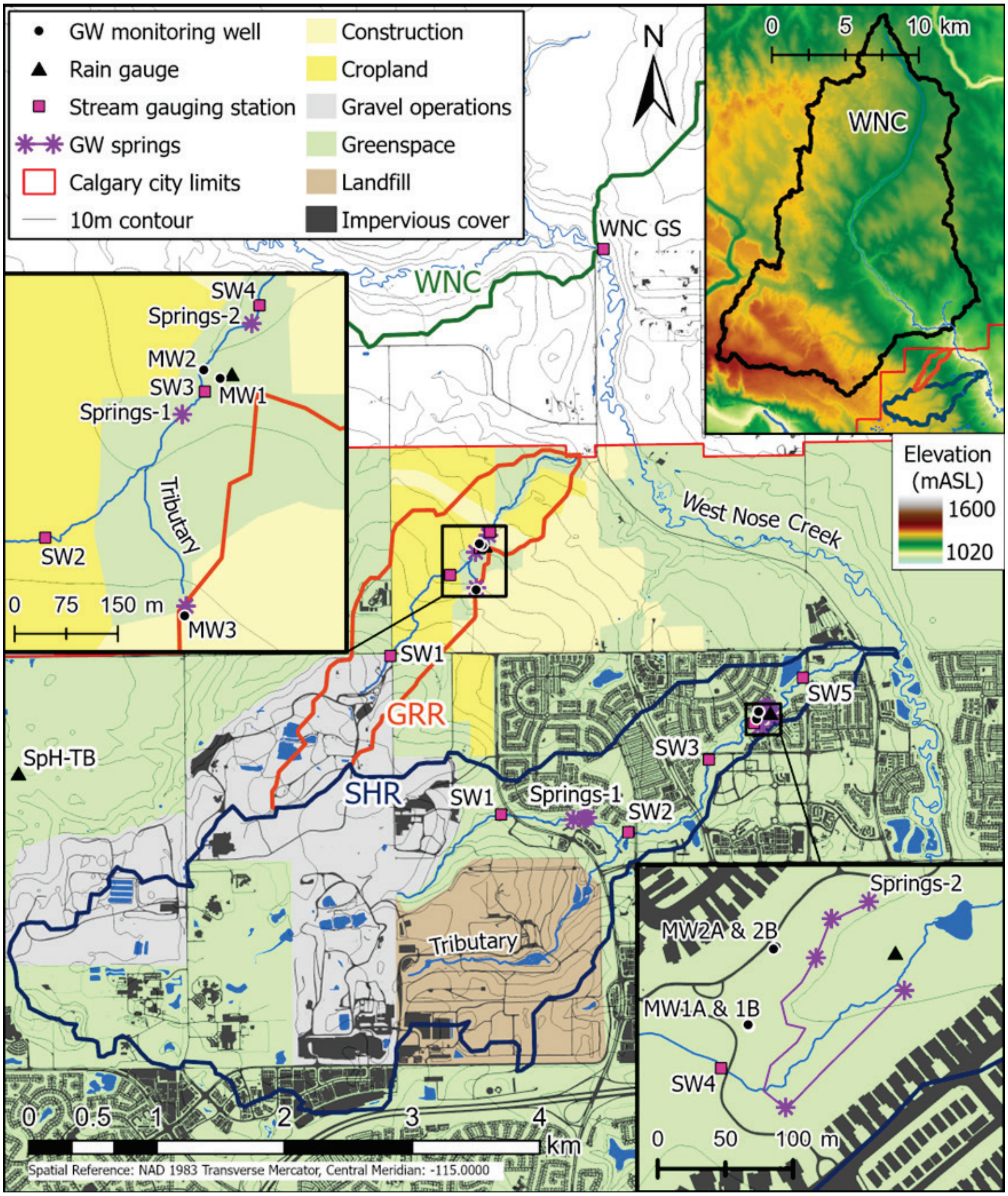

Figure 2. Map with outlines of SHR (blue; developed) and GRR (orange; developing) relative to WNC (green). Main map and inset maps show the locations of monitoring equipment, groundwater springs, and relevant land use. Land use is representative of conditions circa July 2022 and was delineated manually (Johnson, 2024). The top-right inset map shows SHR, GRR, and WNC relative to the regional topography. mASL: meters above sea level.

and gravel extraction operations. SHR is considered to represent developed urban land use and consists of residential, commercial, and industrial uses. The stream riparian areas situated in the lower-lying ravine are largely preserved as greenspace and account for 8% of the total SHR catchment area. Two noteworthy land uses within the SHR catchment are the landfill and gravel extraction operations that account for 50% of the total catchment area and may play a role in the hydrologic function of the catchment.

The second Glacier Ridge ravine (GRR) catchment is 2.03 km^2 in area with an estimated impervious cover of 5% (City of Calgary, 2023). GRR was selected to represent pre-development conditions for this study as it was largely undeveloped at the start of the project, with primarily agricultural land use consisting of actively farmed cropland, actively grazed pastureland, and non-grazed grasslands. The same gravel extraction operation occurring in the headwater portion of SHR also extends into the headwater portion of the GRR catchment and accounts for 29% of the total catchment area. GRR construction development began in 2021 on the lands east of the catchment and by the end of the 2025 field season construction extended well into the study area and had crossed to the northwest side of the stream. GRR is being developed similarly to SHR with a mix of residential, commercial and industrial land use.

Both catchments feature small streams that originate from the same topographic high to the southwest. The topographic high is characterized by pre-Pleistocene gravel deposits that are the target of gravel extraction operations and a potential source of groundwater recharge. The SHR and GRR streams generally flow from the southwest to the northeast, eventually contributing to West Nose Creek. Within the study area, SHR stream is 5,800 m in length and GRR stream is 3,000 m long. Both SHR and GRR have permanent and semi-permanent reaches fed by prominent groundwater discharge areas or springs. The geology in this area is comprised of surficial glacial tills of the Lochend Drift and Balzac Formations (Moran, 1986) that overlies bedrock of the Paskapoo Formation, which represents an important water bearing unit for the region (Barker et al., 2011).

2.1.1 Monitoring Equipment

Within the SHR and GRR catchments, streamflow gauging stations were installed at multiple locations along each stream and groundwater monitoring wells were installed near prominent groundwater discharge locations (**Figure 2**). Drilling and monitoring well installation at SHR was completed in fall 2020, and drilling and well installation at GRR was completed in summer 2021. Automated water level loggers were installed at, and water samples were collected from, all stream gauging and groundwater monitoring well locations. Tipping bucket rain gauges were installed in both catchments, and an eddy-covariance micrometeorological station was installed in SHR to measure water vapour fluxes (i.e., evapotranspiration and sublimation). Hydrologic data was collected largely during the ice-free months from April to October. Further details on the monitoring equipment is available in Johnson (2024).

Additional snow survey locations and runoff plots were installed in both SHR and GRR later in the study period (2023-2025) to better assess snow distribution and the role of midwinter and spring melts in contributing to runoff and infiltration in the riparian ravines.

2.1.2 Streamflow Analysis and Hydrograph Separation

Differential streamflow gauging was used to understand how streamflow varied along the streams and through the flow season. Flow duration curves for each gauging station were also evaluated to understand the variability in flow rates over the study period.

Two hydrograph separation techniques were used to analyze streamflow data at the event and seasonal scale. Graphical hydrograph separation using a modified straight-line technique was used to separate the quick flow (Q_f) portion of the hydrograph from the baseflow portion of streamflow (Q_b). Q_f is the portion of streamflow that responds rapidly to precipitation inputs, whereas Q_b is the slower baseflow portion that is gradually released from storage, with Q_b typically presumed to represent the groundwater contribution. The method was applied at the seasonal timescale. Two-component tracer-based hydrograph separation was used to characterize the surface and subsurface flow paths of streamflow generation for individual rainfall/runoff events. The method relies on measured streamflow tracer concentrations prior to and during rainfall events as well as tracer concentrations in the rainfall. For this study, tracer sampling included stable isotopes of water (^{18}O and ^{2}H) collected using autosamplers and electrical conductivity (EC) from dedicated loggers deployed at SHR-SW5 and GRR-SW4. EC was chosen as the tracer for this study due to the significant difference in pre-event and event values, and the ability to collect high-resolution data during events. EC-based hydrograph separations were tested against the more traditional isotopic tracer data for selected events and the results were consistent (Johnson, 2024).

2.2 West Nose Creek and Spy Hill Station

West Nose Creek (WNC) was utilized in this project because it is a largely rural prairie watershed that is close in proximity to the urban SHR catchment and peri-urban GRR catchment. WNC has long-term (>15 years) streamflow and groundwater dataset that served as a useful pre-development baseline comparison for results from SHR and GRR. The stream gauging station that defines the WNC catchment is located upstream from the confluences of the SHR and GRR streams, which both flow into WNC farther downstream (**Figure 1**). The area of the WNC catchment (244 km^2) is much larger than SHR and GRR, but shares similar geologic and climatic characteristics. Farmed cropland and grazed pasturelands are the primary land uses within the WNC catchment (Hayashi and Farrow, 2014).

The Spy Hill station is a hydrological observatory operated by the UofC that includes both surface and groundwater monitoring equipment. Although not situated in the WNC catchment, the data from the Spy Hill station has historically been used for meteorological monitoring of the WNC area. Monitoring equipment and data relevant to this study were precipitation data recorded with the tipping bucket rain gauge (SpH-TB in **Figure 2**) and a co-located all-weather precipitation gauge (Geonor) for monitoring rainfall and snowfall totals. Monitoring well data from the Spy Hill site also provide an indication of groundwater levels in the vicinity of the WNC, SHR, and GRR watersheds.

2.3 Okotoks Bioretention Facility

The OBF study site is located in the Town of Okotoks on the north side of the Sheep River adjacent to the town's wastewater treatment facility. The site is comprised of a “macroscale” bioretention system and connected vegetated bioswales, and a smaller research area that contains 24 engineered bioretention mesocosm cells (**Figure 3**). The design and installation of the macro- and

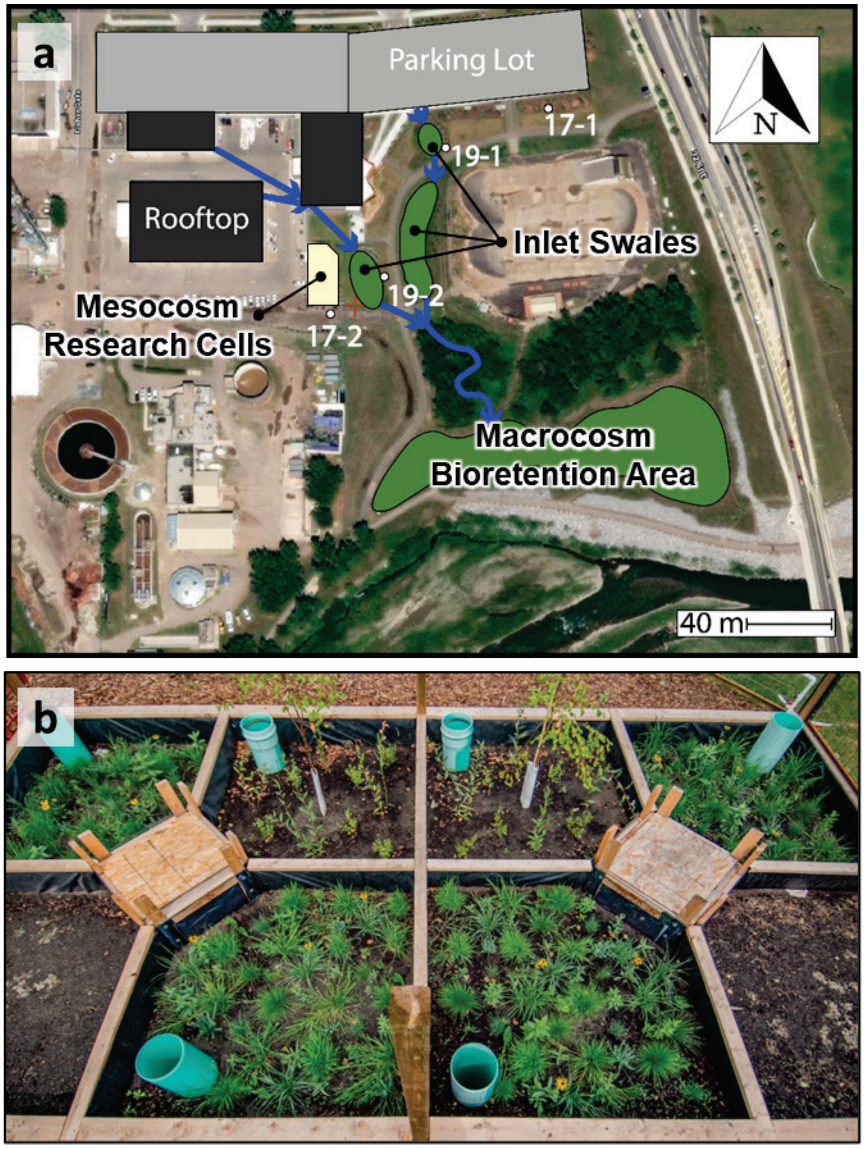

Figure 3. Okotoks Bioretention Facility (a) aerial view image of the full site, and (b) photograph of eight (of 24) mesocosm test cells in the research area. The top diagram (a) shows the location of the mesocosm research cells, and stormwater inlet swales that feed into the main macrocosm bioretention area. Dark and light grey shading represents the parking lot and rooftop sources of runoff, while blue arrows show the direction of stormwater flow through the system. The four monitoring wells shown as white dots were used to record the water table position beneath the adjacent swales (19-1, 19-2) and in background regions across the site (17-1, 17-2).

meso-scale systems was completed in 2016 as a collaboration between UofC and the Town of Okotoks. Research on the mesocosm test cells involved monitoring of hydrological performance (Task 1) and water quality performance (Task 3) that were initiated as part of the previously mentioned joint NSERC CRD project. The results of that research are highlighted briefly in this report for the sake of completeness, although they were not directly funded by Alberta Innovates. For this study, the OBF site was further leveraged to examine augmented groundwater recharge from bioretention swales (Task 1) as well as performance of the mesocosm bioretention cells under frozen ground conditions (Task 4).

2.3.1 OBF Mesocosm Cells

The bioretention mesocosm cells (Figure 3b) at the OBF site were originally used by Skorobogatov (2023) to observe the influence of design parameters on bioretention performance, and to understand how performance changed over multiple field seasons. The research performed by Skorobogatov (2023) was based on simulated rainfall events and water application was restricted to the summer months. This project builds upon the work by Skorobogatov (2023) by including water application to the bioretention cells during the winter and early spring periods when soils were entirely or partially frozen (Elliot, 2023).

The facility contains 24 lined bioretention cells that are approximately 1.8 m x 1.8 m x 1.2m (**Figure 4**). The cells were constructed with three different growing media, three types of vegetation, and two impervious to pervious (IP) ratios. The cells are organized into three groups of eight cells based on media type, with different combinations of vegetation and IP ratio throughout each group. There

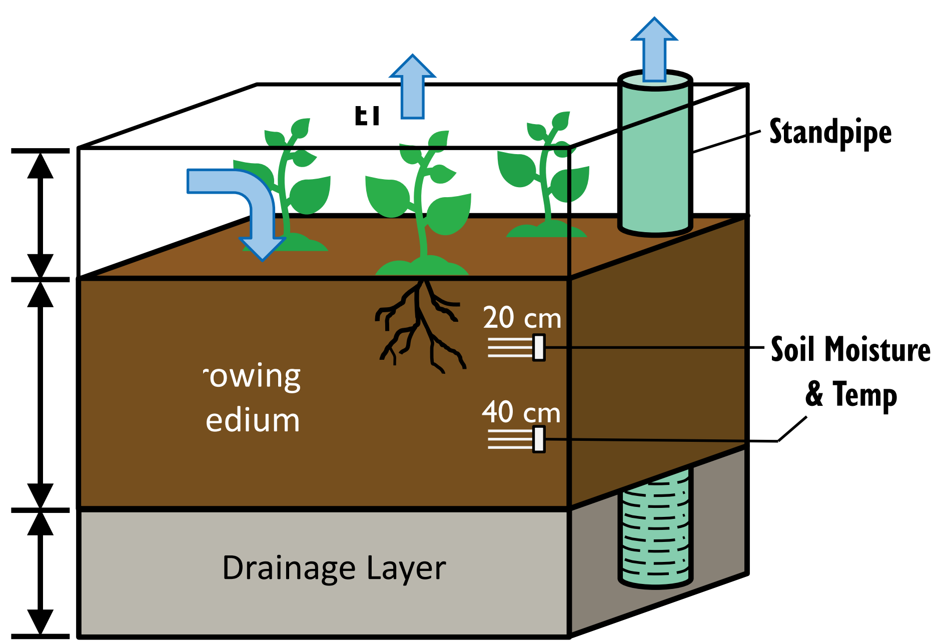

Figure 4. Schematic diagram of a bioretention test cell at the OBF used for artificial stormwater application. Blue arrows show the water budget components that were monitored, including water inflow, drainage outflow, and evapotranspiration (ET), as well as internal changes in soil moisture and soil temperature at two depths in the growing medium. The OBF site contains 24 total test cells consisting of three different growing media types.

were three types of growing media; two sandy loam materials, referred to as media 70 and media 40, and one clay loam referred to as CL. The sandy loam 40 and 70 media values refer to the targeted hydraulic conductivity in millimeters per hour (mm/hr), based on local LID guidelines. The CL media was an experimental mixture of clay loam and wood chips. Three types of vegetation were planted, including woody, herbaceous, and a grassy control. Each group of eight media-type cells contained four (4) herbaceous cells, two (2) woody cells, and two (2) control cells. Details of the species planted for each cell type are included in Skorobogatov (2023). The IP ratios tested were 15:1 (IP15) and 30:1 (IP30). Cells 1,2,6,7, and 8 in each group received a volume of water equivalent to 15:1, and cells 3,4,5 received twice as much water to be equivalent to a 30:1 IP ratio.

The facility is located outdoors, so the cells are fully exposed to the elements and freeze-thaw cycles throughout the year. Each cell was constructed with a 30cm thick drainage layer at the base, 60cm of growing medium, and 30cm of freeboard at the top to allow for ponding (**Figure 4**). A 30cm diameter perforated drainage standpipe was situated in the corner of each cell to allow water to be pumped from the drainage layer.

The summer-focused research of Skorobogatov (2023) involved monitoring of the hydrological and water quality performance of the 24 mesocosm bioretention cells between 2017 and 2020. A series of simulated rainfall/runoff events were conducted each growing season (May-October), with 20-25 events of different magnitudes each year from 2018 to 2020 (72 events total), with approximately 5 days between events. The volume of water applied to each cell was determined by the cell's designated IP ratio, surface area, and the size of the event. Simulated events included volumes equivalent to 4mm, 9mm, 14 mm, and 24mm precipitation events, and each magnitude was repeated at selected frequencies and intervals to imitate the magnitude and frequency of historical rainfall patterns in Calgary (Skorobogatov 2023). Simulated events involved applying water on all cells, allowing the water to infiltrate, and pumping out the drainage layer on the day of the water application, the following day, and the day prior to the next simulated event. As a complement to the water quality research on the mesocosm cells, eight (8) additional aboveground cells were constructed and monitored to investigate the effectiveness of six different soil media amendments for reducing phosphorous (P) leaching from bioretention systems (Task 3).

The winter-focused research of Elliot (2024) was similar in that hydrologic and water treatment performance of the 24 mesocosm cells were assessed, however, all simulated events were conducted under frozen ground conditions. Field activities consisted of three simulated melt events with tracer-infused water applied to all bioretention cells over two the 2021 and 2022 field seasons. In 2021, a single simulated event was completed on March 31 (S21 denotes Spring 2021) to mimic a single spring melt event. In 2022, two simulated events were carried out, including one midwinter melt on March 1 (M22 denotes Midwinter 2022), followed by a spring melt event on March 23, 2022 (S22 denotes Spring 2022). The 2022 events mimic the influence of midwinter melting and refreezing conditions that occur during chinooks that are common in southwestern Alberta. Fluorobenzoic acid (FBA) tracers were applied with the simulated meltwater to differentiate infiltrating water between events and from antecedent water. Each simulated event consisted of applying stormwater to the cell, then pumping and sampling the effluent water from the drainage layer after 3 hours, the following day (24 hr), and after 3 days (72 hr). The first effluent was sampled after 1 hr to assess early tracer breakthrough, but the cells were not pumped. Water samples after An event magnitude of 9 mm was chosen for the S21 and S22 events, and the water was applied over a period of approximately 10 to 20 minutes. This magnitude was selected to maximize the volume of water that could be applied without overtopping the cells if water did not rapidly infiltrate, and to remain consistent with event sizing during the summer experiments. The midwinter M22 event was smaller at 2 mm, typical of smaller midwinter melt and refreezing events in the Calgary area.

For all simulated events (summer and winter/spring), monitoring was conducted to evaluate hydrological and water quality performance. Infiltration rates at the surface of each cell were recorded as water was applied, and the volume of effluent pumped from the drainage standpipe was recorded. In-situ soil sensors were available at two depths (20 cm and 40 cm) within each cell (Figure 4) to record liquid soil moisture and soil temperature during and between infiltration events. The soil moisture data was used to assist with estimating antecedent soil moisture and water retention, while the soil temperature data was used to assess soil freeze-thaw condition. Water samples were collected from the drainage effluent and analyzed for nutrient parameters that included various forms of nitrogen (N) and phosphorous (P). For the purposes of this project, the reporting will focus on the chemical analysis data for Nitrate-N (NO3-N), total nitrogen (TN), reactive phosphorus (RP), and total phosphorus (TP).

In the winter events, a snow survey was completed prior to the M22 event (only event with significant snow cover) to quantify the amount of snow-water equivalent (SWE) on the cells prior to infiltration. In addition, the S22 events included water level transducers installed in the drainage standpipes to record exfiltration rates at higher temporal resolution (5 min intervals). Effluent water samples for all winter/spring events were analyzed for the FBA tracers. The three selected tracers were: pentafluorobenzoic acid (PFBA) for the S21 simulated event, 2,4,5-trifluorobenzoic acid (TFBA) for M22, and 2,6-difluorobenzoic acid (DFBA) for S22.

2.3.2 Inlet Bioswale Monitoring

Surface and groundwater monitoring focused on the OBF bioswale inlets was conducted to address gaps in understanding the function of these unlined systems in cold climates and as potential groundwater recharge sources. The OBF macrocosm bioretention system included a series of vegetated depressions or bioswales (Figure 3a). The design intent of the macro-scale system was to channel stormwater from the rooftop and parking lot catchments, through vegetated bioswales, and into a large, 2900 m^2 open bioretention area comprised of engineered absorbent landscaping fill material located south of a small stand of trees (Figure 3a). Following construction, preliminary field observations revealed that most stormwater infiltration occurred in the inlet swales (little stormwater reached the main southern bioretention area in 2018). As a result, the two northernmost bioswales, designated 19-1 and 19-2, became the focus of investigation. The swale at 19-1 receives stormwater input from the parking lots to the north, and the swale at 19-2 receives stormwater input from the rooftops of the buildings and surrounding pavement at the site.

The bioswales were constructed as an excavated depression lined with a 60 cm thick mixture of unscreened loam, hardwood mulch, and compost in a 60/30/10 ratio. The mulch and compost mixture were added to increase total organic content to support treatment of potential contaminants in the infiltrating waters. The engineered fill material overlays natural alluvial aquifer materials in proximity to the Sheep River, which consisted of coarse sands and gravels.

Monitoring of the bioswales included borehole drilling and monitoring well installation, groundwater levels and chemistry, meteorological data, bioswale runoff inflow and outflow, and soil moisture monitoring (Hall, 2021). Four boreholes were drilled across the site through the unconfined, alluvial aquifer materials and groundwater monitoring wells were constructed in each. Two wells (17-1 and 17-2) were situated to record background groundwater conditions at the site, while the other two wells (19-1 and19-2) were positioned adjacent to the bioswales to capture groundwater level fluctuations attributed to bioswale infiltration. All wells included pressure transducers to record groundwater levels at hourly intervals. Groundwater samples were collected every 2-4 weeks for analysis of total nitrogen and total phosphorous.

To characterize flows through the bioswales, V-notch weirs were installed at the inlet and outlet of each swale. Pressure transducers were used to record water levels behind each weir at 5-min intervals. In association, meteorological data (barometric pressure, air temperature, relative humidity, precipitation, wind speed, and incident solar radiation) were recorded at an on-site meteorological station to characterize both precipitation and evapotranspiration (Hall, 2021). Vertically-nested soil moisture sensors were installed in each bioswale (from 20-100 cm) to monitor changes in soil moisture storage.

Groundwater recharge estimates beneath the bioswales were estimated using two independent methods: a water budget technique and a groundwater mounding technique. Recharge was estimated using the following water budget equation:

$$R = P + Q_{in} - Q_{out} - \Delta S - ET \quad (1)$$

where R is recharge [L^3/T], P is direct precipitation onto the swale [L^3/T], Q_{in} and Q_{out} are stormwater flow into and out of the swale [L^3/T], ΔS is the change in the total volume of stored water within the swale including soil moisture [L^3/T], and ET is the evapotranspirative loss from the system [L^3/T]. Recharge estimates using the groundwater mounding technique relied on the application of the Hantush (1967) analytical solution, which was fitted to groundwater level observations from the monitoring wells (Hall, 2021). Necessary aquifer parameters were estimated for specific yield (S_y) using laboratory drainage tests and for saturated hydraulic conductivity (K_s) using pumping test data from wells 19-1 and 19-2.

2.4 Highland Park and Cambrians Heights Rain Gardens

The hydrologic performance and water budget was studied for two community rain gardens in northcentral Calgary, denoted as the Highland Park (HP) and Cambrian Heights (CH) sites (Figure 1). Both rain gardens were constructed between July and November 2021, with a larger garden installed next to the Highland Park community centre, and a smaller garden installed next to the Cambrian Heights community centre. The HP rain garden has an internal footprint of 152 m^2 (Figure 5b) and IP ratio of approximately 3.1:1. The smaller CH rain garden has an internal footprint of 5.3 m^2 (Figure 5a)and a greater IP ratio of approximately 6.2:1. Both rain gardens were constructed by removing native surficial soil and replacing it with screened loam, which will be referred to as growing media. The growing media thickness was 45 cm at HP and 30 cm at CH. Berms were built up around the perimeter of both gardens to allow for 15-20 cm of ponded water to accumulate. In September 2021, each garden was planted with native herbaceous perennials, with HP also including 12 small woody plants (willow shrubs). Rain garden vegetation gradually

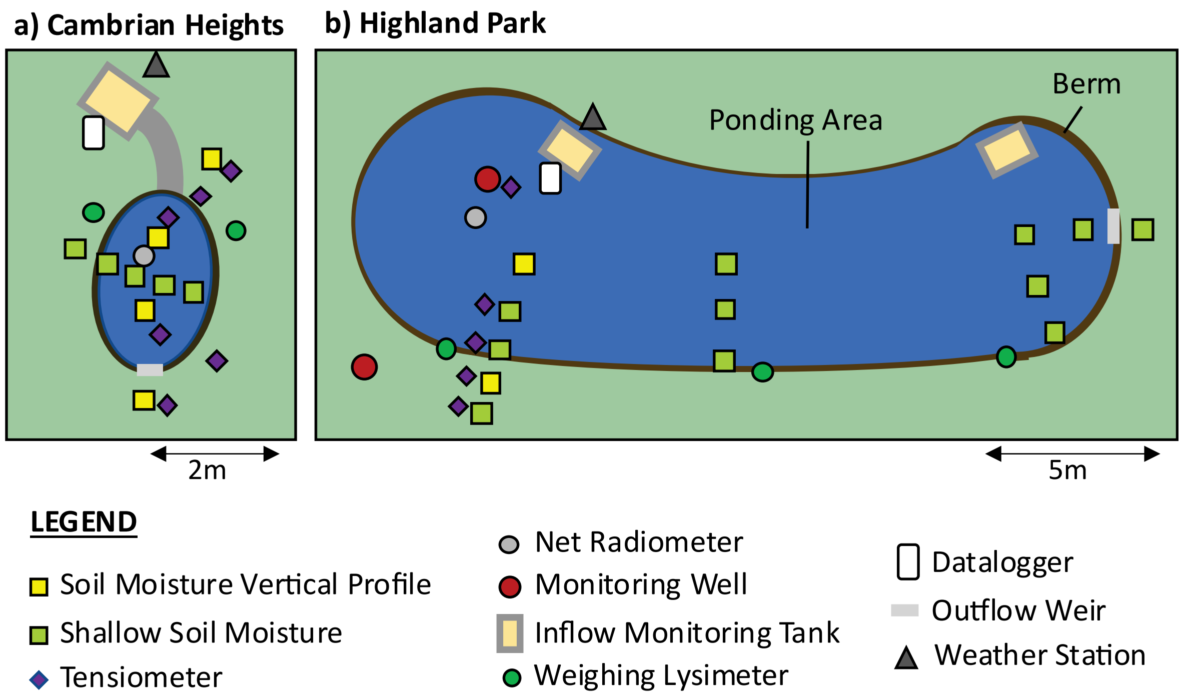

Figure 5. Schematic diagram (not to scale) of monitoring instrumentation installed at rain garden facilities in (a) Cambrian Heights, and (b) Highland Park.

became established over the first two field seasons and was nearly fully established by the 2023 season (Figure 6).

2.4.1 Monitoring Equipment

During and after construction, hydrological monitoring instrumentation was installed in and around each of the rain gardens (**Figure 5**) to evaluate water movement and storage and to evaluate relevant water budget components for each garden. Hydrological monitoring included precipitation (tipping bucket rain gauge), rainwater inflow and outflow (inflow monitoring tanks and outflow weirs), ponded water levels (pressure transducers), soil moisture and temperature (soil moisture sensors), soil water potential (tensiometers), evapotranspiration (weighing lysimeters), meteorological data for evapotranspiration estimation (weather stations and net radiometers), and groundwater levels at HP (monitoring wells). All monitoring equipment was recorded and logged automatically, with the exception of the shallow soil moisture sensors and the weighing lysimeters that required manual monitoring. Further details on the monitoring equipment installed at both rain gardens is available in Ilg (2025).

2.4.2 Simulated Events

Monitoring of natural precipitation events was conducted in all field seasons following rain garden construction, however, it was hampered in some instances when rainfall was less frequent. For example, the 2023 field season experienced extended drought conditions. To augment the natural

Figure 6. Photographs of rain garden sites showing instrumentation and evolution of vegetative cover. Cambrian Heights rain garden in (a) September 2021 during the construction phase, (b) August 2022 after one full growing season, and (c) June 2023 showing established vegetation. Highland Park rain garden in (d) October 2021 during the construction phase, (e) June 2022 after a large rain event in the first full growing season, and (f) June 2023 after near complete establishment of the native plants.

precipitation, simulated rainfall events were conducted at both sites in 2023 and 2024 by applying known volumes of water from the municipal supply (CH) or from a water supply truck (HP). These simulated events offered an opportunity to evaluate how the rain gardens responded to larger precipitation events that are typically infrequent (e.g., once every 5 to 10 years). Simulated events were generally spaced 48 hours apart to further enable comparisons of the rain garden performance under both "dry" and "wet" antecedent soil moisture conditions. The simulated events were designed to replicate a 1 hour, 25 mm rainfall, attempting to replicate the relatively large and short-lasting convective storms typical for the region (Taylor et al., 2011). Events of this magnitude and duration would have a return period of approximately 5 to 10 years based on intensity-duration-frequency (IDF) data for Calgary (Shephard et al., 2014). An additional larger event was conducted at each site in August 2024, with ~30 m^3 (48 mm) of water applied over 1.5 hr at HP, and 3.5 m^3 (91 mm) of water applied over 1.5 hr at CH. These larger events replicated precipitation events with a return frequency of 100 years or greater based on the same IDF curves, attempting to evaluate garden performance in storms well beyond their designed capacity. Since the timing of simulated events was controlled, manual readings (e.g., shallow) could be planned and taken more frequently than was typical of natural events.

2.4.3 Water Budget and Subsurface Flow Analysis

Ilg (2025) undertook analysis to quantify water budget components and characterize subsurface flow processes for both sites using detailed data from the 2023 and 2024 field seasons. The water budget technique was employed to estimate seepage below the rain gardens on both seasonal and event scales. A similar water approach to that used at the OBF bioswales, except that water volumes were normalized to the internal garden footprint area and thus represent a depth of water. The rain garden water budget was defined as follows:

$$P + Q_{in} - ET - Q_{out} - S = \Delta S_{SM} + \Delta S_{SW} \tag{2}$$

where P is direct precipitation onto the garden (mm), Q_{in} is roof runoff into the garden (mm), ET is evapotranspiration (mm), Q_{out} is the surface outflow from the garden (mm), S is seepage (mm), ΔS_{SM} is the change in water volume stored as soil moisture in the garden growing media (mm), and ΔS_{SW} is the change in the total volume of surface ponded water (mm). For this study, seepage (S) is defined as water that flowed out of the garden growing media and into underlying native soil, and it was calculated as a water budget residual value since the remaining variables in the equation were measured or estimated as part of the field monitoring.

Seasonal water budgets were constructed for the growing season from mid-May to mid-October. The specific start and end dates varied by year depending on when equipment was deployed at the start or removed at the end to protect select sensors from freezing (e.g., tensiometers, inflow tank water levels). Water budgets were also calculated at the scale of individual rainfall events. For this study, an event was defined as a period with greater than 2 mm of precipitation, occurring after more than 12 hours from any previously recorded precipitation. An event was considered to have ended when precipitation ceased. To estimate soil moisture changes for event-based water budgets, a combination of soil moisture readings from automated (HydraProbe) and manual (TDR - Time domain reflectometry) sensors installed in the growing media was employed to maximize spatial and temporal coverage.

To assess vertical and lateral flows subsurface flows away from the rain gardens, monitoring well and tensiometer (measures soil water matric potential) data were utilized. The water table fluctuation (WTF) method (Healy and Cook, 2002) was employed to estimate groundwater recharge to the water table at HP. The method requires measurement of water table fluctuations, recorded with pressure transducers in the monitoring wells, and an estimate of the specific yield (Sy) of native sediments, which was estimated using soil moisture data from the native soils below the rain garden. The extent of lateral flows were evaluated using transects of tensiometers at multiple depths that extended from inside the rain garden to several meters outside the garden (Figure 5b). Similarly, the volumes and fate of lateral water flow were estimated using soil moisture data.

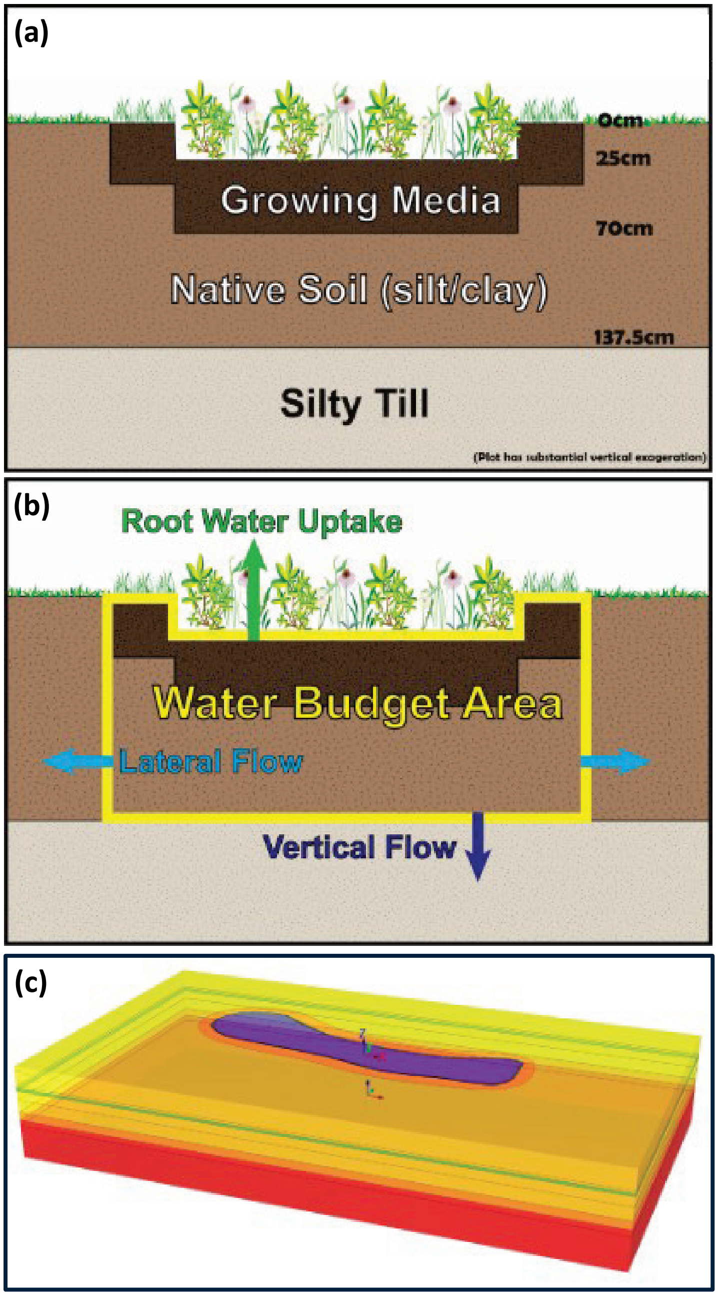

Figure 7. Conceptual approach and model domain for 3D flow simulations of the HP rain garden, showing (a) schematic model geological cross-section, (b) subsurface control volume with relevant water budget components, and (c) isometric view of 3D model domain showing soil moisture conditions during a rainfall event. All images not to scale.

2.4.4 LID Numerical Simulations

To better support evaluations of LID performance and the influence of LID design parameters, numerical simulations of water flow were completed using the variably saturated flow model Hydrus-3D. Two main types of flow simulation were completed and both utilized the HP rain garden as the conceptual basis for simulations and the HP monitoring data was used for model calibration and verification. First, preliminary 2-dimensional (2D) numerical simulations were completed to assess vertical and lateral flow potential beneath a rain garden under varying antecedent moisture conditions, subsurface hydraulic conductivity (Ks), and precipitation events (Merrett, 2023).

The 2D simulations formed the basis for subsequent, more detailed 3D simulations that were based on the geological conditions at the HP rain garden and calibrated against field monitoring data (Figure 7). Sensitivity analyses were conducted to examine the influence of rain garden design parameters and subsurface hydraulic properties (growing media and native sediments) on flow dynamics. Specifically, subsurface water fluxes and water budget contributions were quantified to better assess water flow and storage conditions beneath and adjacent to the garden.

The field data and simulations were also used to support complementary modeling and hydrological tool development being conducted by project partners (City of Calgary). The results were incorporated into PCSWMM models to refine LID modules for application in City of Calgary LID design and implementation guidance (City of Calgary, 2013 and 2016).

3.0 Results

The research results from different sites and from different facets of the project often contribute to more than one key objective or project task. Hence, the results will be presented here grouped by site, with identification of how they contribute to different tasks where applicable. For the sake of brevity, results will focus on the most important findings and point to other sources for readers seeking more complete details.

3.1 Sage Hill and Glacier Ridge Paired Watersheds

The hydrograph data from SHR (developed) and GRR (undeveloped/developing) were compared at both seasonal and event scales, to ascertain the influence of urban development on flow conditions. Data from the WNC watershed was also included where available and appropriate, as a comparison to a largely rural, undeveloped watershed. Seasonal hydrographs of total stream flow (Q_s) for the farthest downstream monitoring stations in SHR and GRR during the ice-free period (April to October) of 2022 are presented in Figure 8. Overall, the seasonal flow regime of the SHR stream was distinct from that of GRR and WNC. This trend is highlighted by the relatively small increase in flows for SHR in June compared to GRR and WNC, and by the lack of a corresponding recession limb in July and August. In essence, streamflow response between events, known as baseflow (Q_b), is much flatter for SHR than it is for either GRR or WNC. The streamflow response to precipitation events also appears to be less prominent in SHR compared to GRR and WNC (Task 2).

SHR streamflow also appeared to have an anomalously large flow that started August 30 and extended into early September (Figure 8). The increase in flow does not correspond with any associated precipitation and was attributed to a confirmed release of water from an upgradient

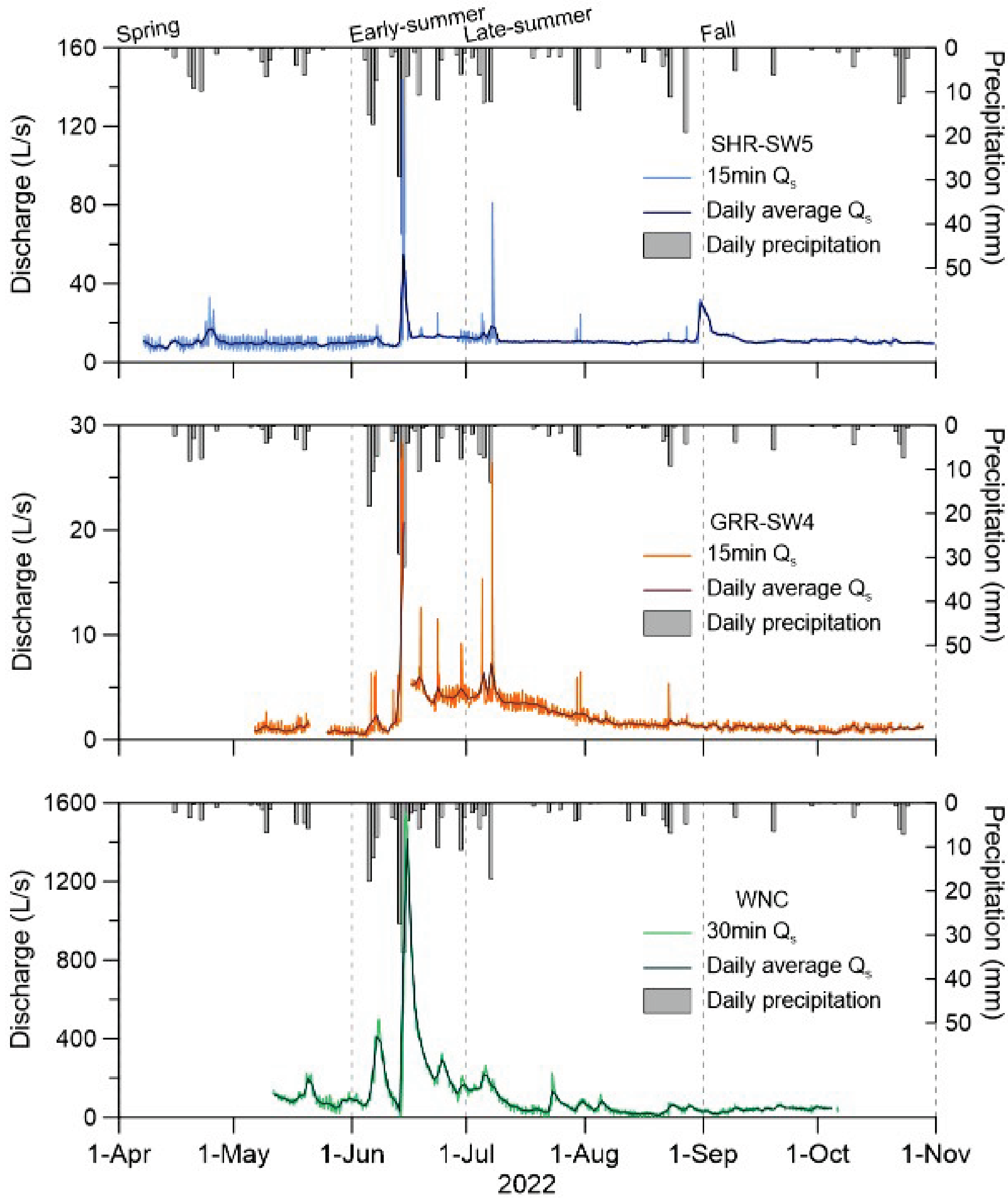

Figure 8. Hydrograph and daily precipitation for SHR-SW5, GRR-SW4, and WNC in 2022. Daily precipitation was recorded for each individual catchment at SHR-TB, GRR-TB, and SpH-TB. Spring is defined by the months of April-May, Early-summer is June, Late-summer is July-August, and Fall is September-October. Precipitation data starts on April 7, due to instrument deployment timing.

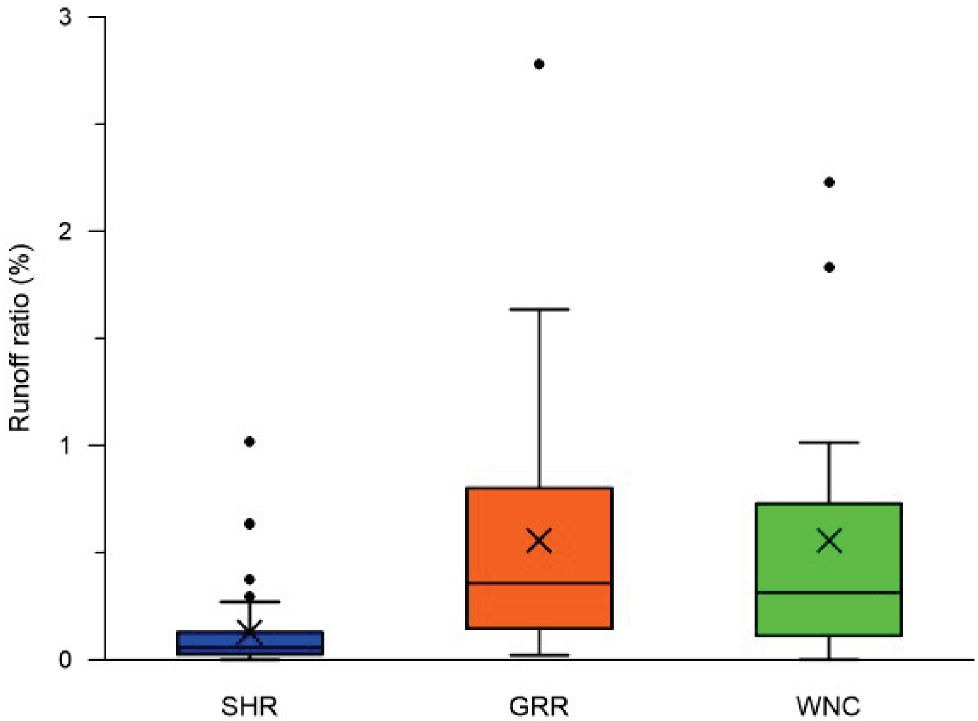

Figure 9. Comparison of runoff ratios from SHR-SW5, GRR-SW4, and WNC for 2022. Each runoff ratio was calculated using the contributing area to the stream gauging station used in this analysis.

stormwater pond operated by the City of Calgary. The data suggest clear differences in streamflow response between the developed (SHR) and undeveloped/developing (GRR/WNC) at both event and seasonal scales (Task 2).

During rainfall events, hydrographs were graphically separated into quick flow, Q_f, and baseflow, Q_b, components, and runoff ratios were calculated as quick flow divided by the total precipitation input. The runoff ratios calculated for individual stormflow events from all three catchments in 2022 is shown in Figure 9. Overall, the runoff ratios in all catchments were small (< 3%), again with distinct differences between the developed and undeveloped locations. Runoff ratios were smaller than most values reported in the literature, and indicate the majority of precipitation in the catchments does not contribute to Q_f, likely due to the capture of precipitation by low relief, undulating terrain and subsequent loss to evapotranspiration (van der Kamp and Hayashi, 2009; Ehsanzadeh et al., 2016).

Despite the low overall runoff ratios, the more urbanized SHR catchment demonstrated considerably lower runoff ratios than GRR and WNC as well as a smaller interquartile range (Figure 9). The data collectively indicate that GRR and WNC have similar capabilities of transforming precipitation into runoff, which was expected given the similar land use characteristics for these two catchments in 2022. The size difference between the GRR and WNC watersheds played a secondary role. What was surprising was the much lower runoff ratios for the SHR catchment, which was counter to expectation since urban development is normally assumed to increase Q_f due to increased impervious landcover. Less runoff production within SHR catchment may be due to a proportionally smaller effective drainage area compared to GRR and WNC (Ehsanzadeh et al., 2012). Based on satellite data, approximately 93% of the SHR-SW5 drainage area represents land uses that are drained by some sort of stormwater management system, including roadways, industrial operations (e.g., landfill, gravel extraction), and other residential or commercial properties. These stormwater management systems capture or re-route the majority of stormwater away from the headwater stream. Therefore, the difference in runoff response in SHR relative to GRR and WNC is attributed urban development and alteration by stormwater management systems that reduce the effective drainage area (Task 2).

Additional tracer-based hydrograph separation results (not shown; see Johnson, 2024) confirmed the graphical hydrograph separation results, and indicated that the GRR catchment contributed event water (i.e., precipitation sourced) at a rate more than three times greater than the SHR catchment for precipitation events of equivalent magnitude. Further, the isotopic data showed that pre-event water, which is normally presumed to represent groundwater, represented the majority of streamflow even during peaks in streamflow. This suggests that both SHR and GRR catchments are controlled largely by groundwater contributions to the streamflow, even during runoff events, and the more developed SHR catchment had a comparatively greater groundwater contributions than GRR (Task 2).

Groundwater monitoring data also suggest important differences in the seasonal baseflow response between watersheds. To explore the relationship between streamflow and groundwater, baseflow contributions to streamflow (Q_b) were separated from the total streamflow (Q_s) for SHR-SW5 and GRR-SW4 and then compared to local groundwater fluctuations (Figure 10). On a daily average basis, groundwater baseflow constituted 95% of the total flow volume at SHR-SW5 and 86% of the total flow volume at GRR-SW4 (Figure 10a). Groundwater is clearly an important streamflow component in both watersheds (Task 2).

Figure 10 compares baseflow trends to relative groundwater levels near prominent groundwater discharge areas within the catchments. An arbitrary datum is used to reference the relative groundwater levels for comparison purposes. All groundwater levels demonstrate a seasonal fluctuation. SHR-MW2A, SHR-MW2B, and GRR-MW3 have sharp responses to precipitation throughout the season due to higher local K_s values, whereas GRR-MW1 is completed in a lower conductivity unit causing water levels to respond more slowly (Figure 10b). Stream baseflow in GRR followed a similar trend to groundwater levels, with peaks occurring in June and July and then declining levels from August to November (Figure 10a). In contrast, streamflow and groundwater trends did not appear to correlate as well in the SHR catchment, as groundwater followed similar seasonal fluctuations to that seen in the GRR catchment, yet stream baseflow remained relatively constant. More detailed analysis of SW-GW connectivity (data not shown; see Johnson, 2024) revealed that streamflow in SHR may actually be driving groundwater levels locally during events. This implies that streamflow in the SHR is being temporarily stored in groundwater during stormflow events (termed bank storage) due to the conductive gravel deposits adjacent to the stream. It appears geologic heterogeneity is influencing the streamflow regimes in the catchments, in addition to development status (Task 2).

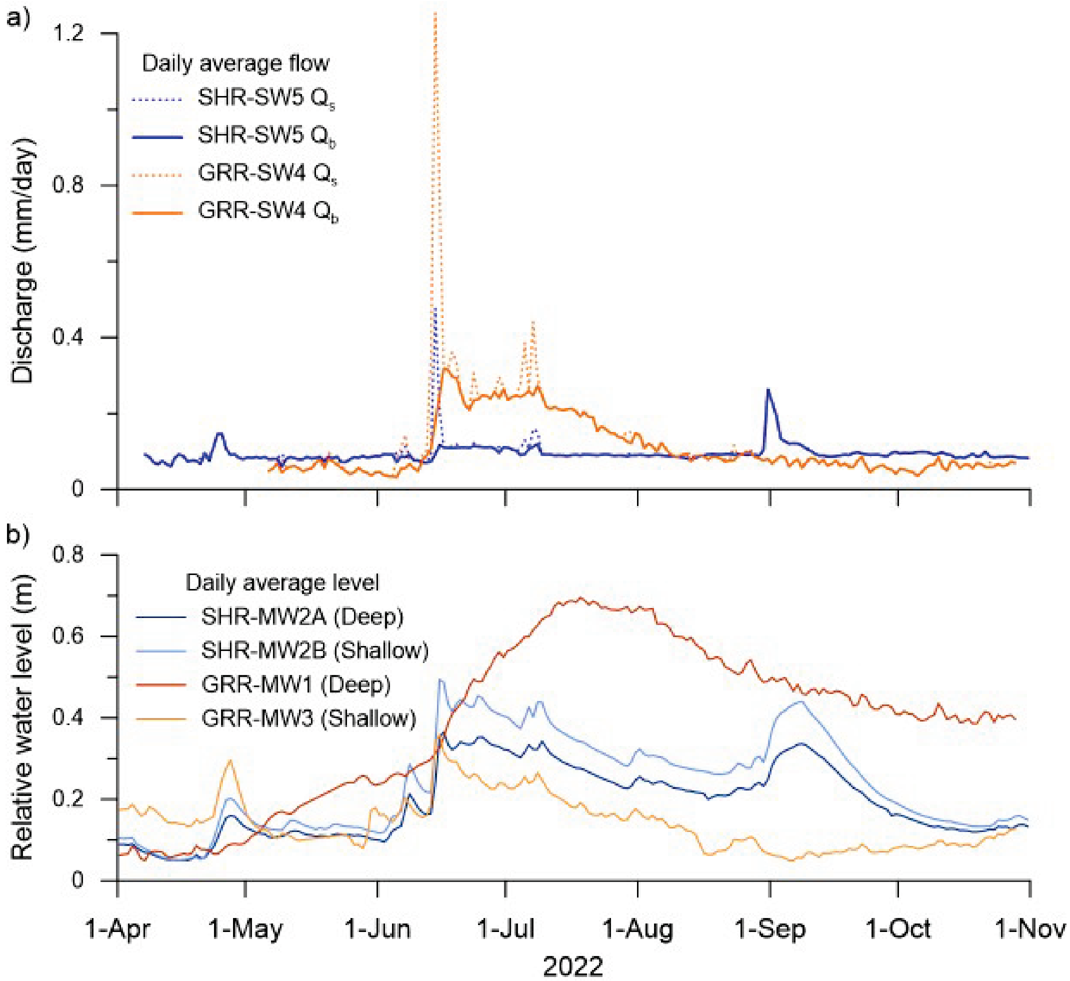

Figure 10. Comparison of daily average stream discharge (Q_s) to daily average groundwater level fluctuations. a) Daily average baseflow (Q_b) (solid lines) separated from the daily average streamflow (Q_s) (dotted lines) for SHR and GRR in 2022. b) Daily average local groundwater levels from shallow wells (light colors) in the glacial overburden and deep wells (dark colors) completed at the overburden-bedrock interface. Groundwater levels are reported relative to an arbitrary datum to compare relative fluctuations.

Patterns of spatial and temporal variability in flow along the streams further exemplified the differences between catchments (Figure 11). Stream discharge in SHR varied considerably along the length of the stream, indicating important gains and losses of flow that are attributed to the SW-GW interactions. Significant gains in streamflow in the SHR-SW1 to SHR-SW2 reach and the SHR-SW4 to SHR-SW5 reach were coincident with major groundwater springs and local tributaries, which most likely contributed to the gains. The streamflow losses between SHR-SW2 and SHR-SW4 are primarily attributed to the infiltration of water into hydraulically conductive sediments beneath or adjacent to the stream channel and ET losses from the stream surface or riparian vegetation. The observed losses are consistent with the literature, showing the influence of connections to high K_s gravels observed in SHR and the semi-arid climate (McMahon and Nathan, 2021; Winter, 2007). Despite the significant spatial variability, the SHR flows at each gauging station remained relatively consistent throughout the season, maintaining the spatial pattern throughout the year. The temporal consistency of SHR flows does not appear to be directly linked groundwater fluctuations, suggesting the groundwater springs contributing to flow may be

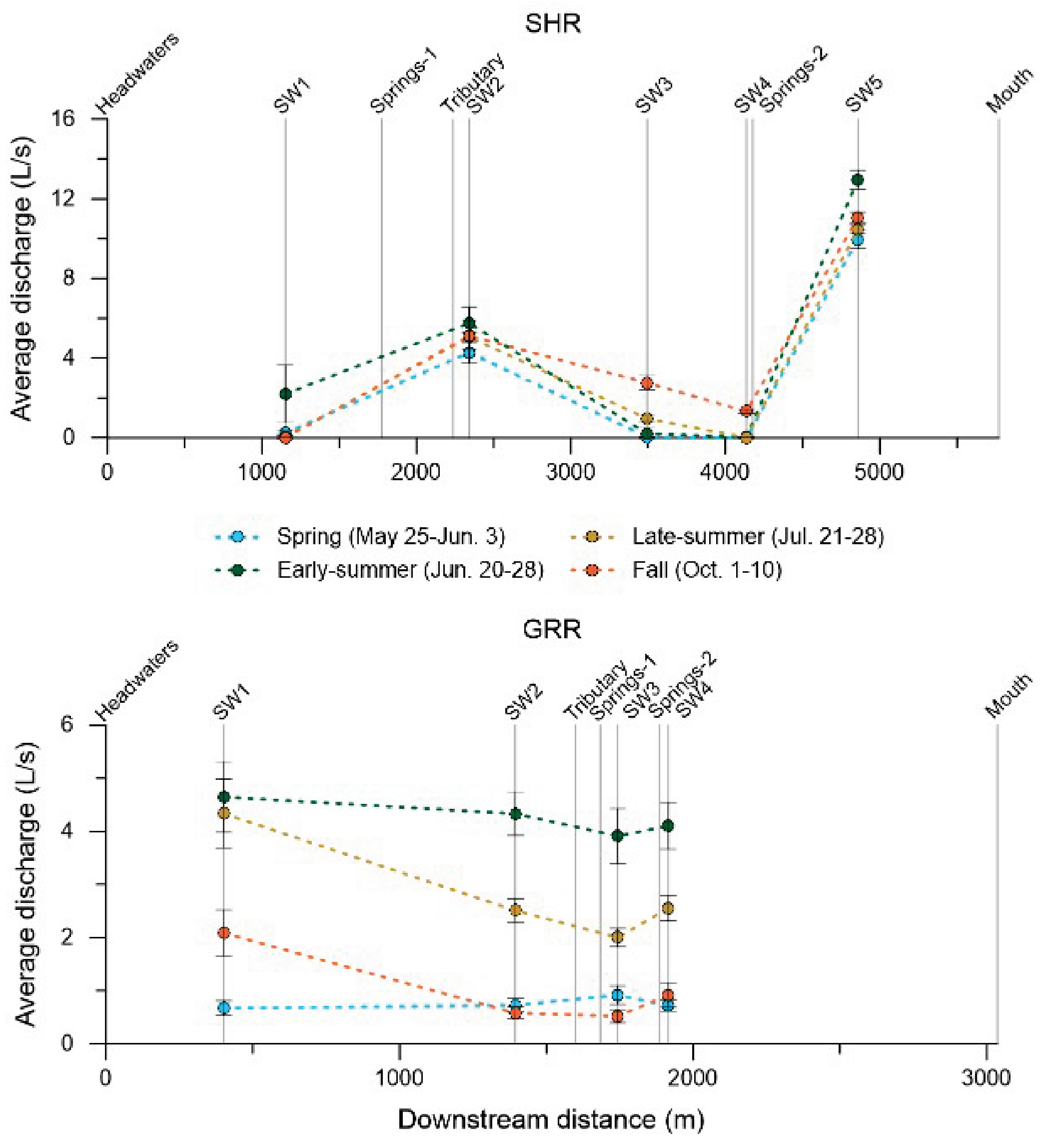

Figure 11. Differential gauging plot for SHR and GRR in 2022. Each data point is the mean of the daily flows for a 9–11-day period representative of the Spring, Early-summer, Late-summer, and Fall phases of the flow season. The dotted lines are straight line interpretations of the gaining and losing fluxes and represent the net change in streamflow for a given reach. The exact locations of the gaining and losing fluxes require higher resolution streamflow measurements. Error bars are the standard deviation of the daily average flows used to calculate the mean for that given period.

recharged farther afield or an influence of stormwater detention ponds. Further high-resolution monitoring is necessary to fully understand the streamflow dynamics.

Unlike SHR, the GRR catchment demonstrated considerable temporal variability throughout the flow season, with relatively consistent flows between gauging stations indicating much less spatial variability (Figure 11). The original source of streamflow in GRR is not well understood because flow emanates from private property that was not accessible during this study. For much of the year, except for the spring season, reach between GRR-SW1 and GRR-SW3 generally shows net losses throughout the flow season. Even the relatively smalls gains between GRR-SW3 and GRR-SW3 are modest and could reflect uncertainty in the data. The geologic conditions along the measured reaches of the GRR stream are comprised mainly of low hydraulic conductivity till that likely limits infiltration into the streambed, making evapotranspiration the primary transmission loss process. Streamflow at all four GRR gauging stations followed the same temporal trend, which was consistent with the rise and fall of groundwater reported above: low flows in the Spring, followed by seasonal high flows in Early-summer, followed by a decrease in flows through Late-summer and Fall (Figure 10 and Figure 11). Differential gauging in GRR suggests that transmission loss is less prominent between gauging stations and that low conductivity substrate promotes temporal variation of streamflow over spatial variation (Task 2).

3.2 OBF Mesocosm Cells

The OBF mesocosm research was intended to evaluate both the hydrologic and water treatment performance of bioretention systems and the associate impacts of design parameters (notably media type, vegetation, and IP ratio). The following subsections will separate the results into growing season hydrologic performance (Task 1), growing season water quality performance (Task 3), and the influence of winter season frozen ground conditions on overall performance (Task 4).

3.2.1 Hydrologic Performance - Growing Season

Hydrologic performance of bioretention systems was evaluated in terms of infiltration dynamics as well as water retention capability, which is central to the function of these types of LID systems. Over the study period, irrespective of the mesocosm types, there was substantial variability in the infiltration rates over time as shown in Figure 12. The mean infiltration rate values were about an order of magnitude higher than the anticipated 40 to 70 mm/hr values (City of Calgary, 2016) suggested by local LID guidelines. Moreover, there was an increasing trend across the years, where the mean infiltration was 286 mm/hr for the first event and 875 mm/hr for the last (Figure 12a). The OBF mesocosms cells were exposed to variable environmental conditions, including variable wetting, drying, and freeze-thaw cycles, and contained differing vegetation types. Both factors have been shown to enhance infiltration capacity over time. The increasing trend over multiple years has important design implications, as it contradicts the conventionally expected decline in infiltration rates over time that can result from media clogging at the surface (Task1).

Figure 12b also shows that there was considerable variability in the infiltration rates based on the magnitude of simulated events. There was considerable difference in the range of infiltration rates for different event magnitudes with 4 mm events having the greatest range and highest values measured. Median infiltration rates were equal to 510, 420, 384, and 390 mm/hr for 4, 9, 14, and 24 mm simulated event magnitudes, respectively (Figure 12b). With freely available water and unsaturated soils, infiltration rates will gradually decline over time and eventually reach a quasi-

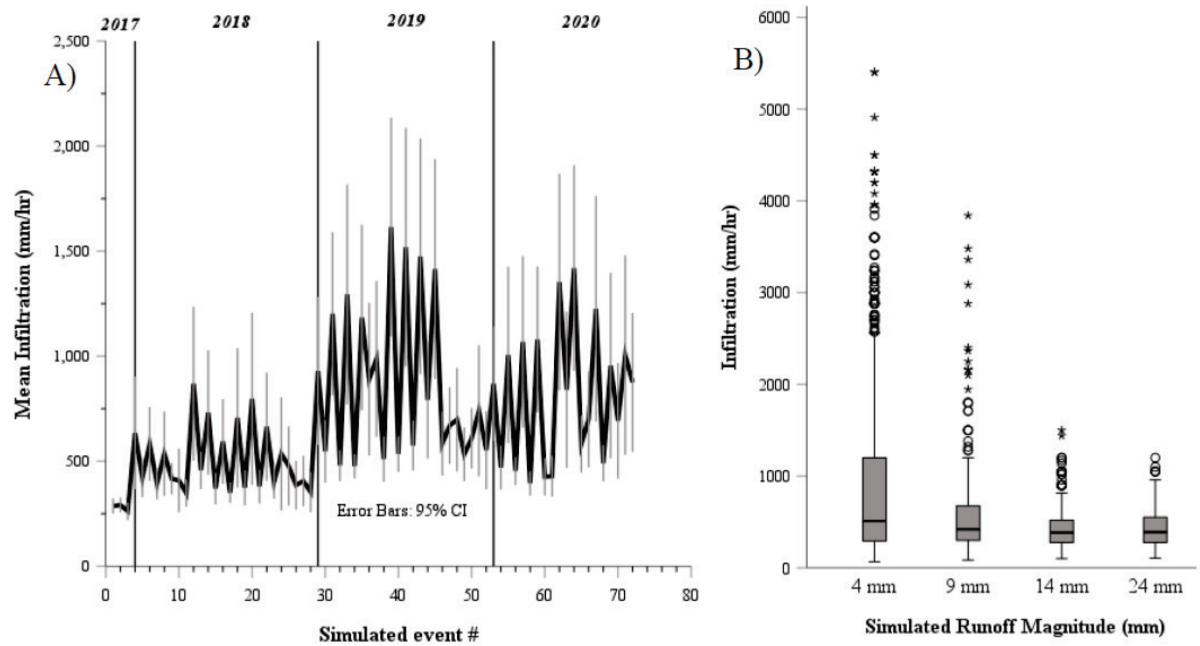

Figure 12. Infiltration performance showing (a) temporal evolution of infiltration capacity over time (the simulated event number), solid black line indicating the mean infiltration across 24 mesocosms, bars representing 95% confidence intervals (CI); and (b) The relationship between infiltration and simulated event magnitude, whiskers representing the 95% confidence interval (CI), empty circles are for potential outliers outside the 1.5-times inter-quartile range (1.5xIQR), and stars represent extreme outliers outside 3-times the inter-quartile range (3xIQR).

steady state condition. Infiltration for smaller simulated events likely never reached the quasi-steady state conditions, leading to the higher infiltration rates and greater variability observed for these events (Task 2).

All design parameters (i.e., growing media type, vegetation, and IP ratio) had an influence on infiltration performance, but there were complex interrelations between design parameters and over time. To gain a better understanding of the impacts of design parameters on infiltration rate, the temporal variability of infiltration rates specific to the design parameters are shown in Figure 13. The data again reveals the generally increasing infiltration rates over time (with the simulated event number), with distinct differences in these trends based on LID design. More specifically, there was a consistent difference in the slopes of regression lines associated with the different IP ratios, namely, mesocosms of the IP ratio of 15 had a greater positive slope than those of the IP ratio of 30, suggesting that the mesocosms with the higher IP ratio of 30 were subject to a lesser increase in infiltration rate over time. Differences in growing media were statistically significant ($p<0.01$), with media 70 (287 mm/hr) having the lowest mean infiltration rate, followed by media 40 (479 mm/hr) and CL media (1086 mm/hr). Notably the sand-based media (40 and 70) had significantly lower infiltration rates than the clay-loam based CL media, which contradicts the conventional notion of using textural classification as the main design parameter controlling infiltration capacity. The increased infiltration in CL media is attributed to the development of structural pores in the clay-based media, which has been shown to result in preferential flow and more rapid infiltration (see more in Section 3.2.3). Infiltration was also significantly impacted by

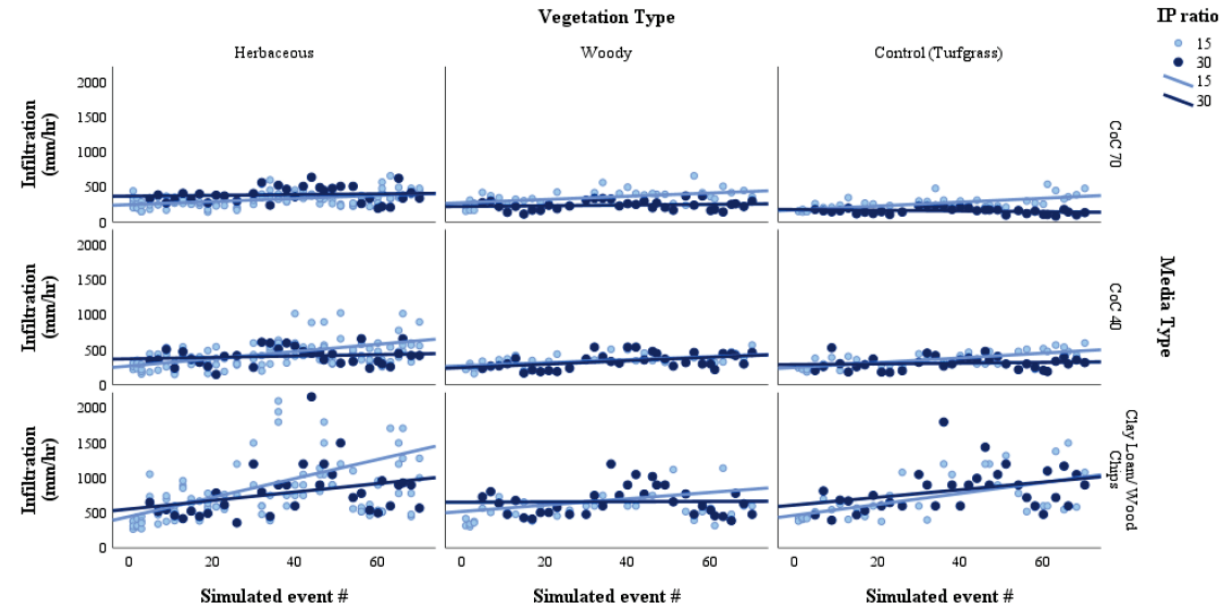

Figure 13. Temporal variation (along with the simulated event number) of the infiltration rates across design parameters. The solid lines are the linear regression lines.

vegetation type, with herbaceous vegetation having significantly greater infiltration rates than the woody or turfgrass control mesocosms. Mean infiltration rates were 886, 529, and 509 mm/hr for herbaceous, woody, and control vegetation mesocosms, respectively. This finding underscores the importance of vegetation selection for bioretention systems and positive impact on infiltration performance, yet it appears to deviate from the current state of research that shows woody media generally having the largest infiltration impact followed by herbaceous plants (Técher and Berthier, 2023) (Task 1).

In contrast to the infiltration results, water retention performance gradually decreased in importance over the entire study period and the significance of media type declined dramatically in later years (data not shown; Skorobogatov, 2023). Mean percent water retention (PWR) was 16.1%, which was lower than typical water retention reported for bioretention systems in the literature that vary from 19% to 86% (Davis, 2008; Hathaway et al., 2014; Hatt et al., 2009; Hunt et al., 2006; Li et al., 2009). The findings point out the physical limitations to runoff capture and water retention associated with media storage. In addition, seasonality was observed as generally less exfiltrate was collected in the middle of summer compared to the beginning and end of growing seasons (data not shown; Skorobogatov, 2023). The relative importance of seasonality increased over time as vegetation became more mature. Peaks in water retention occurred around mid-August, which corresponds well with the notion of higher average ET being observed during the warm summer months (Task 1).

Figure 14 shows the variations in PWR and volumetric water retention (VWR) by all 24 mesocosms among the different event magnitudes and IP ratios. Over the study period, there were 36 events of 4 mm, 13 events of 9 mm, 15 events of 14 mm, and 8 events of 24 mm magnitude applied to the mesocosms. Mean PWR values were 14.8, 18.3, 18.8, and 13.2% for simulated events of 4, 9, 14, and 24 mm magnitudes, respectively. The consistency of PWR across event size in this study runs

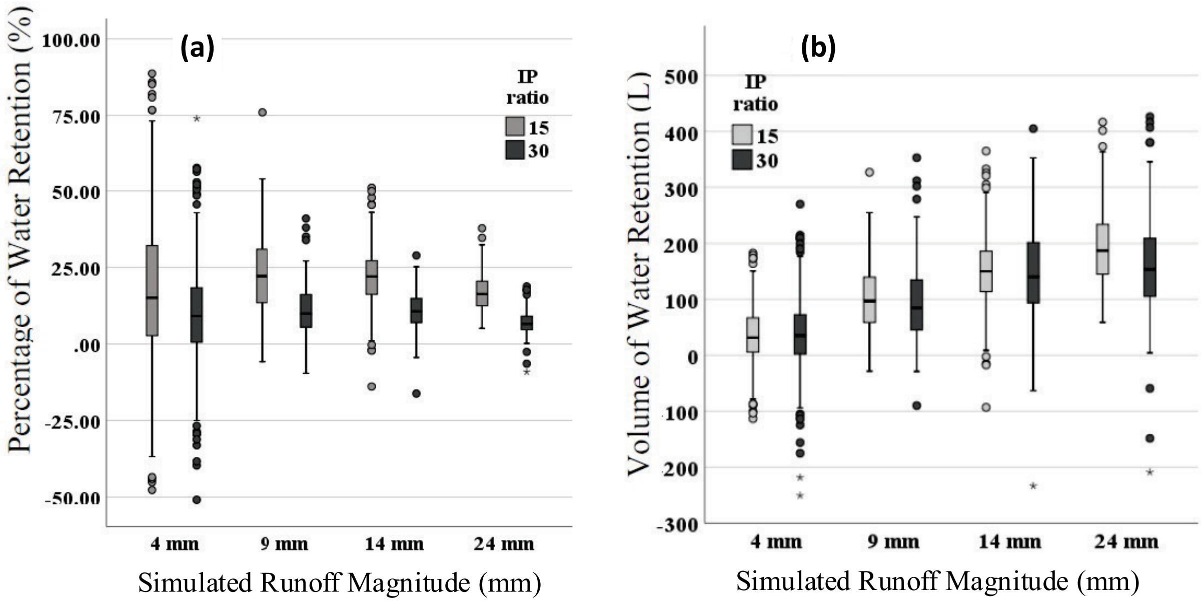

Figure 14. Relationship between simulated event magnitude and water retention expressed as (a) percentage water retention, and (b) volume of water retention. Circles are outliers at 1.5 interquartile range (IQR), and stars are outliers at 3.0 IQR.

counter to other studies (Davis, 2008) that have indicated greater PWR when bioretention systems are exposed to smaller events. The impact of event size is more apparent in the VWR results, which appeared to increase with increasing event magnitude with the mean VWR values of 37, 100, 151, and 184 L across the 4, 9, 14, and 24 mm events, respectively (Figure 14b). Care must be taken when interpreting the impact of the runoff event magnitude as its effect can be confounded by the antecedent, vegetation, and temporal conditions (e.g., antecedent soil moisture, seasonality, vegetation maturity) associated with different events. The relationship between VWR and antecedent growing media moisture condition in 2019 exemplifies this point (Figure 15). Of note is that the negative VWR corresponded with a negative value for the antecedent media storage. There was a linear relationship between the antecedent media storage and VWR, but it had a relatively moderate R^2 (0.26), likely due to the complexity of interactions described above (Task 1).

Overall, the results have demonstrated the importance of plant-media interactions in controlling hydraulic behaviour of the bioretention systems as a result of time-varying environmental exposure and plant root-induced changes. Similarly, evaluation of ET as a water removal mechanism confirmed the impact of media-vegetation interactions on ET (data not shown; Skorobogatov, 2023). Although the effect of design variables (i.e., vegetation and media types) on ET is not as significant as that of climatic variables, there was a significant difference in ET (particularly in the surface layer) among the different growing media, with the greatest ET from woody mesocosms. The effects of the design variables, especially vegetation, became more prominent over time. These findings suggest the need for optimizing bioretention systems with consideration to the role of these design variables in bioretention performance (Task 1).

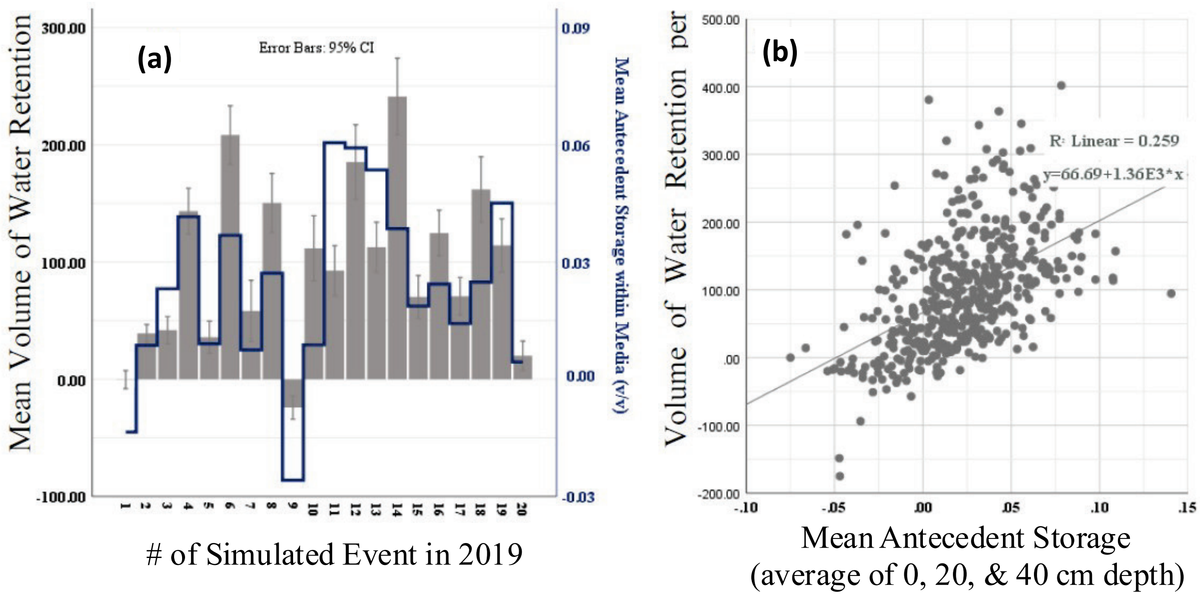

Figure 15. Relationship between volume retained per event and antecedent media storage; (a) mean of 24 mesocosms per simulated event, and (b) per simulated event per mesocosm.

3.2.2 Water Quality Performance - Growing Season

Bioretention systems are designed to improve the water quality of stormwater runoff, yet this multi-year analysis showed significant leaching of dissolved nutrients when using conventional bioretention media. Rather than pollutant removal, growing media type had a significant impact on effluent concentrations, with considerable leaching of both N and P (Figure 16). The sand-based media (40 and 70) had the highest reactive phosphorous (RP) and nitrate (NO3) concentrations in the source media, leading to effluent concentrations that significantly exceeded the concentrations in the influent source water. Further, the relative ratio of effluent concentration to either influent (applied) concentrations or media extract concentrations, suggests that the degree of leaching was greatest for sand-based media. The degree of leaching for P was greater than for N, which may be attributed to biogeochemical reactions (e.g., denitrification) in the soil profile. In addition, P leaching was persistent across the years while extractable P contents within the media were within the typical targets for bioretention systems. The consequences of these findings are considerable since effluent leaching of nutrients can have a major impact on groundwater and downstream surface water bodies. It is critical that bioretention system designs are properly amended to mitigate leaching and potential downstream impacts. The more unique clay-based and organic rich CL media had much better water quality performance relative to sand-based media, providing an avenue for further exploration to assess the potential benefits and risk in relation to nutrient leaching (Task 3).

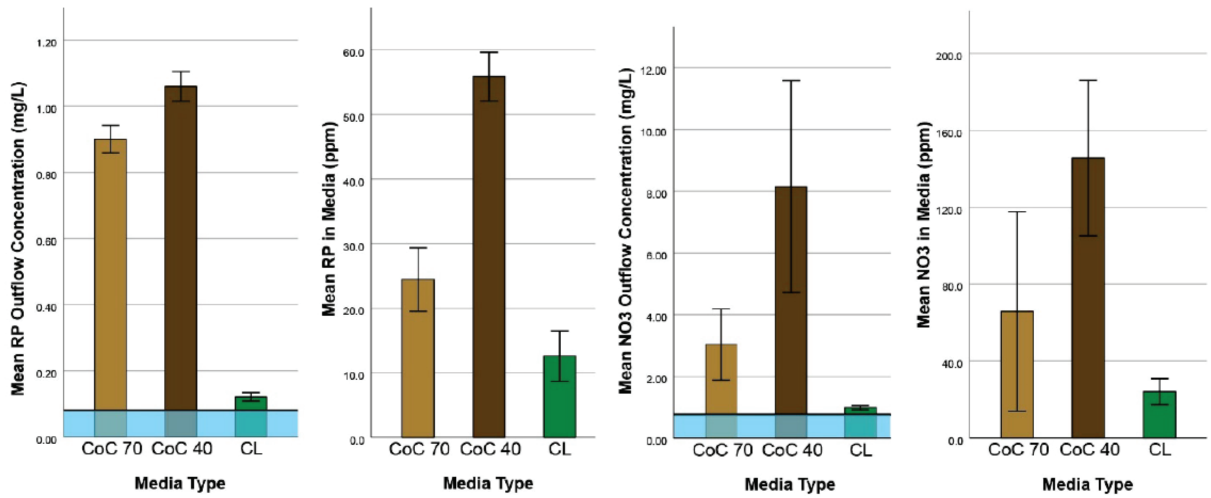

Figure 16. Mean nutrient concentrations in simulated runoff effluent and corresponding extractable media nutrient content for each media type. Reactive phosphorous (RP) and nitrate-N (NO3) nutrient components are shown. Influent nutrient concentrations are shown as the blue baseline on the effluent graphs.

Hydrologic loading had little effect on P leaching, meaning that greater runoff volume to the mesocosms did not cause a significant decrease in concentration. This could translate to a greater potential downstream threat with conventional bioretention systems in the face of increased intensity and magnitude of storm events under a changing climate. On the other hand, a dilution effect was observed with the increased hydrologic loading for the leaching of N, thereby somewhat reducing risks from storm events with larger magnitudes.

Leaching of N (Figure 17) and organics (not shown) had a statistically significant decreasing trend over time, particularly in the early years of study. Differences in nitrate-N effluent concentration between the CL and media 40/media 70 was dramatic with the sand-based media having initial effluent concentrations two orders of magnitude greater than those of the CL media, followed by a gradual move toward more similar values among the three media types in later events (Figure 17). The effects of media, vegetation, and IP ratio were all statistically significant based on linear mixed method (LMM) analysis. Statistically, the nitrate-N effect coefficient of media 40 was 2.7-times higher than that of media 70, which is consistent with the data shown in Figure 16. Among the vegetation types, woody vegetation was found to correspond to the lowest effluent concentrations based on the effect coefficient, whereas nitrate-N effluent concentrations were significantly higher for the IP ratio of 15 than for the IP ratio of 30. The effect of IP ratio points to a limited source scenario in which more water volume would yield a lower effluent concentration (i.e., diluting effect). Substantial variability and significant changes over time were observed for the different mesocosms, which underscores the need for long-term performance data on these nature-based systems. Given that initial leaching may be unavoidable in LID bioretention systems, targeted management strategies are required to support future implementation to ensure any receiving water bodies are protected from the impacts of the initial nutrient flush (Task 1).

To examine the efficiency of soil amendments for reducing phosphorus (P) leaching, testing was conducted on above-ground bioretention cells as reported by Zhang et al. (2023). Briefly, testing consisted of six amended and two control cells that were constructed and monitored in the 2020

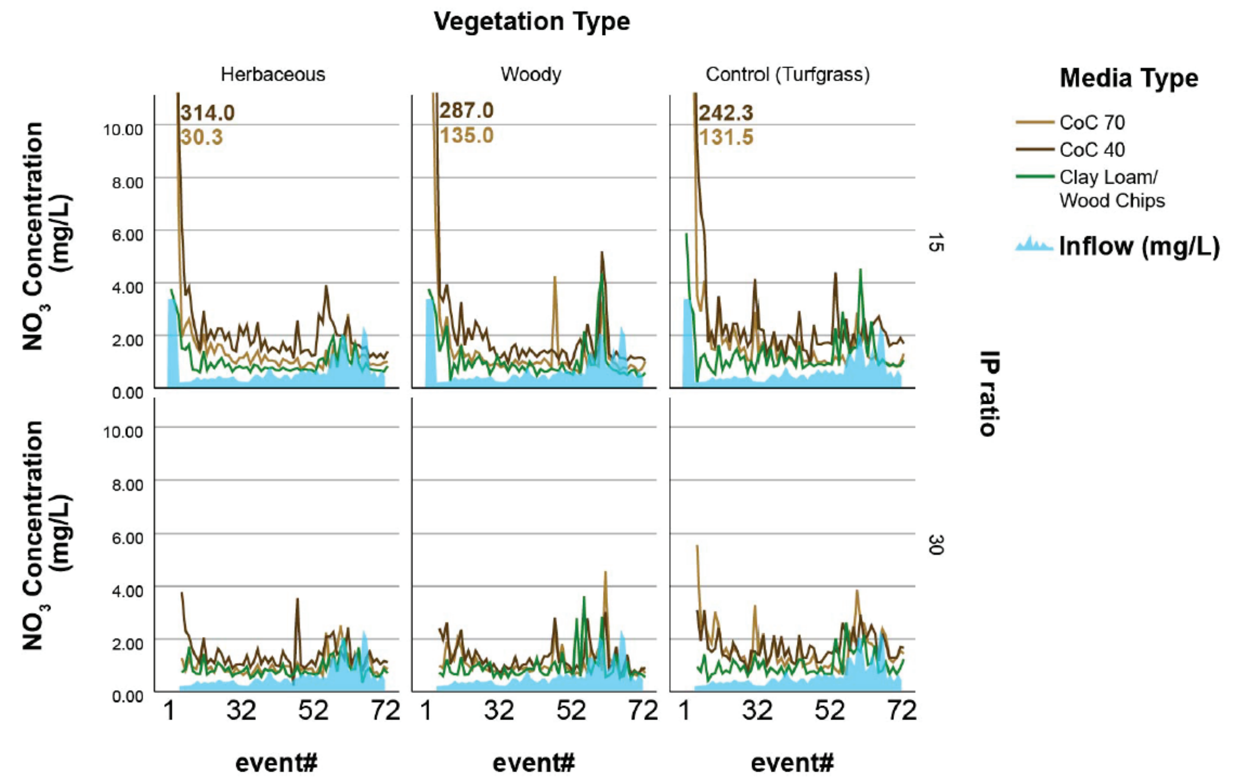

Figure 17. Nitrate-N leaching across the simulated events and design factors. Numbers in top-left of the plots indicates the peak nitrate-N concentration recorded if values are off scale.

and 2021 growing seasons. Media 40 was used as it released the most P, and amendments consisted of two iron-based (SM and PF), two aluminum-based (WTR, AA), and two sodium-based (EGG, DRY) products. Results showed that all amendments had the capability of preventing or mitigating P leaching from bioretention systems to varying degrees, with the water treatment residual (WTR) outperforming all other amendments, followed by the activated aluminum (AA) and sorptiveMEDIA (SM) amendments (not shown; see Zhang et al., 2023). In addition, some amendments (i.e., drywall (DRY), WTR, and SM) were also found to be beneficial in reducing the N leaching to a slight degree, whereas eggshell (EGG) introduced an extra source of N leached. There was no obvious influence of amendments on water retention performance, although there were differences in vegetation and antecedent soil moisture in some amendment cells relative to control cells, which might imply an influence on hydrologic behaviour (Task 3).

3.2.3 Winter Season Performance

Infiltration rates from the winter 2021/2022 simulated events under frozen ground conditions are show in Figure 18 alongside the summer 2021 events when the ground was completely thawed. While there were slight variations in infiltration rates between the S21, M22, and S22 events, the differences were not statistically significant ($p=0.86$, K-W). Media type had a significant influence on infiltration under frozen conditions, where CL cells had the highest average infiltration rate of 233 mm/hr, media 40 was lower at 108 mm/hr, and media 70 cells had the lowest rate of 58 mm/hr. The influence of media type was similar to that observed under summer conditions, however, infiltration rates were significantly lower under frozen conditions with an average reduction of ~80% ($p<1.7\times10^{-10}$) compared to unfrozen infiltration rates (Task 4).

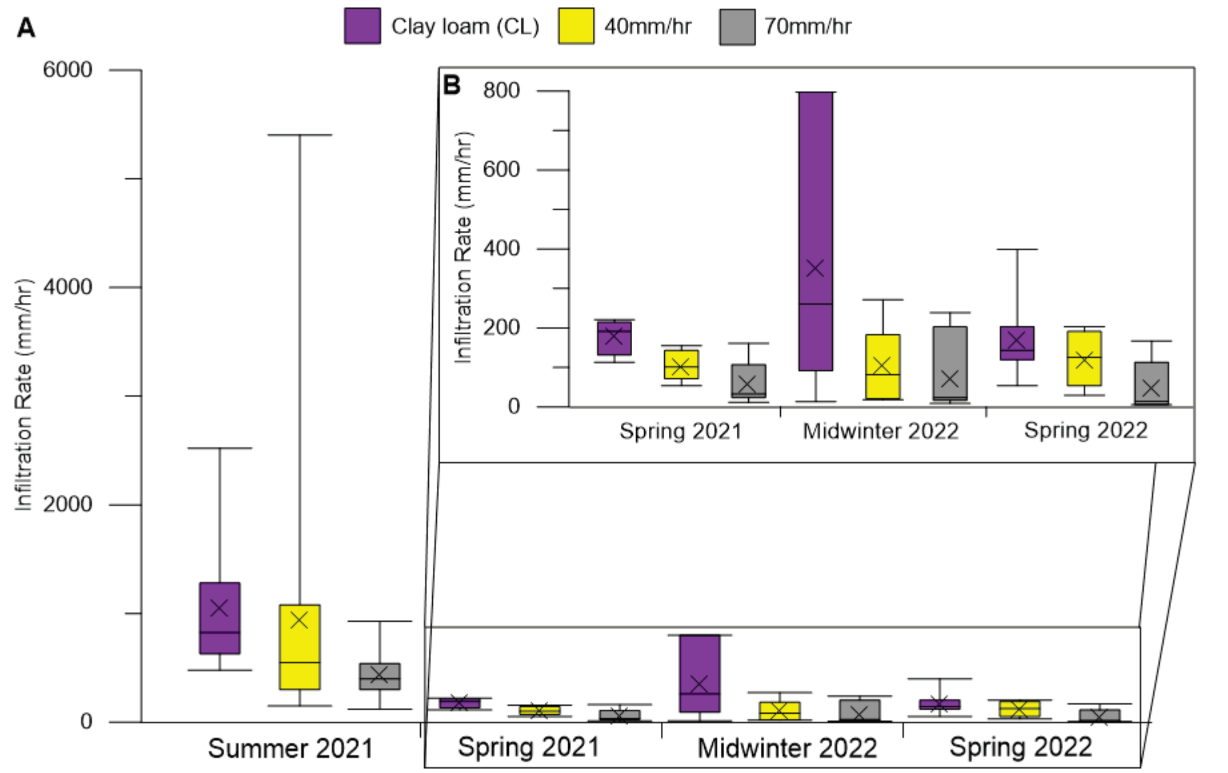

Figure 18. (A) Bioretention cell infiltration rates for simulated frozen and unfrozen events based on media type. (B) Magnification of infiltration rates under frozen conditions. Colored boxes represent the lower and upper quartiles, with the centre line denoting the median, and x denoting the mean. Whiskers represent the extreme values.

The reduction in infiltration rate during the frozen events, compared to unfrozen, varied considerably based on the bioretention design parameters, with IP ratio having the largest influence. The IP 15 cells had an average reduction in infiltration rate of 89%, whereas the IP 30 cells had a 65% reduction ($p=6.1\times10^{-5}$). As a result, IP 30 cells ended up having higher infiltration rates than IP 15 cells under frozen conditions, which is opposite to the trend under frozen conditions (data not shown; Elliot 2023). These findings are believed to be the result of macropore flow dominating the flow systems, which is discussed in more detail below. In terms of media type, CL cells saw the smallest infiltration rate reduction (74%) relative to unfrozen conditions on average, followed by media 40 (80%), and media 70 was the most affected (85%) ($p=0.036$). There was no statistically significant influence of vegetation type on infiltration rate reductions under frozen conditions. IP ratio had the largest influence of all construction parameters (Task 4).

The influence of frozen ground conditions on percent water retention (PWR) was relatively small in comparison to the above-noted infiltration influence. PWR was comparable under frozen and unfrozen conditions, with mean PWR under frozen conditions of 20% slightly lower than the mean unfrozen value of 25% ($p=0.046$). PWR during spring melt did not change significantly between the S21 and S22 events, despite the inclusion of the midwinter melt M22 event and subsequent refreezing (Figure 19). Under frozen conditions, PWR was largely governed by media type (Figure 19). For the S21 simulated event, CL cells (12%) had the lowest mean PWR under frozen conditions, media 40 (17%) was slightly higher, and media 70 (23%) was the highest, however,

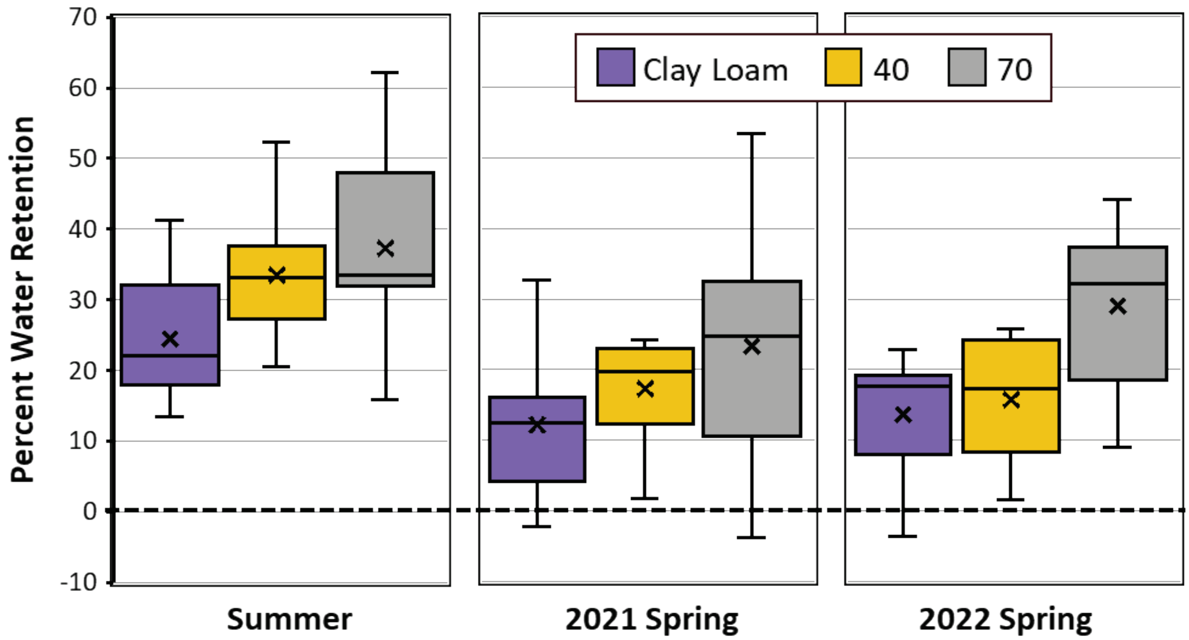

Figure 19. Percent water retention for unfrozen (Average of Summer events) and frozen (Spring 2021 -S21 and Spring 2022 - S22) simulated events based on media type. The box represents the lower and upper quartiles, with the centre line denoting the median, and x denoting the mean. Whiskers represent the extreme values.

these differences were not significant (p=0.18). There were statistically significant differences in the S22 event (Figure 19), with PWR values for media 70 cells (mean=33%) significantly higher than both CL (15%) and media 40 (17%) cells (p=0.041). Vegetation and IP ratio had very little effect on PWR, however, this inherently means that the IP30 cells retained more water than the IP15 cells in terms of total water volume (Task 4).

Preferential flow was the key driver of hydrologic performance in the bioretention cells. Further analysis using chemical tracers and physical methods (data not shown; Elliot, 2023) demonstrated that hydrologic performance under frozen conditions (and likely unfrozen conditions) was strongly influenced by preferential flow through the growing media. On average, preferential flow was estimated to represent between 49 to 70% of total effluent discharge from the cells. The degree of preferential flow was controlled by media type based on two key factors: (1) clay content high enough to support macropores, and (2) organic matter content that breaks up the soil aggregates. The methods of estimating preferential flow all concluded that CL had the greatest preferential flow potential, media 40 had the second highest, and media 70 had the lowest. While the CL and 40 media both clearly facilitated high amounts preferential flow, the 70 media displayed more matrix flow characteristics, which explains the higher water retention performance. Preferential flow reduces interaction with the soil matrix, leading the CL and 40 media to be largely unaffected by antecedence moisture prior to media freeze and refreeze of infiltrating midwinter melt water. These results are consistent with the conceptual model of snowmelt infiltration in frozen soils put forward by Mohammed et al. (2018), where air-filled macropores create conduits for preferential flow. As a consequence, finer-grained soils (like CL) often have greater potential for rapid infiltration under frozen conditions than coarser-grained, sandy soils (like 40 and 70 media).

Water quality performance under frozen conditions was highly variable, with the differences primarily dependent on media type and vegetation. Most bioretention cells were leaching RP, TP, and nitrate-N in the spring melt events, and removing total nitrogen (TN) from the applied water with variations caused by media type (not shown) and vegetation (Figure 20). P concentrations in

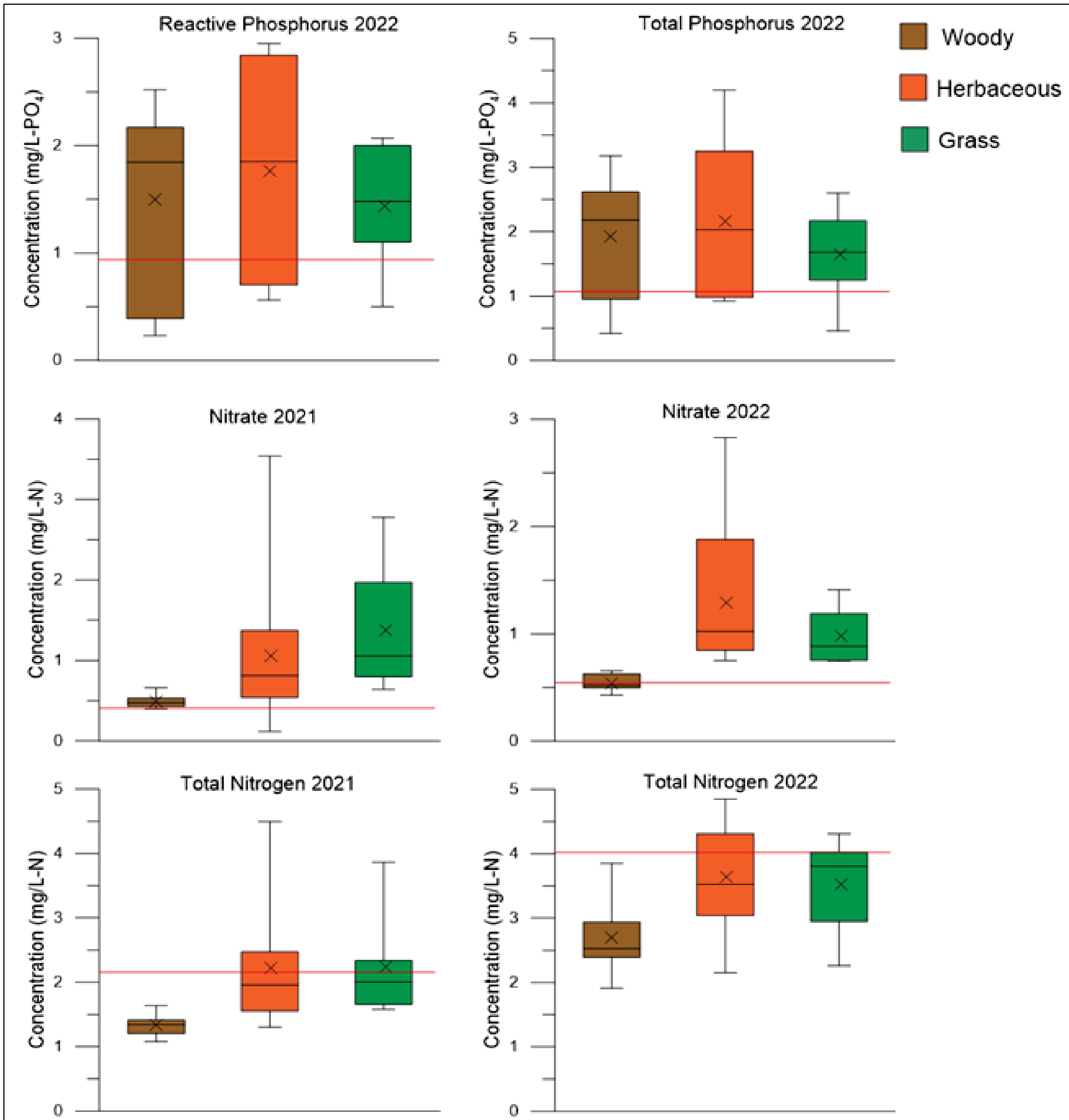

Figure 20. Nutrient concentrations from cell outflows from the Spring 2021 and Spring 2022 frozen simulated events based on vegetation type. The red lines indicate inflow concentrations. The box represents the lower and upper quartiles, with the centre line denoting the median, and x denoting the mean. Whiskers represent the extreme values.

effluent were largely controlled by media type (data not shown; Elliot 2023), where CL consistently had the lowest P concentrations, with occasional reductions relative to applied meltwater, and media 70 typically had the highest concentrations. While vegetation had limited influence on effluent RP and TP concentrations, it was the main driver in nitrate-N and TN concentrations (Figure 20). Woody vegetation had significantly lower nitrate-N and TN concentrations in effluent relative to cells with herbaceous and grassy vegetation, and there were no significant differences in concentration between the herbaceous and grassy cells. IP ratio also had no significant impacts on effluent nutrient concentrations (Tasks 3 and 4).

While there were no major differences in effluent nutrient concentrations between frozen and unfrozen events, the presence of preferential flow appeared to influence water quality. These influences were mixed as preferential flow caused bypassing of the soil matrix and thereby limited leaching of nutrients from the growing media. However, preferential flow also likely limited nutrient removal processes, such as microbial uptake and conversion, plant uptake, sorption, and filtration. Phosphorus concentrations were slightly elevated in the inflows and outflows during the spring melt events relative to unfrozen events, and outflow concentrations were largely dependent on media type, lacking the influence of vegetation seen in the unfrozen simulated events. Nitrogen concentrations in the effluent were similar under frozen and unfrozen conditions, despite higher inflow concentrations during the frozen events. Nitrate concentrations in effluent were dependent on vegetation type (Figure 20) and similarly lacked the influence of media noted in the unfrozen events. The differences in performance between summer and winter conditions may be influenced by the lack of vegetation and the relative decrease in microbial processes and chemical transformations under frozen conditions (Tasks 3 and 4).

3.3 OBF Inlet Bioswales

Through use of pairs of strategically placed monitoring wells at the OBF site, the localized groundwater mounding signal beneath vegetated bioswales 19-1 and 19-2 was isolated and used to monitor GW-SW interactions between the surface swale and the water table year-round. Groundwater recharge was estimated using the analytical solution of Hantush (1967) fitted to groundwater mounding data, as well as a water budget calculation applied to the bioswales. Figure 21 shows the estimated recharge volumes beneath the two bioswales using both methods, normalized by the surface of area of the contributing catchment. For comparison, the black 1:1 line shown in Figure 21 represents a simple calculation of the total runoff volume from the contributing areas (e.g., parking lots, rooftops) for a given precipitation event, using an appropriate runoff coefficient for impervious surfaces and assuming all runoff water became groundwater recharge. Recharge estimated using the groundwater mounding equation was greater than the calculated 1:1 runoff volume for each event in almost every case, and on average was three times greater than the 1:1 volumes. In contrast, water budget estimates of recharge remained close to the 1:1 line for all observed events. The 1:1 recharge line for 19-2 has a lesser slope than the 1:1 line at 19-1 due to the lower imperviousness percentage of the 19-2 contributing catchment. What is clear from these results is that the bioswales can function as a source of groundwater recharge in the right geological setting, enabling managed aquifer recharge as a realistic water management strategy (Tasks 1 and 5).

Observations during a high intensity storm event outside the monitoring period noted overland flow out of swale 19-1 and into the next downstream swale before infiltrating, showing that loss of water

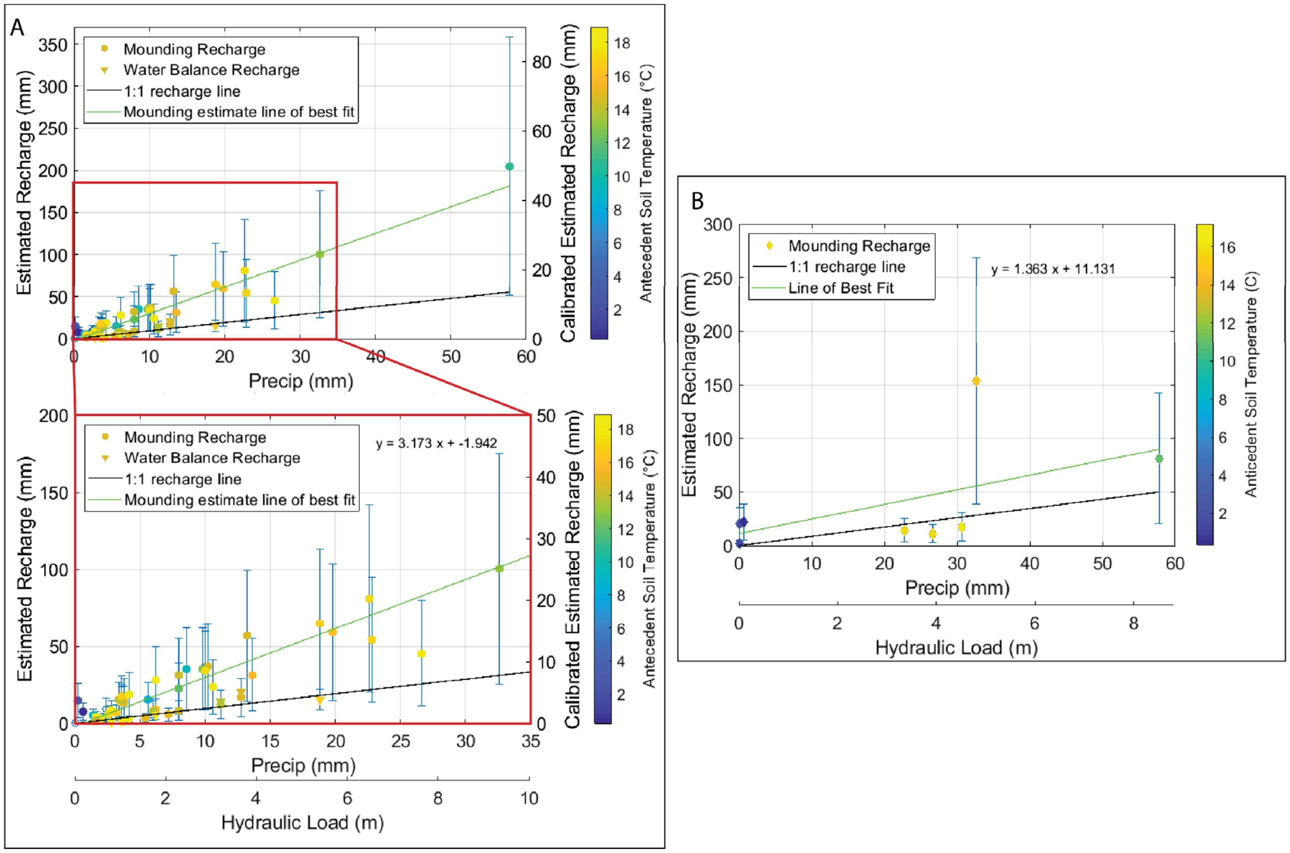

Figure 21. Groundwater recharge estimates for storm events at (a) bioswale 19-1 and (b) bioswale 19-2 showing mounding estimates (circles) and water budget estimates (triangle). The black line represents a 1:1 recharge relationship based on the runoff coefficient for the catchment. "Hydraulic Load" is the estimated volume of runoff into the swale divided by swale area. The green trend-line displays the linear-regression relationship mounding recharge estimates. Right-hand Y axis applies only to the recharge data estimated through mounding and shows the recharge estimates obtained using the calibrated estimate of saturated hydraulic conductivity.

via overland flow occurs when storm magnitude and intensity are high enough. Water budget estimates are believed to be reliable for all but two of the events, which had sufficiently large precipitation intensities and likely violated the assumption of no-outflow via overland flow assumed for the water budget calculations. In those cases, violation of this assumption would cause the water budget method to overestimate recharge.

A key finding in this study relates to the distinct differences in hydrologic response between bioswale 19-1 and 19-2 (Figure 21), which were largely the result of subsurface geologic conditions. The lag time between surface water input and groundwater table response was four and a half times greater at 19-2 than the lag time at 19-1. The average event duration for 19-2 was an order of magnitude larger than the average event duration of 19-1. The greater average recharge volume and event length at 19-2 is attributed to the nature of the events that were able to produce a measurable groundwater mound beneath 19-2. Surface ponding in 19-2 would generally last for days whereas surface ponding in 19-1 would dissipate within an hour. The mounding approach was only able to account for events where there was an observable groundwater mound beneath the swale. The difference in infiltration and ponding dynamics between the two swales drastically altered the types of precipitation or melt events that were needed to observe groundwater mounding. Small precipitation events that would pond and quickly infiltrate in 19-1 would generate ponded conditions at 19-2 over the course of multiple days, and yet produce no observable groundwater mound. This extended ponding period would exacerbate the influence of evapotranspiration and increase the likelihood of loss from the system through overland outflow if subsequent precipitation events discharged into an already full recharge pond. If precipitation events were not large enough to produce enough volume to overcome evapotranspiration, soil moisture storage capacity, and the slower infiltration rate at 19-2, then the mounding impact at the water table was difficult (if not impossible) to quantify. As a result, only large events were observed to produce mounding beneath 19-2 (Task 1).

The actual volume of recharge at Swale 19-1 was expected to be equal to or less than the calculated influent runoff volumes for each storm event, due to the rapid infiltration and efficient subsurface drainage observed at that swale. Water budget estimations of recharge were within +/-50% of calculated runoff volumes for each event, while estimates of recharge obtained using the mounding formula were on average 317% greater than calculated runoff volumes. The greater than expected groundwater mounding estimates indicate that this method is systematically overestimating the recharge rate. The overestimation is believed to result from violations of key assumptions in Hantush's 1967 solution, most notably assumptions of homogeneous and isotropic aquifer conditions. The local alluvial aquifer is known to be highly heterogeneous and anisotropic, being comprised of interbedded layers of clay, silt, sand, and gravel. The resulting variability in hydraulic parameters (K_s and S_y) and aquifer thickness can dramatically change the estimated recharge rates. Additional testing by Hall (2021) was conducted by varying *Ks* to fit the groundwater mounding recharge estimates to the water budget estimates (see right axis of Figure 21a). This "calibration" approach may provide an avenue for practitioners to utilize the groundwater mounding approach with more confidence. One key advantage of the groundwater mounding approach is that it was able to identify recharge events when there was no obvious rainfall and snowmelt was a significant contributor to recharge (i.e., late fall and early spring), thereby providing another tool to assess the hydrologic performance of bioswales and their potential usage for managed aquifer recharge (Tasks 1 and 5).

3.4 Highland Park and Cambrian Heights Rain Gardens

3.4.1 Seasonal Water Budgets

The seasonal water budgets for both rain garden sites are presented as equivalent water depths (i.e., volume of water normalized by rain garden area) in Figure 22 for the 2023 and 2024 field seasons. In 2023, HP recorded 1226 mm of total inflow and 1371 mm in 2024. In 2023, CH recorded 2434 mm of total inflow and 2002 mm in 2024. The increased inflow at CH relative to HP is the result of the smaller garden and larger IP ratio at CH directing more water into the garden. Also note that the total volumes of applied water also include any water applied by the maintenance crew to support plant establishment as well as the simulated rainfall events noted in Section 2.4.2 (Task 1).

ET over the monitoring seasons was estimated to be 587–652 mm (4.0–4.2 mm d^{-1}) and was greater at CH (612–652 mm) compared to HP (587–625 mm), although these differences are within the range of estimated uncertainty (Figure 22). Note that the lysimeter-aligned ET values used in this study likely overestimated actual ET slightly (see Ilg, 2025), however, the differences are

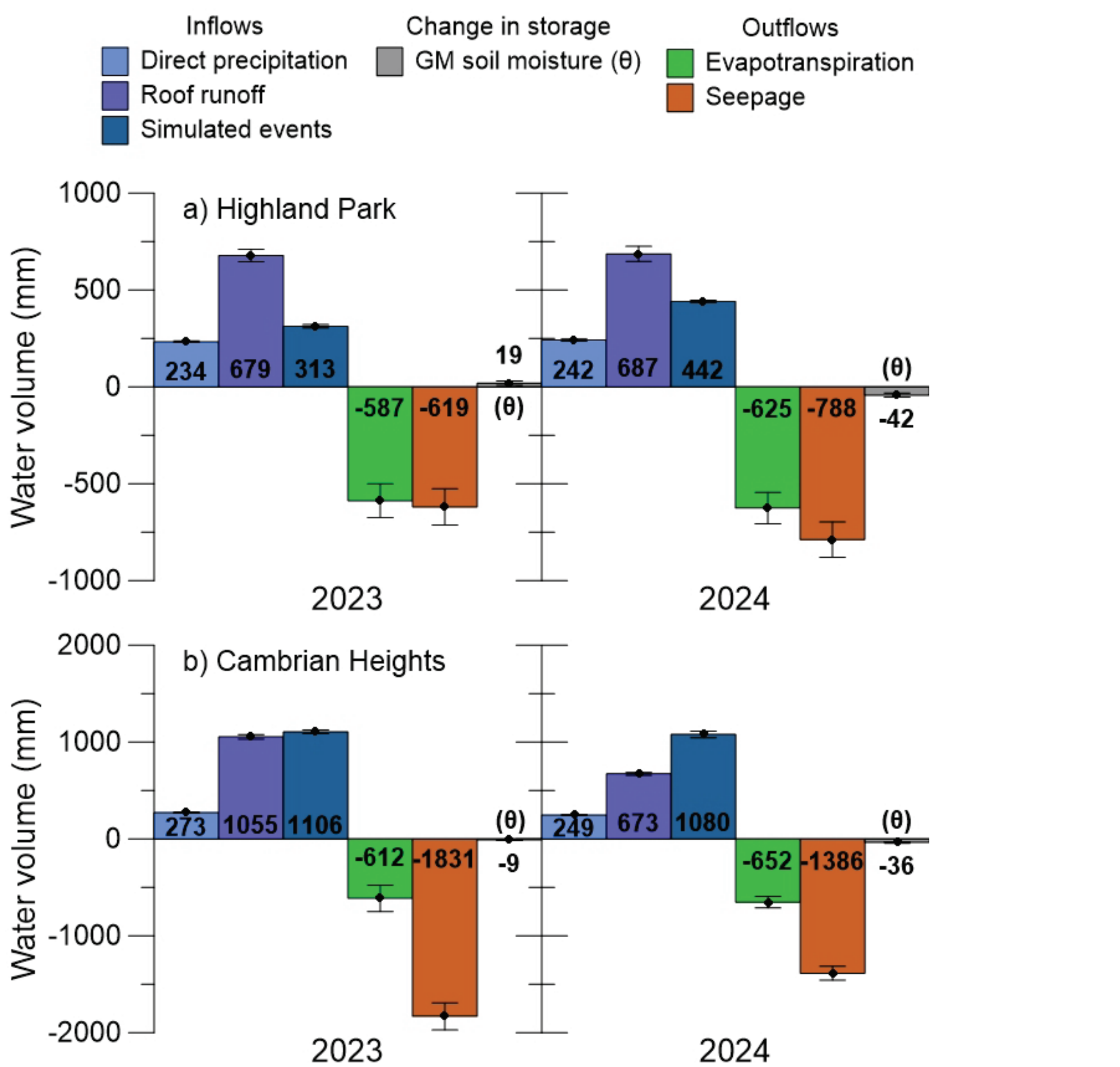

Figure 22. Seasonal water budgets of the Highland Park (HP) and Cambrian Heights (CH) rain gardens, depicted as equivalent water depth (mm) normalized to the garden area. Water budgets ran from May 24–October 16 in 2023, and May 13–October 15 in 2024.

considered small (likely <10% and no more than 20%). Overestimating ET results in a corresponding underestimation in seepage as the residual of the water budget. Underestimating seepage is considered a reasonable conservative approach and does not significantly alter any interpretations or conclusions. That said, ET observed in this study is well above this average actual evapotranspiration (AET) measured at Calgary international airport, likely because the large volumes of runoff water added to the garden meant that available soil moisture was a minimally limiting factor, and the AET estimates are regional ones that does not consider the localized ET enhancing conditions of rain gardens. Owing to this, the rain garden ET values are more comparable to the 609–697 mm of growing season (May–October) ET estimated from the nearby OBF bioretention cells (Skorobogatov, 2023) which also received large runoff volumes, albeit with substantially higher IP ratios (15–30:1) than the rain gardens (Task 1).

At HP, 46–48% of inflow over the monitoring seasons was accounted for through ET, and 51–57% through seepage (Figure 22). At CH, ET accounted for 25–33% of inflow, and seepage for 69–75%. Both processes are therefore important components of the water budget on a seasonal basis, with seepage accounting for slightly more of the water budget than ET at HP, and significantly more at CH. In all cases, water stored as growing media soil moisture accounted for very small amounts (<4%) of the water budget. It is important to recognize that seepage out of the growing media and into subsurface sediments below the rain gardens is not currently factored in their design. The findings of this study suggest that designs for unlined LID systems should consider subsurface seepage as it is a major component of rain garden function, even in the relatively low-permeability sediments encountered at CH and HP sites, which are common across Alberta (Task 1).

No underdrain or subsurface liner was present at the CH and HP sites, and no overflow was observed, meaning these rain gardens effectively had a 100% stormwater removal efficiency over the study period. If implemented on a watershed scale, the seasonal water budgets indicate that rain gardens could store and remove a large volume of stormwater runoff, resulting in reduced peak surface flows and less total surface water runoff directed into stormwater infrastructure (Hoghooghi et al., 2018).

3.4.2 Event Water Budgets

Water budgets were constructed for all precipitation events larger than 3 mm for the 2023 and 2024 seasons, resulting in 25 events at HP and 31 events at CH over this period. The water budget behaviour differed substantially at shorter timescales as compared to seasonal scales, owing to

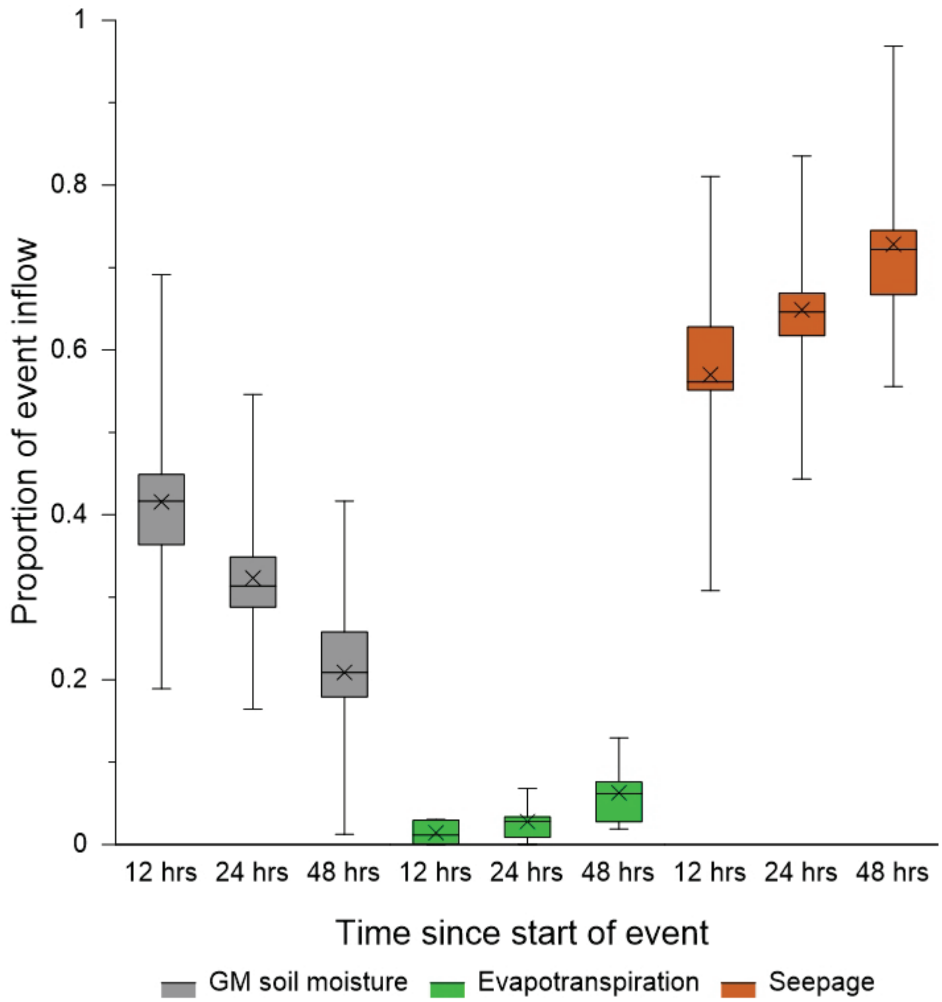

Figure 23. Event scale water budgets at the Highland Park rain garden 12, 24, and 48 hours after the start of nine large precipitation events (>25 mm) in 2023 and 2024. GM soil moisture refers to water stored in the growing media and seepage refers to water that drained out of the growing media. The box represents the upper and lower quartiles, the centre line denotes the median, the x denotes the mean, and whiskers represent the extreme values.

the reduced time available for water to either drain or evapotranspire. As expected, seepage from the rain gardens was generally greater when the growing media antecedent soil moisture was wetter (data not shown; Ilg, 2025). Seepage also exhibited a threshold behavior, increasing linearly with precipitation more rapidly for large events (>25 mm) than for small events (<25 mm) (Task 1).

Water budgets for large events, including simulated events (>25 mm) were created for periods 12, 24, and 48 hours after the start of the event at each site. Larger events represent the circumstances when rain gardens can become most valuable regarding flood prevention, and when they might start approaching their water retention limits (Li et al., 2009). In 2023 and 2024, nine large events occurred and were analyzed at HP (four natural), and ten events at CH (four natural). Figure 23 shows the water budget components from these large events at HP, revealing that soil moisture

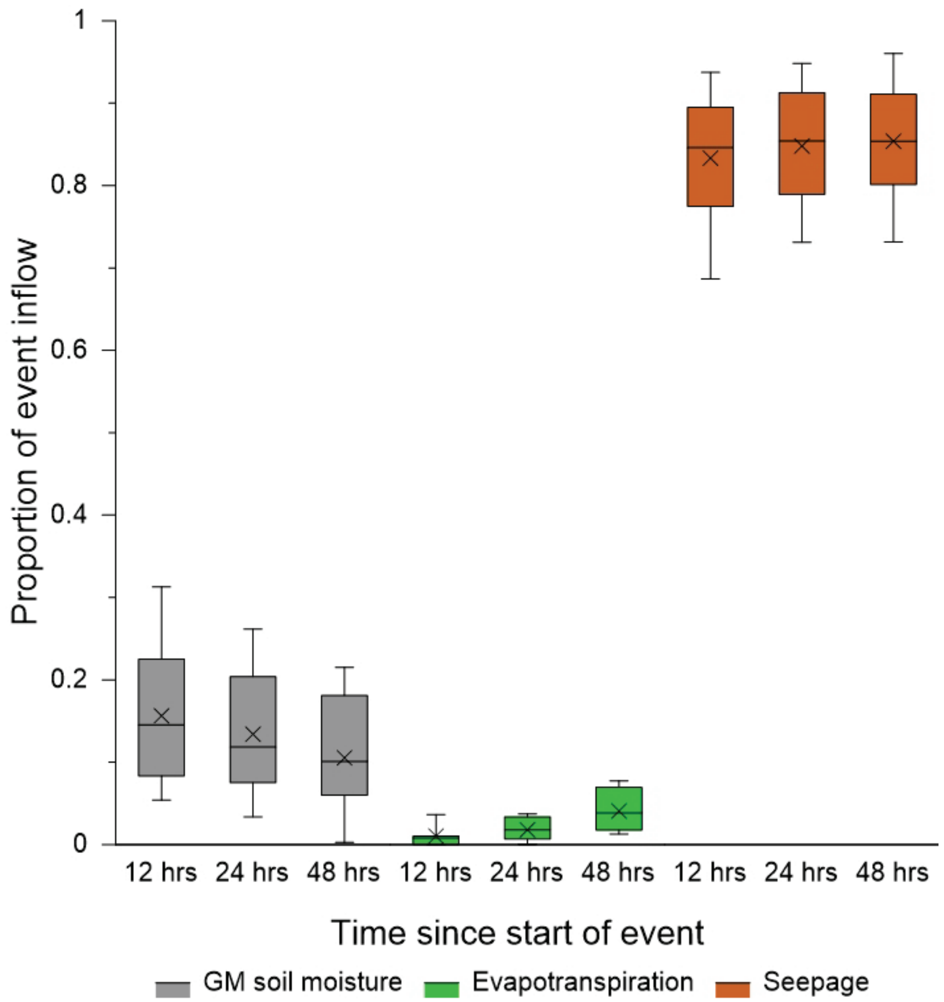

Figure 24. Event scale water budgets at the Cambrian Heights rain garden 12, 24, and 48 hours after the start of ten large precipitation events (>25 mm) in 2023 and 2024. GM soil moisture refers to water stored in the growing media and seepage refers to water that drained out of the growing media. The box represents the upper and lower quartiles, the centre line denotes the median, the x denotes then mean, and whiskers represent the extreme values.

storage, ET, and seepage on average accounted for 21%, 6%, and 73% of inflow, respectively, after 48 hours. At CH (Figure 24), the same processes accounted for 11%, 4%, and 85% of inflow respectively, after 48 hours. At both sites, seepage losses represented the largest water budget component for these large events, and soil moisture storage was a lesser, but still important, component. Water budget results were similar with varying water budget intervals, with seepage and ET increasing for longer interval periods, at the expense of reduced soil moisture storage. ET was a small component of the event scale water budgets, which contrasts with the seasonal scale water budgets where ET was a substantial component. ET water removal capacity is limited during and shortly after an event, with ET increasing over longer timescales and is the primary mechanism responsible for removing water between events. When compared to the other processes of storage and seepage, ET clearly is much slower, removing water over multiple days and potentially weeks (Task 1).

Simulated rain events provided a unique opportunity to examine hydrologic processes in greater detail and hourly water budgets for each simulated event at HP are presented in Figure 25. As a subset of the larger events, the plots highlight once again that for large events, most applied water ended up as seepage, with ET playing a minor role over shorter timescales. Growing media soil moisture storage was also an important contributing component. The smaller IP ratio and greater depth of growing media at HP enabled the garden to retain more water in the growing media

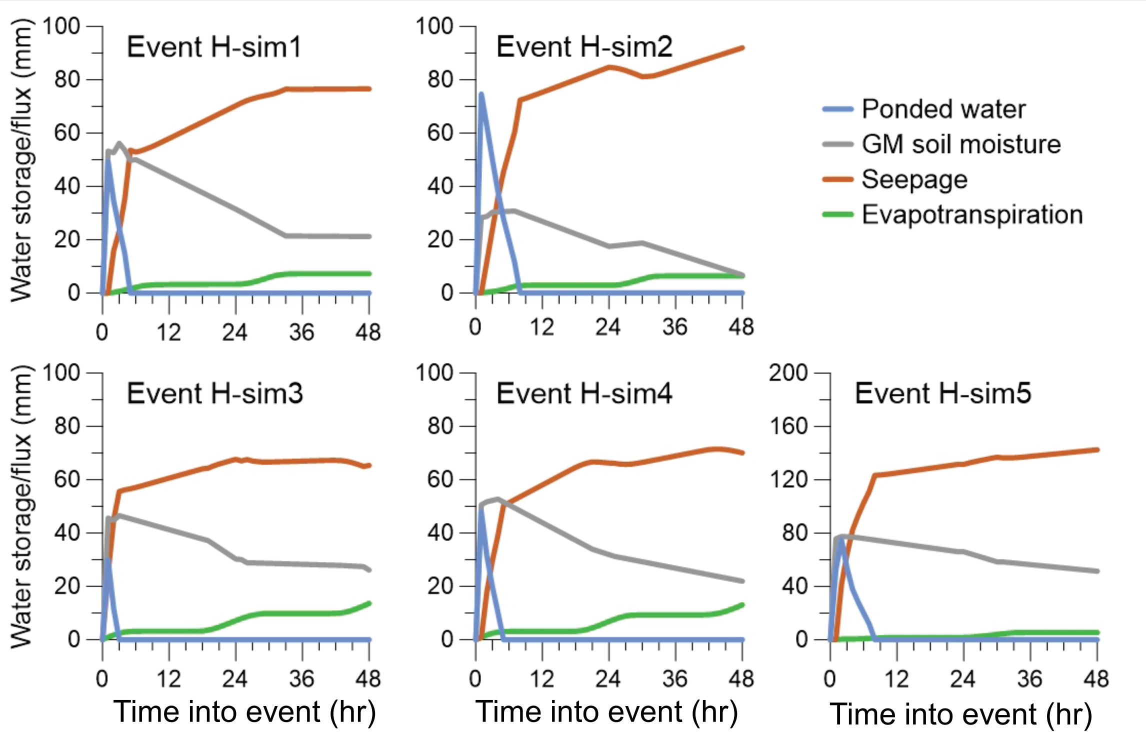

Figure 25. Water budget calculated in hourly intervals for the five simulated events at Highland Park in 2023 and 2024. All events simulated approximately 26 mm of rainfall, except H-sim5 which simulated a 48 mm rainfall. Soil moisture refers to water stored in the growing media and seepage refers to water that has drained out of the growing media.

compared to CH (data not shown; Ilg, 2025). The simulated events exemplify how well the rain gardens performed through the early stages of their operating lifespan. Even during the largest simulated events (H-sim5, Figure 25), replicating short but intense storms with return periods greater than 100 years, there was no surface overflow. These findings show the rain gardens continue to function for events larger than the design capacity, due to seepage below the gardens that is not accounted for directly in the design specifications. Effectively, the results suggest that these gardens may be oversized and that the IP ratios could potentially be increased while largely maintaining their functionality. This approach would need to be taken cautiously, however, as some studies (Asleson et al., 2009; Le Coustumer et al., 2012) have noted that LID performance can decrease overtime due to sediment clogging of the growing media, which was not observed in this study.

3.4.3 Infiltration

There were seven events with enough ponding to allow infiltration rate calculations at HP (two natural), and four events at CH (two natural). Infiltration rates are presented in Figure 26. At HP, flooded infiltration rates ranged from 16–35 mm hr^{-1} (mean = 21 mm hr^{-1}), and at CH from 248–350 mm hr^{-1} (mean = 304 mm hr^{-1}). All flooded rates far exceeded the lower end of City of Calgary subsurface percolation rate calculations for LIDs, which range from 0.5 to 100 mm hr^{-1} (City of Calgary, 2016). Field saturated hydraulic conductivity (K_{fs}) was estimated for each rain garden using a modified Philip-Dunne (MPD) infiltrometer and are presented alongside the ponded infiltration rates since the numbers are comparable under saturated/ponded infiltration conditions (Figure 26). The MPD method overestimated the garden-scale infiltration rate by around an order of magnitude. Since the MPD device is relatively small (<20 cm diameter) and infiltrates small volume of water, it measured the K_{fs} of the surficial growing media. In contrast, garden-scale flooding tests measured the infiltration rate of the entire garden, which includes the influence of the low conductivity native soil that underlies and surrounds the garden. Due to this limitation, small-scale estimates of infiltration capacity (such as MPD or other ring infiltrometers) should be viewed with caution, since they do not necessarily reflect the native soil below the growing media that can be the limiting factor for infiltration (Task 1).

Another key finding was that the duration of ponding was limited. During larger events, substantial standing water was observed at HP for a maximum duration of eight to nine hours (Figure 25), and at CH the maximum duration was less than two hours (data not shown). Ponding durations were at both sites were well below the maximum allowable time of 24 hours set out by the City of Calgary (City of Calgary, 2016) to prevent plant mortality and the creation of spawning grounds for mosquitos (Task 1).

3.4.4 Vertical and Lateral Subsurface Flows

The groundwater monitoring for HP showed both seasonal and event-scale trends, as well as variations between years. For example, the prolonged regional drought heading into 2023, caused by lower-than-average precipitation in 2021 and 2022 (as measured at Spyhill), resulted in lower groundwater levels in 2023 compared to 2024. The resulting year-to-year differences in regional groundwater levels likely contributed to differences in groundwater response measured at HP, effectively increasing subsurface storage capacity in drier years (e.g., 2023) compared to wetter years (e.g., 2024). As a result, groundwater mounding was observed at HP in response to rainfall/runoff events, with far more events and more total estimated recharge in 2024 compared to

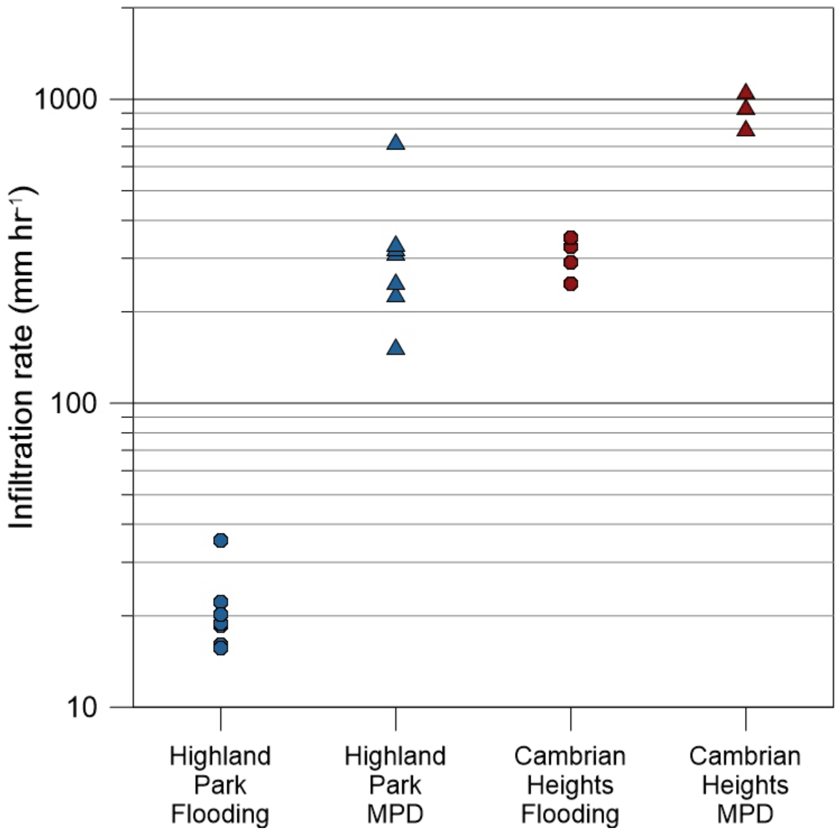

Figure 26. Infiltration rates calculated at each rain garden using two methods: (1) flooding tests where infiltration rate was estimated by observing the rate at which ponded water level declined during large precipitation events, and (2) spot measurements using the MPD (Modified Philip-Dunne) infiltrometer.

2023. In 2023, the largest event induced groundwater rise in MW1 (situated directly beneath the garden) was 5 cm, and in 2024 there were ten events with groundwater level rises greater than 10 cm. In MW2, located 1.5 m outside the garden, two events in 2024 exceeded a groundwater rise of 10 cm. The largest event (H24-25) on September 12, resulted in a 115 cm groundwater rise in MW1 and a 68 cm rise in MW2 (Figure 27). Groundwater mounds were short lived, typically dissipating within 1–2 days, although the groundwater levels following event H24-25 took approximately five days to return to pre-event levels (Tasks 1 and 2).

The WTF method for estimating groundwater recharge was applied to all events in 2023 and 2024 with distinct water table rises greater than ~3 cm. The WTF estimated recharge was 7 mm in 2023, and 315 mm in 2024. In general, more recharge was observed during larger events with greater precipitation and seepage. Relative to the seepage values calculated from seasonal water budgets above, groundwater recharge accounted for 1% of seepage in 2023, and 40% in 2024. The substantial differences between seasons show the distinctly different groundwater recharge dynamics that can occur from year to year. The 2024 value is likely slightly overestimated as a result of assumptions in the WTF method, specific yield estimate, and inflow measurements (Ilg, 2025), however, the measured differences in groundwater recharge between years are still considerable and a reflection of subsurface storage conditions and the timing and magnitude of precipitation events across years (Tasks 1 and 2).

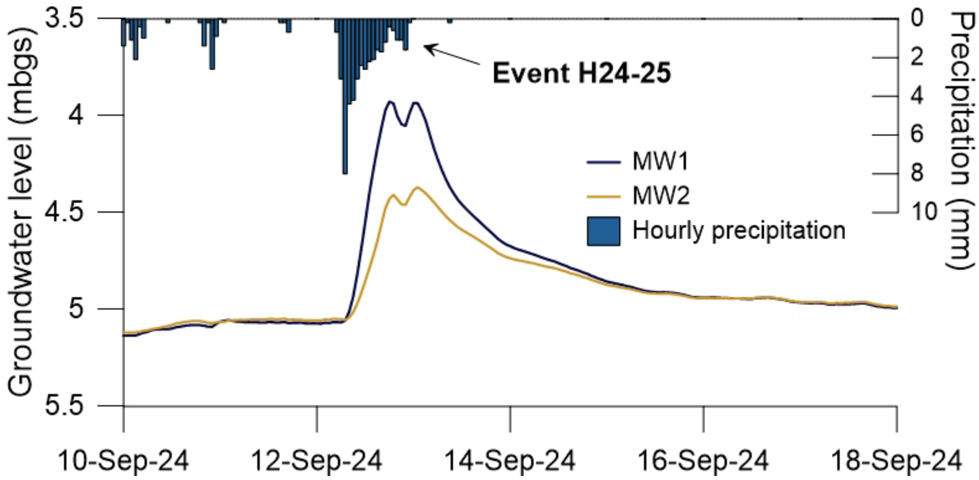

Figure 27. Groundwater response to event H24-25 and daily precipitation at Highland Park rain garden from September 10-18, 2024. Groundwater level is depicted as depth relative to the ground surface at MW1.

Tensiometers were used to assess lateral subsurface flow at both rain gardens via measurement of soil matric potential (data not shown; Ilg, 2025). Differences in matric potential enable the directions and lateral extent of subsurface flow to be determined, but the data cannot be used to quantify lateral fluxes or flow volumes. In brief, strong lateral flow was observed within ~1 m of each garden after large precipitation events, particularly when antecedent moisture conditions were wetter. At shallower depths, represented by the 35 cm depth tensiometers at HP, lateral flow was limited to less than 2 m outside the garden. At depths of 75 cm, lateral flow was observed out to ~2 m when the antecedent soil moisture was high, but it never reached ~3 m distance. Similarly, observations from the HP monitoring well MW2, showed a rise in the water table extending laterally out from the garden >1.5 m on several occasions. The deepest tensiometers at CH (130 cm) often exhibited lateral flow extending out ~2 m, and it likely extended slightly farther but no sensors were installed at greater distances. When lateral flow occurred at these farther (~2 m) distances, the soil remained unsaturated, and the flow was delayed by up to a few days after the rainfall/runoff event. Like HP, lateral flow extended farther from the garden at CH after the second of the consecutive simulated events, when the antecedent moisture content was higher. The CH rain garden has previously been modeled, and similar lateral flow observations were made (Merrett, 2023). Lateral water flow is an important concern for urban infrastructure that surrounds rain gardens, such as basements and roads/pathways, and these findings provide valuable measured data to assist in establishing appropriate setback distances for rain gardens and similar infiltration-based LIDs in Alberta. These results suggest a setback of 2–3 m from LID installations would mitigate most lateral flow concerns for roads and pathways with shallow (<1 m) bases. Deeper infrastructure, including building foundations, would benefit from a setback greater than 3 m, which supports the current City of Calgary (2016) recommendation of 3–5 m (Tasks 1 and 5).

3.5 Numerical Simulations

Initial 2D simulations by Merrett (2023) highlighted the lateral flow potential around the rain gardens, but here we will focus on the results of the more detailed 3D simulations of the HP garden. The 3D simulations were conducted by varying the hydraulic conductivity of different soil layers (Figure 7a) to assess the impact on water budgets and lateral/vertical flow. Contrary to common assumptions about infiltration-based LID systems, the hydraulic conductivity of

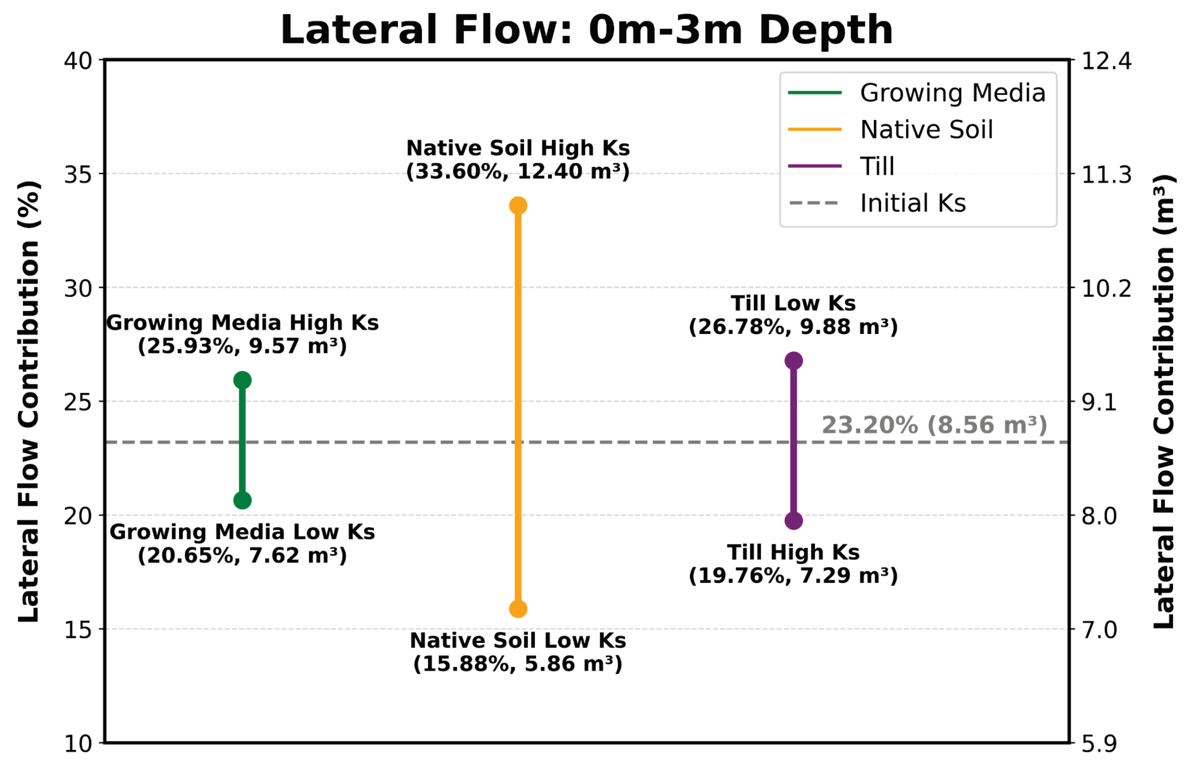

Figure 28. Simulated influence of varying hydraulic conductivity (K_s) on lateral flow away from the rain garden for different soil layers. Values are expressed relative to the initial calibrated K_s values for each layer, using percent difference (left axis) and total volumetric flow (right axis). See Figure 7a for soil layer delineation.

sediments outside the engineered growing media exerted the greatest control on lateral and vertical fluxes. Figure 28 shows the impact of increasing or decreasing K_s by a factor of five (5) on lateral flows, with the native subsoil having the greatest impact on flow dynamics followed by the deeper till unit. Growing media properties had the least influence on flow. This result has important implications for rain garden design, pointing to the need for careful evaluation of subsurface soil characteristics, which have an influence similar to or greater than the properties of the growing media. Overall, approximately 25% of the inflow to the garden is expected to escape laterally outside the garden footprint. It was also noted that lateral flow was largely limited to within 3m of the garden edge, confirming the field observations reported above (Task 5).

In terms of water budget, the timescale of evaluation dictated the importance of different hydrologic system components. As observed in the field, wetter pre-event soil conditions dramatically increased lateral and vertical flow. Under dry antecedent moisture conditions, soil moisture storage was the largest water budget component, averaging 48% of total inflows for all scenarios, compared to 36% of water lost to deep vertical flow and 10% lost to lateral flow (Figure 29a). In contrast, under wet conditions vertical flow comprised 47% of inflow on average, lateral flows increased to 16% and soil moisture storage accounted for 24% (Figure 29b). Even though lateral and vertical flow were substantially affected by antecedent moisture conditions, systemic

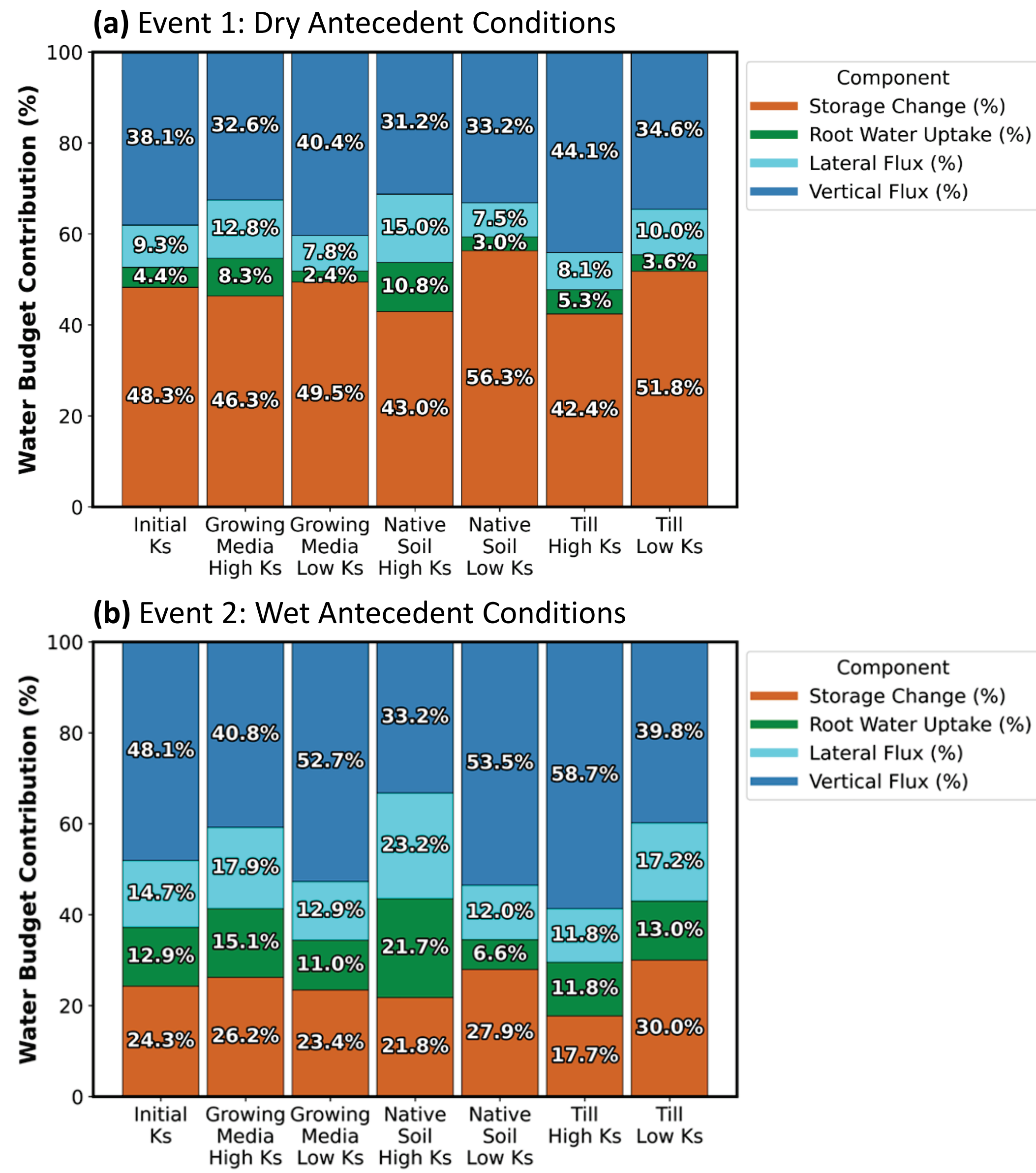

Figure 29. Simulated influence of varying hydraulic conductivity (K_s) for different soil layers on event-based rain garden water budget components for two large (26 mm) events under (a) dry antecedent soil moisture, and (b) wet antecedent soil moisture conditions. Values are expressed as a percentage of total runoff inflow to the garden for each modeled scenario. See Figure 7a for soil layer delineation.

drainage patterns remained relatively consistent across scenarios. The influence of hydraulic conductivity changes was more pronounced under wetter antecedent conditions, but the interplay between layers had a pronounced influence on the magnitude of both vertical and lateral water fluxes (Task 5).

Modeled water budgets showed that soil moisture storage plays an important role during individual events; however, over longer time periods, this storage decreased substantially as root water uptake became increasingly important. Over the entire simulation period, root water uptake (ET) returned 49% of runoff inflows to the atmosphere across all seven simulated scenarios (Figure 30), whereas vertical and lateral water fluxes accounted for 29% and 23% of total inflows, respectively. Soil moisture storage over longer time frames was minimal (Task 5).

In general, the 3D rain garden simulation results were very consistent with all available field data, providing confidence in the model and enabling usage of model results to further test and refine the hydraulic performance of rain gardens and other infiltration-based LID systems. The model results clearly point to the importance of understanding the composition and distribution of soils and sediments surrounding the rain gardens as they have a major control on subsurface flow dynamics. Both the field data and numerical simulations from this project were used by various project partners (e.g., ALIDP, City of Calgary) to support decision-making and refine assessment tools for evaluating LID hydraulic performance. The details of these collaborations and related ongoing studies is outlined in greater detail in Sections 5.0 and 8.0.

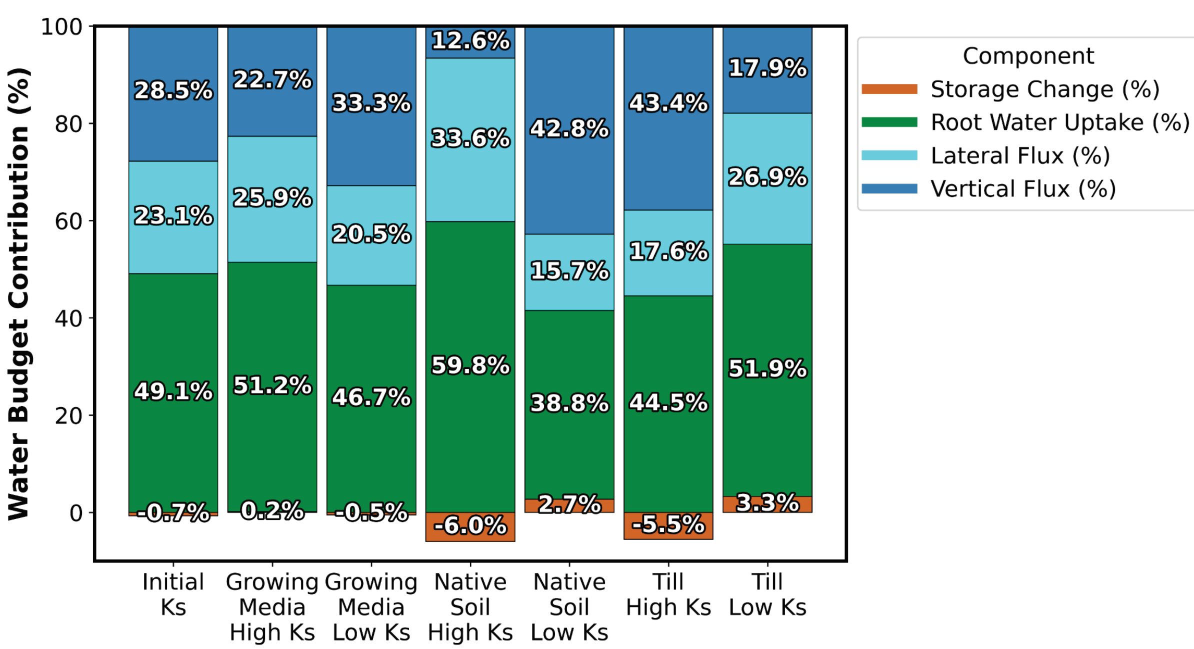

Figure 30. Simulated influence of varying hydraulic conductivity (K_s) for different soil layers on total cumulative rain garden water budget components for all events over the full simulation period. Values are expressed as a percentage of total runoff inflow to the garden for each modeled scenario. See Figure 7a for soil layer delineation.

4.0 Key Learnings

This project has produced numerous important results from the breadth of field studies and numerical simulations that were undertaken. The key project learnings can broadly be stated as follows:

- Surface water-groundwater interactions were critically important to local and watershed-scale hydrologic function and the understanding of these processes gained from this study can support improved water management.
- Groundwater is the primary contributor to prairie streams in the region, but urban development had a clear impact on streamflow.
- The LID systems tested functioned as effective stormwater management tools and the results of this project can further strengthen their hydrologic and water treatment performance.

The following subsections briefly outline key project learnings that contribute to the first five project objectives and tasks. Contributions to the knowledge dissemination task (Task 6) will be summarized later in the document.

4.1 Task 1 Hydrologic Performance of LID Systems

- The OBF bioretention mesocosms with differing growing media exhibited significant differences in water retention performance at the onset of the study period, yet became increasingly similar over time. In contrast, the impact of vegetation type between mesocosms gradually increased over time as plants became established.
- Bioretention mesocosms demonstrated an increasing trend in infiltration rates over time, which is the opposite of the conventional expectation of decreasing infiltration due to media clogging. Media type and vegetation had the most significant impacts on infiltration rates, with clay-rich CL media having the highest infiltration rates and the greatest increases over time.
- Water retention was limited in the bioretention mesocosms (mean PWR = 16%), meaning these systems may have limited hydrologic benefit for that purpose. The limited storage capacity of the systems also meant that total water retention did not scale with increasing IP ratio.
- Strong interactions between design parameters of media type, vegetation, IP ratio had important influences on both hydrologic and water quality performance. In particular, the importance of plant-media interactions were significant due to the evolution of soil properties (e.g., soil structure development, freeze-thaw) and plant root establishment over time.
- Measured infiltration rates in the OBF mesocosms exhibited an overall increasing trend through time. Among the three media types, the clay-loam media had the highest infiltration rates, showing promise for future LID implementation.
- Hydrologic performance of many infiltration-based LID systems, including bioswales and rain gardens, was controlled by the subsurface geologic conditions and thus there is a need to ensure facilities are appropriately sited and designed.

- The OBF bioswales were incredibly effective at enhancing stormwater runoff infiltration and, based on the subsurface conditions (sand and gravel-based sediments), functioned as effective conduits for groundwater recharge.
- The rain gardens functioned very effectively to reduce surface water runoff (no recorded surface outflow in four years of monitoring).
- Rain garden water budget components changed depending on the timescale under consideration. At seasonal scales, evapotranspiration via plant water uptake was an important water budget component, but played little role in short-term (i.e., event scale) water budgets.
- Subsurface seepage was a key process in rain garden performance, routing approximately 50-70% of runoff water into the subsurface below and around the rain gardens over seasonal timeframes. Large rainfall events (>25 mm) further enhanced seepage out of the rain gardens.
- The CH rain garden had more seepage and less ET than the larger HP rain garden, which was attributed to a combination of higher IP ratio, thinner growing media, and smaller footprint (i.e., larger perimeter to area ratio).
- For the rain gardens, roughly 10-40% of water was retained in the growing media as soil moisture within the first 48 hours following large events, indicating the relevance of short-term growing media storage to overall hydrologic performance.
- Infiltration rates for engineered growing media used in LID designs exceeded the specified infiltration rates in all systems tested (i.e., bioswales, bioretention, rain gardens), likely resulting from preferential flow and increased biopore/root development over time. Enhanced infiltration has benefits for flood protection and groundwater recharge, but brings with it increased risks for subsurface infrastructure and potentially reduced water treatment performance.
- The rain gardens maintained effective hydrologic performance for large rainfall events that exceeded their design capacity, largely due to the subsurface hydraulic connections that increase the overall storage volume.

4.2 Task 2 Pre- and Post-Development SW-GW Interactions

- SW-GW interactions were across the landscape from groundwater recharge zones to groundwater discharge zones. LID systems displayed enhanced surface water infiltration that increased groundwater discharged. Likewise, groundwater discharge was critical in supporting streamflow during and between precipitation events.
- Paired watershed data suggested clear differences in streamflow response between the developed (SHR) and undeveloped/developing (GRR/WNC) at both event and seasonal scales. At seasonal scales, baseflow in the developed watershed was consistent through much of the year, whereas in the undeveloped watershed there was a strong seasonal signal in response to groundwater level fluctuations.
- Spatial variability in streamflow was common, with water gained and lost along different stream reaches primarily attributed to connectivity with groundwater as determined by the hydraulic properties of the underlying geologic materials.
- During individual rainfall events, runoff in the developed watershed was much lower than in the undeveloped watersheds which goes against most conventional understanding. The

unique hydrologic behaviour was attributed to capture and rerouting of water away from the urban stream by stormwater infrastructure.

- Groundwater was the primary source of flow to prairie streams in both developed and undeveloped catchments. Baseflow separation and stable water isotopes showed that 95% and 86% of the cumulative streamflow volume in SHR and GRR, respectively, was sourced from groundwater.

4.3 Task 3 Water Quality Performance Assessment

- Research at the OBF site revealed significant leaching of nutrients and organics from the bioretention cells, especially in the earliest stages after construction, meaning that the system effectively increased nutrient loads downstream rather than providing water quality treatment as intended.
- Leaching of nitrogen was very significant in the early stages, particularly in the sand-based media, and decreased over time, whereas phosphorus leaching was more problematic since it persisted over multiple years.
- Interactions among different design factors (media type, vegetation, and IP ratio) were important as they each contributed to water quality performance in varying, and often complex, ways.
- Hydrologic loading (IP ratio) had little effect on P concentrations in effluent, which effectively means increased P loading for downstream aquatic environments. N concentrations, by comparison, were diluted by higher IP ratio loading rates.
- The novel CL media, composed of clay-loam and wood chips, had the least leaching of the three media used in the bioretention mesocosms and highlighted the potential benefits of this media for improved water treatment.
- Soil amendments were shown to be effective at preventing or mitigating P leaching from bioretention systems, with the water treatment residual (WTR) product showing the most promise.

4.4 Task 4 Frozen Ground Hydrology

- The OBF bioretention systems continued to function from a hydrologic perspective even during frozen ground conditions. Infiltration rates during simulated snowmelts were reduced by 80% relative to unfrozen summer conditions, but still sufficient to manage the magnitudes of water inflows tested during this project.
- IP ratio and media type had the most significant impact on flow, with CL media and IP 30 cells having the largest infiltration rates.
- Water retention was not strongly influenced by frozen soil conditions, due to the relatively small water retention capability of the mesocosm cells even under unfrozen conditions and the importance of preferential flow.
- Overall hydrologic performance was largely based on media type, and more specifically, the ability of the media to support preferential flow under frozen conditions. Clay-based CL media showed improved hydrologic performance and important potential as a viable alternative media type for infiltration-based LID systems.
- Preferential flow also limited the effects of pore clogging from refreezing of midwinter meltwater, as no significant difference in infiltration rate was noted following the midwinter melt event.

- Coarse-grained bioretention media performed poorly relative to finer-grained media, particularly in terms of infiltration capability. This trend was exacerbated under frozen ground conditions.
- Nutrient (N and P) performance of the bioretention cells was comparable between frozen and unfrozen conditions, with most cells leaching relatively low concentrations of nutrients. Nutrient leaching or removal was largely dependent on media type, but vegetation also played a role in reducing N leaching.

4.5 Task 5 Hydrologic Assessment Tools

- Water table mounding methods for estimating groundwater recharge, including analytical approaches and the WTF method, were able to produce reliable estimates of groundwater recharge, but require careful estimation and application of hydraulic properties.
- Lateral flow around unlined LID systems (e.g., rain gardens) extended from 2-3 m away from the infiltrating source under typical southern Alberta climate and soil conditions, with greater lateral flow deeper in the soil profile. The magnitude and extent of lateral flow are enhanced by wetter antecedent soil moisture conditions.
- Subsurface geologic conditions are essential to consider in LID designs, as modest changes in hydraulic properties can markedly alter the water flow and storage dynamics that dictate overall hydraulic performance.
- 3D simulations of rain gardens were able to quantify water budget components, showing roughly 50% of inflow is routed to ET and another 50% to subsurface drainage at seasonal time scales.
- Hydrologic data and numerical simulation results from the project were utilized to refine LID system designs, support software-based LID assessment, and inform additional monitoring needs in related studies for a range of project partners.
- The consistency of simulated and measured data sets lent confidence to the results from numerical models, and further enables evaluation of an array of design factors and hypothetical scenarios to support improved stormwater management.

5.0 Outcomes and Impacts

This project generated substantial advances in understanding the coupled surface water–groundwater processes that govern watershed hydrology in Alberta's urban and peri-urban settings. The integrated field investigations and numerical simulations provided a multi-scale assessment of SW-GW connectivity and valuable insights into infiltration-based LID system performance and their influence on groundwater recharge. Most importantly, we have achieved the project outcomes by providing empirical evidence to support improved water management decisions, and training highly qualified personnel (HQP) who will amplify the project impact by applying their knowledge and expertise to address relevant water security problems. Project outcomes in relation to the proposed performance metrics are categorized in the following subsections.

5.1 Performance Metric: Highly Qualified Personnel (HQP) Training

Perhaps the most important impact of this project is the training of multiple HQP, including technicians and students at all levels (BSc, MSc, and PhD). This project provided a valuable multidisciplinary training environment. Through hands-on fieldwork, data interpretation, and collaboration with project partners, HQP gained practical experience that enhances their career readiness while building societal capacity for evidence-based water resource management. Outside of the project leadership team, HQP conducting thesis-based research or providing technical research support are summarized below.

- 3 PhD Students: Cann, Skorobogatov, Jalali
- 7 MSc Students: Elliot, Hall, Ilg, Johnson, Nasrollahpour, Wyse, Zhang
- 4 BSc Students: Giberson, Merrett, Prevost, Skirten
- 6+ Research assistants and technical staff: Decent, Maxwell-Nikiforuk, Mott, Muenchrath, Nightingale, Shrestha

The HQP trained through this project will continue to generate impact by applying their technical expertise in academic, municipal, consulting, and regulatory sectors. Their experience and practical training will also contribute to advancing future studies and innovation in LID design and integrated watershed management across Alberta and beyond.

5.2 Performance Metric: Best Practices Advanced and Guidelines Informed

The project has directly contributed to the advancement of best practices for water management and approaches for identifying the impacts of urban development on water quantity and quality. Collaborations with project partners in completing the project, as well as connections and discussions in parallel with the research, have been instrumental in shaping the outcomes. Key outcomes are briefly summarized as follows:

- Findings from the OBF and community rain garden studies will directly inform City of Calgary LID Guideline Modules 1 and 2 that deal with hydrogeological considerations and bioretention/bioswale systems, respectively. The results have identified opportunities for upgrading as well as incorporation of new guidance, including soil media specifications, LID setback distances, IP ratios, and hydrogeological characterization.
- We are proposing updated guidance for ALIDP Rain Garden Performance Evaluation.
- Project data from the community rain gardens were utilized to guide City of Calgary development of approaches for simulating infiltration-LID systems, notably the application of 2-layer approaches being led by KWL Consulting.
- Community rain garden results were directly incorporated into the City of Calgary's new Green Stormwater Infrastructure Triple Bottom Line Tool.
- Results demonstrate that bioretention media with moderate clay and silt content (CL media) can achieve high infiltration rates and superior water quality performance compared to conventional sand-based designs.
- Project results highlight the potential to adopt more flexible, performance-based media specifications that lower material costs and broaden sourcing options without compromising hydraulic performance.
- The observed temporal evolution of LID hydrologic and water quality performance emphasizes the need for multi-year performance monitoring to refine best practices and inform adaptive management of LID systems.

- In partnership with the Nose Creek Watershed Partnership (NCWP) and Bow River Basin Council (BRBC), project findings and data have been utilized in the development of NCWP's hydrologic, hydraulic, and water quality model to support watershed management decision-making.
- Project members (Cey and Hayashi) have utilized research findings in advising Alberta Environment and Protected Areas (AEPA) in their development of the Groundwater Management Framework.
- Similarly, project results and expertise have been used to guide Alberta Geological Survey-Alberta Energy Regulator (AGS-AER) with development of aquifer classification system as part of the Southern Alberta Groundwater Evaluation (SAGE) project. This will advance guideline development focused on groundwater protection and integrated SW-GW management.

These contributions strengthen local and regional design standards, advance best practices for LID performance, guide watershed-scale modeling and regulatory efforts, and support development of regional water management plans.

Performance Metric: Presentations and Outreach

The project generated a large, multi-year dataset and produced multiple scientific and knowledge dissemination outputs. Results were shared extensively throughout the project via a combination of professional, academic, and community engagement activities. These activities ensured broad distribution of project outcomes, supporting both practitioner adoption and public awareness of nature-based stormwater management solutions. The following list briefly outlines the key contributing areas, with further details on outreach, engagement and knowledge dissemination activities are outlined in Section 8.0, and details on specific publications, presentations, and theses are provided in Sections 9.0 and 10.0.

- **Scientific publications and student theses**: Project results have been captured in 15 journal articles and student theses to date. Four additional student projects (2 PhD, 1 MSc, 1 BSc) are still in progress and are expected to be completed in the coming year, and several additional peer-viewed publications are anticipated from the research that is ongoing and that already completed.

- **Conference presentations**: A total of 39 presentations have been formally presented or submitted to a wide range of scientific conferences and meetings, with additional presentations emanating from the research expected to continue into the future. Audiences have ranged from targeted, local interest groups (e.g., NCWP and BRBC Science forums) to national and international meetings.

- **Project partner meetings, working groups and advisory activities**: Steering committee meetings with project partner organizations have been held throughout the project. Most importantly, several members of the project team have worked closely with partner organization working groups, other provincial organizations, and industry stakeholders to translate the project outcomes into practice across the province.

- **Educational outreach**: The research sites and project outcomes have been actively used for educational outreach, helping to broaden understanding of water management issues for scientific and non-scientific audiences at all levels.

- **Community engagement**: This research project was designed with community engagement in mind, with all research sites having some degree of public accessibility and others (e.g., rain gardens) being wholly integrated into the communities they are designed to serve. Community support has been instrumental to successful project outcomes. In turn, the research sites have served as valuable platforms for learning and engagement, enhancing collective understanding of sustainable water management.

6.0 Benefits

This project has generated multiple, tangible benefits for Alberta, while strengthening the province's capacity for innovation and leadership in sustainable stormwater management. The project and outcomes directly support cost-effective, resilient, and science-based water management strategies in water-stressed urban regions.

6.1 Economic

- Findings from the OBF mesocosm experiments demonstrate that effective hydraulic and water quality performance can be achieved with less stringent bioretention media specifications, lowering production and sourcing costs for municipalities and developers.
- Improved understanding of media composition, vegetation function, and temporal changes in hydraulic performance will enhance design efficiency and reduce life-cycle costs associated with LID systems.
- Enhanced groundwater recharge and local stormwater management capacity can reduce reliance on expensive water supply and flood control infrastructure, supporting long-term economic resilience in growing communities.
- The research provides new tools and data to better predict hydrologic responses to urbanization, floods, and droughts, thereby helping communities to avoid costly infrastructure damage and adapt to changing climate conditions.
- Appropriate design guidance for LID setback distances and hydrogeologic characterization will help safeguard property values and minimize water-related disruptions to urban infrastructure
- The findings directly support the development industry by ensuring green stormwater systems are efficient and sustainable.

6.2 Environmental

- Valuable new data and modeling tools are available for assessing and mitigating impacts of changing land use and climate on hydrologic systems at the urban-rural interface.
- Coupling of field and numerical results enhances confidence in hydrologic models and provides transferable methods for estimating recharge, evaluating lateral subsurface flow, and simulating water budgets under Alberta's cold-climate conditions.
- Improved understanding of SW-GW connectivity and hydrologic function garnered from this project will enable science-based guidance for policy development and support more holistic management of water resources.

- Results provide quantitative insights into how infiltration-based LID systems can enhance groundwater recharge and improve the sustenance and natural variability in streamflows, thereby enhancing both flood and drought resilience.
- Identification of nutrient leaching risks underscores the importance of proper soil amendments and adaptive design to prevent impacts on groundwater and downstream surface waters.
- The clay-based and organic-rich CL media tested in the OBF mesocosms exhibited superior water treatment and hydraulic performance compared with sand-based media, highlighting opportunities for improved water handling and pollutant mitigation.
- The project contributes to climate adaptation by promoting green infrastructure approaches that improve watershed health, mitigate flooding, and enhance resilience to drought and extreme weather events.
- Outcomes directly advance best management practices for cold-climate LID design, supporting improved environmental performance across Alberta and Canada.

6.3 Social

- Research sites have served as visible, accessible examples of nature-based stormwater solutions and community-focused scientific research, promoting public awareness and engagement in water stewardship and sustainable urban planning.
- The project's collaboration with municipalities and watershed organizations (e.g., NCWP, BRBC, Rocky View County) strengthened regional partnerships in water stewardship and planning.
- Improved design and management of urban stormwater systems safeguard municipal infrastructure, reduce surface and groundwater flooding risks, and enhance the safety and livability of urban communities.
- Enhanced protection of local streams and aquatic habitats through improved water quality and moderated flow regimes.
- The project outcomes also provide health-related benefits by supporting design strategies that can reduce nutrient loading from urban runoff and LID systems.

6.4 Building Innovation Capacity

- The project trained a diverse cohort of HQP (BSc, MSc, and PhD students), equipping them with advanced skills and knowledge to support future needs in the province's water sector.
- HQP are well positioned to contribute to Alberta's academic, consulting, and public sectors, strengthening the province's technical capacity in water resource management.
- The large and diverse datasets generated across the three major field studies form a valuable long-term asset for ongoing innovation in LID design and hydrologic modeling.
- The established field infrastructure and collaborative partnerships will continue to support research, outreach, and technology transfer, helping Alberta maintain leadership in sustainable, climate-resilient water management.

7.0 Recommendations

Based on the outcomes of this project, the following recommendations are proposed to guide future policy, design, and research directions:

1. **Promote adaptive LID design and monitoring.**
   LID design should account for the fact that performance changed over time from construction to long-term operation. Thus, LID designs should reflect this temporal variability and long-term field monitoring is recommended to track how systems evolve through vegetation establishment, seasonal freeze-thaw cycles, soil structure development, and sedimentation. Standardized monitoring protocols would enable data comparability and contribute to a province-wide evidence base for LID system performance.
2. **Incorporate subsurface characterization into all LID planning and design.**
   Site-specific assessment of soil and geologic conditions is essential to predict LID performance that is driven by infiltration, seepage, and groundwater interaction.
3. **Adopt a more flexible approach to bioretention media specifications.**
   Results from the OBF bioretention mesocosms demonstrated that it is possible to achieve the desired hydrologic and treatment performance with less stringent tolerances on media composition. This flexibility could reduce production costs and expand material sourcing options, while maintaining or improving system effectiveness.
4. **Address nutrient leaching in bioretention media.**
   Incorporate media amendments such as water treatment residuals (WTR) to manage P leaching and consider clay-rich or mixed-texture media to reduce N and P losses. Further evaluation is required to confirm their long-term performance, benefits, and risks.
5. **Integrate surface water-groundwater connectivity into watershed planning.**
   Since groundwater is the dominant source of streamflow and infiltration-based LID systems enhance groundwater recharge, water management frameworks should explicitly incorporate these interactions into stormwater design, modeling, and policy. Specifically, this means integrating groundwater recharge into stormwater master plans to maintain baseflow and watershed health.
6. **Advance modelling tools to incorporate groundwater dependent processes.**
   In line with the previous recommendation, expand the use of coupled surface–subsurface hydrologic models to assess LID performance and improve prediction of watershed-scale hydrologic responses by explicitly accounting for groundwater recharge, subsurface flow paths, and downstream baseflow contributions. Continued development and refinement of models will be undertaken to support design optimization, land use and climate change assessments, and long-term watershed-scale planning.
7. **Encourage collaborative implementation and data sharing.**
   Partnerships among municipalities, academia, and provincial agencies should be maintained to coordinate LID monitoring networks and share hydrologic datasets.
8. **Evaluate cumulative watershed-scale benefits.**
   Future studies should assess how distributed LID implementation affects overall watershed resilience, groundwater systems, and aquatic ecosystem health.

8.0 Knowledge Dissemination

Throughout the project, we have maintained our goal of communicating regularly and broadly with a wide range of audiences that would be interested in the project outcomes. Communication plans included engagement with our project partners and related organizations to disseminate information on the project, seek feedback or collaboration opportunities, and conduct educational and outreach activities. Project leaders also regularly participated in technical advisory work on a range of water resource management issues in the province, and team members were consulted by media organizations to comment on relevant water sector issues. The success of the project is reflected in the quality and range of collaborations that have developed from this work, and most importantly from the interest in continued and new collaborations that have sparked further research on water innovations in Alberta.

A summary of relevant knowledge dissemination and collaboration activities is provided here, broken down by primary target audience.

Project Partners and Advisory Groups

- Annual steering committee meetings have been held throughout the project with all project partners participating (AI, AEPA, ALIDP, BRBC, City of Calgary, NCWP, Town of Okotoks, Rocky View County). These steering committee meetings have been designed to facilitate input on research needs and knowledge gaps as identified by project partners, and to disseminate project results. Additional 1:1 meetings with individual project partners also occurred regularly to facilitate further knowledge transfer and collaborations.
- Project team members have been instrumental in supporting the ALIDP Research and Monitoring (RAM) working group, which promotes data and knowledge sharing for LID systems. One of our former team members (Skorobogatov) and one of our project partners (L. van Duin) co-chair the group and multiple team members participated and presented at meetings regularly throughout the project. This collaboration is expected to continue.
- The success of this research project has catalyzed new research initiatives and plans for further collaboration, including establishment of LID-based research in the City of Edmonton (through ALIDP) and plans continued monitoring and analysis of the HP and CH rain gardens with the City of Calgary.
- Team leaders (Cey and Hayashi) have participated in the Nose Creek Watershed Partnership (NCWP) stakeholder group meetings related to NCWP's Hydraulic and Water Quality Model project, and E. Cey is an active participant in the Nose Creek Watershed Modeling Phase III team that meets weekly. This collaboration is expected to continue. Project team members (Cey and Cann) have also presented on project activities and findings to the NCWP board and via the NCWP Science Forum.
- Further collaborations with the NCWP and Rocky View County focused on parallel research to improve soil moisture monitoring in Nose Creek watershed. Team members installed automated soil moisture and weather stations across the watershed to provide data for NCWP model development noted in the previous bullet. UofC has also supported multiple funding proposals submitted by NCWP to improve water stewardship.
- Project team members participated in infiltration testing experiments with ALIDP and industry partners at several field sites, including the rain garden sites established for this research. Results were presented at ALIDP RAM meetings.
- Members of the project team (Cey, Hayashi) contributed to the AEPA working group advising on the Guide to Groundwater Management Frameworks Development.
- Technical advisory support was provided to AGS-AER via their Aquifer Classification Workshop, held in partnership with AEPA.

- The project lead (Cey) collaborated on a related stormwater project with the Calgary Airport Authority as a result of partnerships that arose from this project.
- On multiple occasions, project team members presented research plans and results in seminars or showcase events with various partners. Examples include the BRBC Science Forum, ALIDP Designing for Tomorrow Student Showcase, and City of Calgary Luncheon Seminar Series.

Educational Outreach

- University of Calgary students completing the hydrogeology field course (GLGY 441 and GLGY 649) annually visited the Sage Hill field site for experiential learning of practical field skills in hydrology, hydrogeology, and geophysics. Multiple team members have been involved in this training during the project period (Hayashi, Cey, Johnson, Cann, and Wyse), and we anticipate the site will continue to provide a valuable learning platform moving forward.
- Similar to the previous bullet, students from Southern Alberta Institute of Technology (SAIT) Integrated Watershed Management Program have completed annual field training exercises at the Sage Hill site under the direction of our project team.
- Team members (Ilg, Cann, Wyse, Cey) engaged in public outreach events to educate elementary and secondary school students on water issues. Examples included Water Innovation Day in collaboration with SAIT and Inside Education, and the "What is a resilience garden?" event with Edelweiss Preparatory School. These educational outreach activities were conducted at the community rain garden sites, by visiting classrooms, and in public education seminars.
- The Sage Hill site served as a hands-on learning venue for youth groups, such as the Girl Guides of Alberta. Through interactive visits, multiple classes with children of various ages were introduced to water resource concepts and encouraged to explore, observe, and ask questions about earth systems.

Community Engagement

- The Highland Park rain garden site was the focus of multiple field visits over the study period by visiting scientists and water managers through partnership with the City of Calgary (B. van Duin). Rain garden development, equipment design, and technical demonstrations were presented by the project team (Cey, Elliot, Ilg).
- Various HQP (Elliot, Ilg) and ALIDP partners presented rain garden development plans and findings to the Highland Park and Cambrian Heights Community Associations as part of outreach efforts.
- Team members completed drainage mapping assessments with representatives from the Cambrian Heights Community Association.
- Project leaders (Cey, Hayashi) participated in multiple media stories in relation to water issues in Alberta, including CBC news, QR77 radio, and the Canadian Press.

Scientific Publications and Presentations

Members of the research team also disseminated relevant research findings through various published works (e.g., peer-reviewed publications, conference proceedings, student theses) and participation in a range of scientific conferences, meetings and events. A full list of these publications and presentations are summarized in Sections 9.0 and 10.0. Finally, the project generated a large, multi-year dataset and associate data products that will be made available for ongoing research, model refinement, and watershed planning initiatives.

9.0 Reference List

*** Denotes a contribution from researchers originating directly from this project. These contributions are <u>not repeated</u> in the subsequent Section 10.0 list of project contributions.*

Asleson, B.C., Nestingen, R.S., Gulliver, J.S., Hozalski, R.M., Nieber, J.L. 2009. Performance assessment of rain gardens. *J. Amer. Water Resour. Assoc.*, 45(4), 1019–1031.

Baker D.B., Richards R.P., Loftus T.T., Kramer J.W. 2004. A new flashiness index: Characteristics and applications to Midwestern rivers and streams. *J. Amer. Water Resour. Assoc.*, 40 (2), 503–522.

City of Calgary. 2016. Low Impact Development Guidelines Module 1 - Geotechnical and Hydrogeological Considerations.

City of Calgary. 2016. Low Impact Development Guidelines Module 2 - Bioretention and Bioswales.

City of Calgary. 2023. Impervious Surfaces 2021 Available at: https://data.calgary.ca/Environment/Impervious-Surface-2021/rgsu-3v7u [Accessed April 11, 2023]

Davis, A.P. 2008. Field performance of bioretention: Hydrology impacts. *J. Hydrol. Eng.*, 13, 90-95.

Ehsanzadeh E., Spence C., van der Kamp G., McConkey B. 2012. On the behaviour of dynamic contributing areas and flood frequency curves in North American Prairie watersheds. *J.Hydrol.*, 414–415, 364–373.

Ehsanzadeh E., van der Kamp G., Spence C. 2016. On the changes in long-term streamflow regimes in the North American Prairies. *Hydrol. Sci. J.*, 61 (1), 64–78.

**Elliot, S. 2023. A mesocosm study of bioretention functionality under frozen conditions. MSc thesis, University of Calgary, Calgary, AB.

Environment Canada. 2025 Canadian climate normals. http://climate.weather.gc.ca/climate_normals/index_e.html. [Accessed Sept 14, 2025].

Government of Alberta, 2013. Evaporation and Evapotranspiration in Alberta, in: Alberta Environment and Sustainable Resource Development (Ed.), Development A.E.a.S.R. Edmonton, Alberta, p. 283.

**Hall, G. 2021. Evaluating the effectiveness of bioretention systems for managed aquifer recharge in cold climates. MSc thesis, University of Calgary, Calgary, AB.

Hantush, M.S. 1967. Growth and decay groundwater-mounds in response to uniform percolation. *Water Resour. Res.*, 3, 227-234.

Hathaway, J.M., Brown, R.A., Fu, J.S., Hunt, W.F. 2014. Bioretention function under climate change scenarios in North Carolina, USA. *J. Hydrol.,* 519, 503-511.

Hatt, B.E., Fletcher, T.D., Deletic, A. 2009. Hydrologic and pollutant removal performance of stormwater biofiltration systems at the field scale. *J. Hydrol.*, 365, 310-321.

Hayashi M., & Farrow C.R. 2014. Watershed-scale response of groundwater recharge to inter-annual and inter-decadal variability in precipitation (Alberta, Canada). *Hydrogeol. J.*, 22 (8), 1825–1839.

Healy, R.W., Cook, P.G. 2002. Using groundwater levels to estimate recharge. *Hydrogeol. J.*, 10, 91–109.

Hoghooghi, N., Golden, H.E., Bledsoe, B.P., Barnhart, B.L., Brookes, A.F., Djang, K.S., Halama, J.J., McKane, R.B., Nietch, C.T., Pettus, P.P. 2018. Cumulative effects of Low Impact Development on watershed hydrology in a mixed land-cover system. *Water*, 10(8).

Hunt, W.F., Jarrett, A.R., Smith, J.T., Sharkey, L.J., 2006a. Evaluating bioretention hydrology and nutrient removal at three field sites in North Carolina. *J. Irrig. Drain.*, Eng. 132, 600-608.

**Ilg, D. 2025. Investigating the water budget and subsurface hydrology of two rain gardens in Calgary, Alberta. MSc thesis, University of Calgary, Calgary, AB.

**Johnson, S. 2024. Influence of development on peri-urban headwater streams in Calgary, Alberta. MSc thesis, University of Calgary, Calgary, AB.

Le Coustumer, S., Fletcher, T.D., Deletic, A., Barraud, S., Poelsma, P. 2012. The influence of design parameters on clogging of stormwater biofilters: A large-scale column study. *Water Res.*, 46(20), 6743–6752.

Li, H., Sharkey, L.J., Hunt, W.F., Davis, A.P. 2009. Mitigation of impervious surface hydrology using bioretention in North Carolina and Maryland. *J. Hydrol. Eng.*,14, 407-415.

McMahon T.A., Nathan R.J. 2021. Baseflow and transmission loss: A review. *WIREs Water*, 8 (4): 1–30.

**Merrett, S. 2023. Evaluation of rain garden hydraulic performance through lateral and vertical flow characterization in Hydrus 2D. BSc thesis, University of Calgary, Calgary, AB.

Mohammed, A.A., Kurylyk, B.L., Cey, E.E., Hayashi, M. 2018. Snowmelt infiltration and macropore flow in frozen soils: Overview, knowledge gaps, and a conceptual framework. *Vadose Zone J.*, 17(1), Article 180084.

Moran S.R. 1986. *Surficial Geology of the Calgary Urban Area*. Alberta Research Council Bulletin No. 53: Edmonton, AB, Canada.

Morton, F.I. 1983. Operational estimates of areal evapotranspiration and their significance to the science and practice of hydrology. *J. Hydrol.*, 66(1-4), 1-76.

Shephard, M.W., Mekis, E., Morris, R.J., Feng, Y., Zhang, X., Kilcup, K., Fleetwood, R. 2014. Trends in Canadian short-duration extreme rainfall: Including an Intensity-Duration-Frequency perspective. *Atmosphere - Ocean*, 52(5), 398–417.

**Skorobogatov A. 2023. Multi-year analysis of hydrological and water quality bioretention performance. PhD thesis. University of Calgary, Calgary, AB.

Taylor, N.M., Sills, D.M.L., Hanesiak, J.M., Milbrandt, J.A., Smith, C.D., Strong, G.S., Skone, S.H., McCarthy, P.J., Brimelow, J.C. 2011. The understanding severe thunderstorms and Alberta boundary layers experiment (UNSTABLE) 2008. *Bull. Amer. Meteor. Soc.* 92(6), 739–763.

Técher, D., Berthier, E. 2023. Supporting evidences for vegetation-enhanced stormwater infiltration in bioretention systems: a comprehensive review. *Environ. Sci. Pollut. Res.*, 30, 19705–19724.

van der Kamp G., Hayashi M. 2009. Groundwater-wetland ecosystem interaction in the semiarid glaciated plains of North America. *Hydrogeol. J.*, 17 (1), 203–214.

Winter T.C. 2007. The role of ground water in generating streamflow in headwater areas and in maintaining base flow. *J. Amer. Water Resour. Assoc.,* 43 (1), 15–25.

**Zhang, Y., Skorobogatov, A., He, J., Valeo, C., Chu, A., van Duin, B., van Duin, L. 2023. Mitigation of nutrient leaching from bioretention systems using amendments. *J. Hydrol.*, 618, Article129182.

10.0 Project Publications and Presentations

*A full listing of project contributions to scientific knowledge is provided below, except for those publications and student theses that have already been included in Section 9.0 (denoted by **).*

Cann, B., Cey E. 2023. Modeling and assessing low impact development (LID) and urban impacts on stream transects in the Calgary area, Nose Creek Watershed Partnership Board Meeting, Calgary, AB and Virtual, April 27, 2023.

Cann, B., Cey, E., Hayashi, M., He, J., Chu, A., van Duin, B., van Duin, L. 2023. Hydrological modeling of infiltration-based low impact development. ALIDP 2023 Designing for Tomorrow, Calgary, AB, November 13-16, 2023.

Cann, B., Cey, E., Ilg, D., van Duin, B., van Duin, L., Hayashi, M., He, J., Chu, A. 2025. Exploring subsurface flow dynamics for a rain garden using 3D modeling. Alberta Low Impact Development Partnership (ALIDP) Designing for Tomorrow Live, Edmonton, AB, May 7-9, 2025. *****Most impactful poster & Best overall poster***

Cey, E. 2020 Assessing water connectivity in rural and urban watersheds for improved water management. Alberta Innovates Water Innovation Program Connect Series (Virtual), June 24, 2020.

Cey, E. 2023. Evolving water connectivity in an urbanizing watershed. Nose Creek Watershed Partnership Science Forum, Airdrie, AB, October 12, 2023.

Cey, E. 2024. Water connectivity and green stormwater infrastructure in urbanizing watersheds. ALIDP Green Stormwater Infrastructure Perspectives and Pathways Forward, Part 3 (virtual), April 18, 2024.

Cey, E. 2024. Assessing water connectivity in rural and urban watersheds for improved water management. AI Water Innovation Program Forum, Calgary, AB, May 27-28, 2024.

Cey, E., Ilg., D., Cann, B., Wyse, J., Elliot, S., Johnson, S., Hayashi, M., He, J., Chu, A., van Duin, B., van Duin, L. 2025. Groundwater-surface water connectivity across the spectrum in urbanizing watersheds. Abstract submitted to CWRA Alberta-IAH-CNC Joint Meeting, Edmonton, AB, November 12-14, 2025.

Cey, E., Elliot, S., He, J., Chu, A., Skorobogatov, A., van Duin, B. 2022. Frozen ground performance of engineered bioretention systems in southern Alberta. GAC-MAC-IAH-CNC-CSPG Joint Meeting, Halifax, NS, May 15-18, 2022.

Cey, E., Hayashi, M., He, J., Chu, A., Elliot, S., Johnson, S. 2022. Assessing water connectivity in rural and urban watersheds for improved water management. AI Project Steering Committee Meeting (virtual), Feb. 23, 2022.

Cey, E., Hayashi, M., He, J., Chu, A., Elliot, S., Johnson, S., Ilg, D., Wyse, J., Cann, B., Merrett, S. 2023. Assessing water connectivity in rural and urban watersheds for improved water management. AI Project Steering Committee Meeting (virtual), Mar. 15, 2023.

Cey, E., Ilg, D. 2023. Evolving water connectivity in an urbanizing watershed. ALIDP Research and Monitoring Working Group (virtual), December 15, 2023.

Cey, E., Johnson, S., Hayashi, M., van Duin, B. 2023. Development impacts on groundwater-surface water connections. City of Calgary Research Partner Seminar (virtual), June 27, 2023.

Elliot, S., Cey, E., He, J., Chu, A., Skorobogatov, A., van Duin, L., van Duin, B. 2022. Low impact development functionality in southern Alberta. Bow River Basin Science Forum, Calgary, AB, May 4, 2022.

Elliot, S., Cey, E., He, J., Chu, A., Skorobogatov, A., van Duin, B. 2022. Bioretention functionality under frozen conditions. CWRA 2022 Annual Conference, Canmore, AB, June 5-8, 2022.

Elliot, S., Cey, E., He, J., Skorobogatov, A., van Duin, B. 2022. Okotoks bioretention mesocosm research - frozen condition infiltration testing results. Designing for Tomorrow: Future of Stormwater Management in Alberta, Conference Series, Online, April 21, 2022.

Elliot, S., Cey, E., He, J., Skorobogatov, A., van Duin, B. 2023. Okotoks bioretention frozen media functionality. ALIDP - Designing for Tomorrow Student Showcase (virtual), April 20, 2023.

Hall, G., Skorobogatov, A., Chu, A., Cey, E., and He, J. 2020. Determining the recharge potential of a Low Impact Development system under seasonally frozen conditions. GeoConvention 2020, Calgary, AB (virtual), September 21-23, 2020. *****poster award winner***

Hayashi, M. 2021. Groundwater - surface water connection in prairie watersheds. Alberta Environment and Parks, Science Seminar (virtual), March 23, 2021.

Hayashi, M. 2025. Understanding groundwater - surface water connection for watershed stewardship. Agricultural Service Board of Rocky View County, Balzac, Alberta, March 12, 2025.

Hayashi, M. 2025. Understanding groundwater – surface water interaction for water supply in Alberta watersheds. Red Deer River Watershed Alliance, Red Deer, Alberta, June 20, 2025.

Hayashi, M. 2025. Understanding groundwater - surface water connection for watershed stewardship. Jumpingpound Creek Watershed Stewardship, Jumpingpound, Alberta, November 25, 2024.

Ilg, D., Cann, B., Elliot, S., Cey, E., van Duin, B., van Duin, L., Hayashi, M., He, J., Chu, A. 2025. Rain gardens in action – Investigating the water budget and subsurface flow dynamics of two rain gardens in Calgary, Alberta. Alberta Low Impact Development Partnership (ALIDP) Designing for Tomorrow Live, Edmonton, AB, May 7-9, 2025.

Ilg, D., Elliot, S., Cey, E., van Duin, B., van Duin, L., Hayashi, M., He, J., Chu, A. 2025. Investigation of the water budget and subsurface hydrology of two rain gardens in Calgary, Alberta. GAC-MAC-IAH-CNC Annual Meeting, Ottawa, ON, May 11-14, 2025.

Ilg, D., Elliot, S., Cey, E., van Duin, L., van Duin, B. 2023. Monitoring and assessing the hydrologic performance of two Calgary rain gardens. ALIDP - Designing for Tomorrow Student Showcase (virtual), April 20, 2023.

Ilg, D., Elliot, S., Cey, E., van Duin, L., van Duin, B. 2023. Monitoring and assessing the hydrologic performance of two Calgary rain gardens. City of Calgary Research Partner Seminar, Virtual, June 27, 2023.

Jalali, G., Zhang, Y., Skorobogatov, A., He, J., van Duin, B., van Duin, L. 2023. Characterization of nutrient leaching of amended and non-amended bioretention cells. ALIDP 2023 Designing for Tomorrow, Calgary, AB, November 13-16, 2023. *****student poster award winner***

Jalali, G., Zhang, Y., Skorobogatov, A., He, J., Valeo, C., Chu, A., Huang, J., van Duin, B., van Duin, L. 2024. Nutrient leaching characterization of amended bioretention systems: a field experiment study. CWRA 2024 National Conference, Saskatoon, SK, June 17-19, 2024.

Jalali, G., Zhang, Y., Skorobogatov, A., He, J., Valeo, C., Chu, A., Huang, J., van Duin, B., van Duin, L. 2025. Impact of design on nutrient leaching of bioretention systems. CWRA 2025 National Conference, Penticton, BC, May 25-29, 2025.

Jalali, G., Skorobogatov, A., He, J., Valeo, C., Chu, A., van Duin, B. 2024. Impact of media, vegetation and their interaction on the temporal evolution of nutrient leaching of bioretention systems: A field study. AGU 2024 Annual Meeting, Washington, DC, December 9-13, 2024.

Jalali, G., Skorobogatov, A., He, J., Valeo, C., Chu, A., Huang, J., van Duin, B. 2025. Nutrient leaching dynamics of bioretention systems: the impacts of design parameters and their interactions. Submitted to Science of the Total Environment.

Jalali, G., Zhang, Y., Skorobogatov, A., He, J., Valeo, C., Chu, A., Huang, J., van Duin, B., van Duin, L. 2025. Characterization of nutrient leaching of non-amended and amended bioretention cells. Environmental Science and Pollution Research. Minor Revision Requested.

Johnson, S., Cey, E., Hayashi, M., van Duin, B. 2022. Evaluating the influence of urban development on stream flow in northwest Calgary. Bow River Basin Science Forum, Calgary, AB, May 4, 2022.

Johnson, S., Cey, E., Hayashi, M., van Duin, B. 2022. The impact of urban development on stream flow in northwest Calgary. CWRA 2022 Annual Conference, Canmore, AB, June 5-8, 2022.

Johnson, S., Cey, E., Hayashi, M., van Duin, B. 2023. Understanding surface water-groundwater interactions in developed and undeveloped catchments in northwest Calgary. ALIDP - Designing for Tomorrow Student Showcase (virtual), April 20, 2023.

Nasrollahpour, R. 2021. Impacts of vegetation and growing media on evapotranspiration in bioretention systems, Master's thesis, University of Calgary, Calgary, AB.

Nasrollahpour, R., Skorobogatov, A., He, J., Valeo, C., Chu, A., van Duin. B. 2021. The effects of climatic and design variables on the evapotranspiration of bioretention systems. Hydrotechnical Specialty Conference, CSCE Annual Conference (virtual), May 26-29, 2021.

Nasrollahpour, R., Skorobogatov, A, He, J., Valeo, C., Chu, A., van Duin, B. 2022. The impact of vegetation and media on evapotranspiration in bioretention systems. *Urban Forestry and Urban Greening*, 74, Article 127680.

Prevost, S. 2023. Hydrogeological characterization of springs in the Bighill Creek watershed, BSc thesis, University of Calgary, Calgary, AB.

Prevost, S., Hayashi, M. 2023. Hydrogeological characterization of springs in the Bighill Creek watershed. Bow River Basin Council Science Forum, Calgary, AB, April 26, 2023.

Skirten, J. 2021. Modeling the Water Budget of an urban City of Calgary Rain Garden System with HYDRUS-1D. BSc thesis, University of Calgary, Calgary, AB.

Skorobogatov, A., He, J.X., Chu, A., Valeo, C., van Duin, B. 2020. The impact of media, plants and their interactions on bioretention performance: A review. *Sci. Total Environ.*, 715, Article136918.

Skorobogatov, A., He, J., Chu, A., Valeo, C., van Duin, B. 2020. Stormwater management by bioretention mesocosms - the dynamic role of vegetation and media in the performance. 2nd International Conference on New Horizons in Green Civil Engineering (NHICE-02), August 24-26, 2020.

Skorobogatov, A., Li, X., Nasrollahpour, R., He, J., Valeo, C., Chu, A., van Duin, B. 2021. Dynamic multi-year performance of bioretention mesocosms – patterns of change. Environmental Specialty Conference, CSCE Annual Conference (virtual), May 26-29, 2021.

Zhang, Y. 2023. Mitigation of nutrient leaching from bioretention systems using amendments Master's thesis, University of Calgary, Calgary, AB.

Zhang, Y., Skorobogatov, A., He, J., Chu, A., van Duin, B., van Duin, L. 2021. Bioretention amendments for reducing phosphorus leaching: field investigation. CWRA 2021 Annual Conference (virtual), May 31- June 4, 2021.

Zhang Y., Skorobogatov, A., He, J., Valeo, C., Chu, A., van Duin, B., van Duin, L. 2022. Effects of amendments on bioretention systems: the field and laboratory investigations. CSCE 2022 Annual Conference, Whistler, BC, Canada, May 25-28, 2022.